

UNIVERSITY OF HELSINKI

Master's Thesis

High-throughput evaluation of the combinatorial approach to improve NK cell cancer immunotherapy using anti-cancer drugs in acute myeloid leukaemia

Jonas Bouhlal
Master's Programme in Translational Medicine
Faculty of Medicine
University of Helsinki

March 2022

Table of Contents

Abbreviations	4
Abstract	6
Tiivistelmä	7
1. Introduction	8
1.1 <i>Acute myeloid leukaemia</i>	8
1.1.1 Pathophysiology	9
1.1.2 Classification	11
1.1.3 Prognostic factors	12
1.1.4 Treatment	14
1.1.5 Methods to study acute myeloid leukaemia	20
1.2 <i>Immunology and cancer</i>	21
1.2.1 The human immune system	21
1.2.2 Role of immune system in cancer	22
1.2.2 Natural killer cells	23
1.3 <i>NK cell-based immunotherapy for AML</i>	27
1.4 <i>Drug sensitivity and resistance testing</i>	29
1.5 <i>Combinatorial approaches to improve immunotherapy</i>	31
2. Aims of the Thesis	34
3. Materials and methods	35
3.1 <i>Cell culture related methods</i>	35
3.1.1 Cell lines	35
3.1.2 Cell culture	35
3.1.3 NK cell isolation and expansion	36
3.1.4 Transducing cell lines with luciferase constructs	39
3.1.5 Selection of transduced cell lines – THP-1 and MOLM-14	40
3.1.6 Post-transduction single cell sorting of HEL cell line	41
3.1.7 Freezing and thawing	42
3.2 <i>Drug screening</i>	43
3.2.1 Optimisation	43
3.2.2 DSRT method	44
3.3 <i>Single cell RNA sequencing using hashtag oligos</i>	47
3.3.1 Drug dilutions	47
3.3.2 Pre-hashing optimisation	47
3.3.3 Hashing experiment and preparation for single cell RNA sequencing	48
3.3.4 Single cell sequencing using hashtag oligos	51
3.4 <i>Data analysis</i>	52
3.4.1 Analysis of DSRT data	52
3.4.2 Analysis of scRNA sequencing data	52

4. Results	54
4.1 Effector-target optimisation of different cell lines and different donor effects	54
4.2 DSRT results	55
4.2.1 Data quality	57
4.2.2 Most activating drugs	58
4.2.3 Most inhibiting drugs	68
4.3 Single cell RNA sequencing of MOLM-14	77
4.3.1 Drug selection for transcriptomic analysis and validation experiment	77
4.3.2 MOLM-14 scRNA data analysis	79
4.4 Drug-specific effects and further analysis	84
4.4.1 Pevonedistat activates NK cell mediated killing in both MOLM-14 and THP-1	84
4.4.2 Daporinad enhances NK cell cytotoxicity in MOLM-14 and THP-1	86
4.4.3 Effect of JAK inhibitors are cell line dependent	88
4.4.4 Tacrolimus strongly activates NK cell cytotoxicity in HEL cell line	89
4.4.5 PI3K inhibitors have an inhibitory effect on NK cell cytotoxicity in MOLM-14	90
4.4.6 Effect of FLT3 inhibitors and other broad range TKIs is decreased by NK cells	91
5. Discussion	93
5.1 Significant findings and their potential implications	93
5.2 Shielding effect of NK cells	96
5.3 Assessment of DSRT and scRNA methods	96
5.4 Improvements	97
5.5 Future perspectives and conclusions	99
Acknowledgements	101
References	102
Supplementary material	111

Abbreviations

ADCC	antibody-dependent cell-mediated cytotoxicity
AML	acute myeloid leukaemia
ALL	acute lymphoid leukaemia
APL	acute promyelocytic leukaemia
ATO	arsenic trioxide
ATRA	all-trans retinoic acid
BCL-2	B-cell lymphoma 2
BiKE	bi-specific killer engager antibody
CAR	chimeric antigen receptor
CBF	core binding factor
CD	cluster of differentiation
CEBPA	CCAAT enhancer binding protein alpha
CLP	common lymphoid progenitor
CML	chronic myeloid leukaemia
CRISPR	clustered regularly-interspaced short palindromic repeats
DMSO	dimethyl sulfoxide
DNA	deoxyribonucleic acid
DSRT	drug sensitivity and resistance testing
DSS	drug sensitivity score
EDTA	ethylenediaminetetraacetic acid
ELVA	expressed luciferase viability assay
FAB	French-American-British
FACS	fluorescence-activated cell sorting
FBS	fetal bovine serum
FIMM	Finnish Institute for Molecular Medicine
FLT3	fms like tyrosine kinase 3
GFP	green fluorescent protein
GO	gemtuzumab ozogamicin
GVHD	graft-versus-host-disease
GVL	graft-versus-leukaemia
HCT	hematopoietic cell transplantation
HGNC	HUGO Gene Nomenclature Committee
HLA	human leukocyte antigen
HSC	hematopoietic stem cell
HSP	heat shock protein
HTO	hashtag oligonucleotide
IDH	isocitrate dehydrogenase
IFN	interferon
IL	interleukin
ISM	individualised systems medicine

ITD	internal tandem duplication
KIR	killer immunoglobulin-like receptor
KRAS	Kirsten rat sarcoma virus
LMPP	lymphoid-primed multipotential progenitor
MACS	magnetic cell sorting
MAPK	mitogen-activated protein kinase
MHC	major histocompatibility complex
MLL	mixed-lineage leukaemia
NAE	NEDD8-activating enzyme
NAMPT	nicotinamide phosphoribosyltransferase
NK cell	natural killer cell
NKEM	NK cell culture media
NKP	NK cell progenitor
NOS	not otherwise specified
NPM1	nucleophosmin 1
PBMC	peripheral blood mononuclear cell
PBS	phosphate-buffered saline
PFA	paraformaldehyde
PI3K	phosphoinositide 3-kinase
R10	cell culture media with 10% fetal bovine serum
RNA	ribonucleic acid
scRNA	single cell RNA
scRNAseq	single cell RNA sequencing
sDSS	differential drug sensitivity score
SEER	Surveillance, Epidemiology and End Result program
SMAC	second mitochondria-derived activator of caspase
STAT	signal transducer and activator of transcription
TGF	transforming growth factor
TKI	tyrosine kinase inhibitor
TNF	tumour necrosis factor
TP53	tumour protein 53
TRAIL	tumour necrosis factor-related apoptosis-inducing ligand
TriKE	tri-specific killer engager antibody
JAK	Janus kinase
WHO	World Health Organisation
UCB	umbilical cord blood
UMAP	Uniform Manifold Approximation and Projection

Abstract

Faculty: Faculty of Medicine

Degree programme: Translational Medicine

Study track: Cancer

Author: Jonas Otto Vilhelm Bouhlal

Title: High-throughput evaluation of the combinatorial approach to improve NK cell immunotherapy using anti-cancer drugs in acute myeloid leukaemia

Level: Master's Thesis

Month and year: March 2022

Number of pages: 126

Key words: Immuno-oncology, NK cells, acute myeloid leukaemia, immunotherapy, single cell RNA sequencing, drug sensitivity and resistance testing

Supervisors: Prof. Satu Mustjoki, MD Olli Dufva

Where deposited: University of Helsinki Library

Abstract:

Despite of great advancements in the field of cancer therapy in the past decades, the 5-year survival of acute myeloid leukaemia (AML) patients remains low with high mortality especially in elderly patients, in whom the disease is most often observed. Poor prognosis often results from complex heterogenous molecular abnormalities defining the progress of the disease, while making it more difficult to treat due to intensive treatments only being feasible for younger patients. Our increased understanding of cancer immunology and the potential of immunotherapy has, however, led to promising therapeutic innovations, which give hope for discovering long-lasting and effective treatment options. Natural killer (NK) cell-based immunotherapies are amongst the emerging novel therapeutic approaches that aim to target malignant cells with less toxicity and improved applicability. Using high-throughput drug sensitivity and resistance testing combined with single cell RNA (scRNA) sequencing, this study focused on finding drug compounds that could synergise with NK cells to improve their effectiveness in killing leukemic cells. In this study, many drugs showed promising results in being able to potentiate NK cell cytotoxicity, with dapornad and pevonedistat showing the most notable differences when compared to controls. The potentiating effect of Janus kinase (JAK) inhibitors also suggested a method of increasing NK cell activity against leukemic cells through downregulation of major histocompatibility complex (MHC) class I molecules. In conclusion, findings shed light on the synergetic potential of drugs and NK cells, giving hope for clinically relevant findings following further validation and testing.

Tiivistelmä

Viimeisten vuosikymmenten merkittävistä syöpälääketieteen edistysaskelista huolimatta akuutin myeloisen leukemian (AML:n) 5 vuoden elossaoloennuste on edelleen huono, erityisesti vanhemmissa potilaissa, joissa AML:n ilmaantuvuus on suurimmillaan. Huono elossaoloennuste johtuu usein monimutkaisista heterogeenisistä molekyyli-tason muutoksista, jotka määrittävät taudin etenemisen, mutta ovat vaikeita hoitaa, sillä tehokkaammat hoidot onnistuvat usein vain nuoremmille potilaille. Lisääntynyt syövän immunologian ymmärryksemme ja immunoterapian kehittyminen on kuitenkin johtanut uusiin innovaatioihin syövän hoidossa, jotka antavat toivoa tehokkaiden hoitomuotojen löytymiselle. Luonnolliseen tappajasoluun (NK-solu) perustuva immunoterapia on orastava hoitomuoto, joka kohdistuu pahanlaatuisiin soluihin ollen samalla vähemmän myrkyllinen ja soveltuvampi muihin hoitomuotoihin verrattuna. Käyttäen suurikapasiteettista lääkeaineseulontaa yhdistettynä yksisolu-RNA-sekvensointiin, tutkimuksemme keskittyi löytämään lääkeaineita, joilla on kyky synergiaan NK-solujen kanssa parantaen niiden leukemiasoluihin kohdistettua tappokykyä. Tutkimukssamme löysimme useita lääkeaineita, joilla on kyky edesauttaa NK-solujen tappokykyä, joista erityisesti daporinad ja pevonedistat johtivat huomattaviin eroihin verrattuna kontrolleihin. Janus-kinaasien (JAK) estäjät edesauttoivat myös NK-solujen tappokykyä, osoittaen mahdollisen keinon lisätä NK-solujen aktiivisuutta leukemiasoluja vastaan vähentämällä I-luokan kudosityhteensopivuustekijöitä (MHC) leukemiasolujen pinnalla. Johtopäätöksenä voidaan todeta, että tutkimuksessa tehdyt löydökset osoittavat synergistisen yhteisvaikutuksen mahdollisuuden NK-solujen ja lääkeaineiden välillä, jota hyödyntämällä tulevaisuudessa voisi olla mahdollista hoitaa syöpää tehokkaammin.

1. Introduction

1.1 Acute myeloid leukaemia

Acute myeloid leukaemia (AML) is a cancer of the bone marrow and blood, which is characterised by the abnormally proliferative nature and poor maturation of myeloid clonal cell populations. The malignancy originates from hematopoietic stem cells of the bone marrow and in most cases, it appears *de novo* in previously healthy individuals. However, AML may also arise because of previously used therapies such as ionizing radiation in addition to chemotherapy including antimetabolites, topoisomerase-II-inhibitors, and alkylating agents.¹

AML is the most frequently diagnosed acute leukaemia in adults, accounting for approximately 23.1% of all leukaemias globally.² In the United States alone, AML was responsible for approximately 80 percent of all acute leukaemias in 2018 with the other 20 percent of acute leukaemias originating from the lymphocytic lineage. (SEER Research Data 1975-2018) In 2017, approximately 119,600 cases of AML were diagnosed worldwide, with a median age at diagnosis of approximately 70 years.

Although big leaps have been taken in the treatment of younger AML patients, the prognosis for elderly patients remains poor. In the United States, the relative 5-year survival rate for those over 65 years or older is only 8.9%, compared to that of 60.6% in patients aged 50 years and below. (SEER Research Data 1975-2018) This highlights the relatively poor prognosis in older patients, who require alternative treatment options to improve their long-term survival.³

1.1.1 Pathophysiology

AML originates from the bone marrow where myeloblasts, a form of immature white blood cells, develop abnormally, leading to the accumulation of leukemic myeloblasts which interfere with normal blood cell production. Although AML cannot metastasize like solid cancers, leukaemia cells can spread around the body, leading to a wide range of symptoms. As the disease develops, abnormal leukemic cells proliferate and take up space from healthy cells in the blood and bone marrow.⁴

The genomic landscape of AML has become clearer through advances in next generation sequencing methods, which has led to findings indicating that over 97 percent of AML cases have identifiable somatic mutations.⁵ Whole-genome sequencing analyses have also revealed that, although AML genomes have fewer mutations than most other adult cancers, some can be clearly associated with AML. A whole-genome study of 200 patients revealed a total of 23 genes that were significantly mutated with an average number of 13 mutations per patient, on average of which 5 were recurrently mutated in AML.⁶

Generally, in AML, the genomic alterations often occur without major chromosomal abnormalities, although some chromosomal translocations have been well characterised. Examples of these include the t(8:21) translocation in core-binding factor AML (CBF-AML) and t(15:17) in acute promyelocytic leukaemia (APL).⁷ In 2002, a two-hit model of cooperativity of activating mutations was suggested as a basis for the genetic reasoning behind AML. The model suggested that mutations could be divided into two groups based on their function. Class I mutations include *FLT3-ITD*, *K/NRAS*, *TP53* and *c-KIT* mutations, which can all on their own confer a proliferative and survival advantage to hematopoietic progenitor cells without affecting differentiation. By contrast, class II mutations were suggested not to be able to cause leukaemia when expressed alone but appear to be impairing hematopoietic differentiation. Mutations of this class include *NPM1*, *CEBPA* and *MLL*-related fusion genes for example. The combination of both classes was hypothesized

to lead to an AML phenotype that proliferates more aggressively, has enhanced survivability, and impaired differentiation.⁸

Genetic alterations manifesting in AML lead to increased accumulation of malignant, poorly matured myeloid cells, which tend to collect in the peripheral blood, bone marrow and in monocytic leukaemias often also to the skin and gums. More rarely, malignant cells can also accumulate to other organs such as the brain and heart. Depending on the location of the accumulated malignant cell mass in the body, different clinical manifestations are observed in patients. A combination of bone marrow failure and leukocytosis are most often seen in patients, with symptoms such as thrombocytopenia, anaemia, fatigue, and weight loss. Infections and bleeding are also often observed in AML patients, leading to death if left untreated.⁷

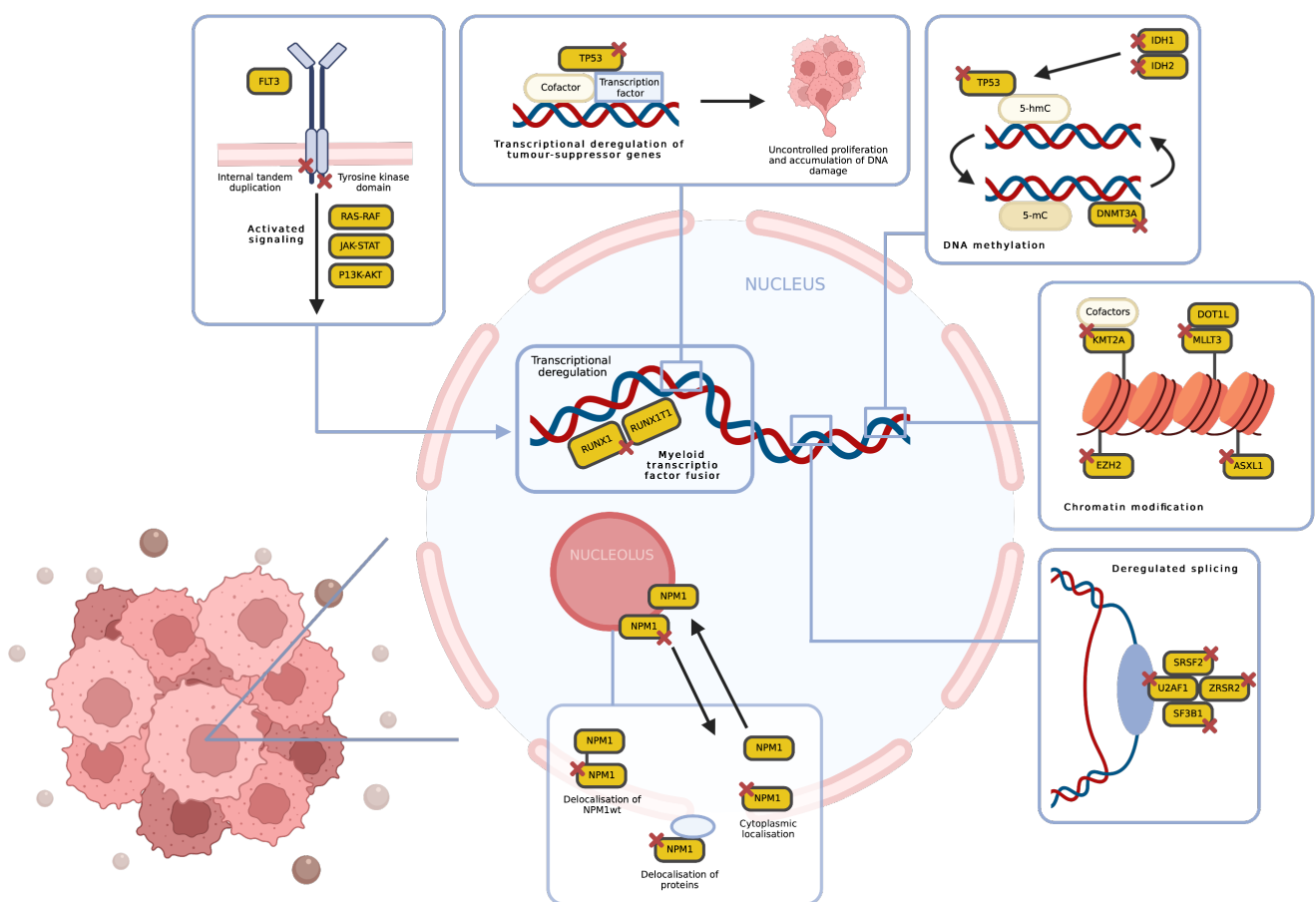


Figure 1. Graphical representation of most common genetic abnormalities observed in AML patients. Mutations are marked as red crosses with effects being highlighted for each abnormality.⁹

1.1.2 Classification

In the 1970's, a group of scientists suggested a classification system for AML to categorise the malignancy into subtypes according to pathological features. At first, the French-American-British (FAB) classification of AML described the malignancy with six subtypes, although the modern classification categorises it into eight subtypes. The subtypes range from M0 to M7, with classification being based on the cell type from which the leukaemia develops from.¹⁰

Although the FAB classification system can be useful, it does not consider the numerous factors, for example the genetics, related to the malignancy and its prognosis. The World Health Organisation (WHO) is responsible for the global management of AML diagnosis and treatment and has developed its own classification system that better incorporates other factors affecting AML prognosis with the attempt to better classify the illness. The latest update by the WHO to the classification system took place in 2016, when underlying genetic defects and predispositions were made a part of the diagnosis.¹¹

Table 1. WHO classification of AML and related neoplasms according to 2016 revision.¹¹

Type of AML or related neoplasm	Genetic abnormalities
AML with recurrent genetic abnormalities	AML with t(8:21)(q22;q22) <i>RUNX1-RUNX1T1</i>
	AML with inv(16)(p13.1q22) or t(16;16)(p13.1;q22) <i>CBFB-MYH11</i>
	AML with t(9;11)(p21.3;q23.3) <i>MLLT3-KMT2A</i>
	AML with inv(3)(q21.3q26.2) or t(3;3)(q21.3;q26.2) <i>GATA2, MECOM</i>
	AML with BCR-ABL1 (<i>provisional</i>)
	AML with mutated <i>NPM1</i>
	AML with biallelic mutations of <i>CEBPA</i>
	AML with mutated <i>RUNX1</i> (<i>provisional</i>)
	megakaryoblastic AML with t(1;22)(p13.3;q13.3) <i>RBM15-MKL1</i>
	APL with <i>PML-RARA</i>
	ML with t(6;9)(p23;q34.1) <i>DEK-NUP214</i>
AML with myelodysplasia-related changes	

Therapy related myeloid neoplasms	
AML not otherwise specified (NOS)	AML with minimal differentiation
	AML without maturation
	AML with maturation
	Acute myelomonocytic leukaemia
	Acute monoblastic or monocytic leukaemia
	Acute erythroid leukaemia
	Pure erythroid leukaemia
	Acute megakaryoblastic leukaemia
Acute panmyelosis with myelofibrosis	

1.1.3 Prognostic factors

Classification of AML is highly linked to the prognosis and hence also the treatment of AML. The cytogenetic and molecular profile of the disease, which is also addressed by the WHO classification system, can be used to group AML patients into prognostic risk groups and is by far the most important parameter for determining prognosis. As in many other cancers, the accurate assessment of prognosis is the key to successful management of AML, as it helps clinicians make decisions between standard and more aggressive treatment options.¹²

Generally, increased age and poor physical condition are factors that are associated with poor prognosis. This is due to reduced tolerability of certain treatment options and other underlying health conditions. Prognosis has also been found to be worse in AML patients with prior hematological conditions or with AML related to prior treatments. In these groups of patients, complete remission is more difficult to achieve, and the overall survival rates are decreased.¹³

Although clinical factors affect prognosis substantially, a more detailed and accurate prognosis factor is obtained through the assessment of cytogenetic changes. Certain chromosomal rearrangements such as t(15;17) and t(8:21) without *c-KIT* mutation are indicators of better prognosis. In patients with such chromosomal rearrangements, overall

survival is significantly increased by 66% in patients aged under 60 years and by 33% in patients over 60 years old. On the other hand, *FLT3-ITD* and *TP53* mutations have been linked to poor prognosis.⁷

As can be seen from Table 2, the assessment of the cytogenetic profile and molecular abnormalities can further increase our understanding of AML on an individual level, enabling more precise diagnosis and treatment. In addition, these can help us develop more targeted therapies for improved therapeutic results.

Table 2. Cytogenetic profiles and molecular abnormalities grouped into prognostic risk group classifications of AML.⁷ These groupings are used to help decide on treatment plans and assess the prognosis.

Prognostic risk group	Cytogenetic profile and molecular abnormalities
Favourable	t(8:21)(q22;q22) without <i>c-KIT</i> mutation
	inv(16)(p13;1q22)
	t(15;17)(q22;q12)
	Mutated <i>NPM1</i> without <i>FLT3-ITD</i> mutation (cytogenetically normal (CN) AML)
	Mutated biallelic <i>CEBPA</i> (CN-AML)
Intermediate	t(8:21)(q22;q22) with mutated <i>c-KIT</i>
	t(9;11)(p22;q23)
	CN-AML other than those in other prognostic risk groups
	Cytogenetic abnormalities not included in other prognostic risk groups
Adverse	<i>TP53</i> mutation, regardless of cytogenetic profile
	CN-AML with <i>FLT3-ITD</i>
	CN-AML with <i>DNMT3A</i>
	CN-AML with <i>KMT2A-PTD</i>
	inv(3)(q21q26.2)
	t(6;9)(p23;q34)
	11q abnormalities other than t(9;11)
	-5 or del(5q)
	-7
Complex karyotype	

1.1.4 Treatment

1.1.4.1 Chemotherapy

Chemotherapy is a type of standardised cancer treatment that relies on the use of one or multiple anti-cancer drugs that inhibit mitosis or induce DNA damage in cells to result in apoptosis. In AML, chemotherapy treatment consists of two phases: induction and consolidation. Induction therapy is the first phase of treatment, which relies on the use of chemotherapy drugs in a short-lasting and intensive manner to eradicate leukemic cells from the blood and reduce the number of blasts in the bone marrow. In the consolidation phase, which takes place after recovery from the induction phase, chemotherapy drugs are administered to patients in cycles to remove the remaining leukaemia cells. Between cycles in the consolidation phase, patients have a period of rest to allow for recovery from the previous cycle of chemotherapy. In addition, for acute promyelocytic leukaemia (APL), post-consolidation chemotherapy can also be given as maintenance therapy using lower doses of chemotherapy drugs.^{14,15}

Drugs used for chemotherapy include antimetabolites, alkylating agents, topoisomerase inhibitors, antitumour antibiotics and anti-microtubule agents. For AML, most often a combination of cytarabine and an anthracycline drug are used. For example, cytarabine, being an antimetabolite, interferes with DNA synthesis in the S phase of the cell cycle. Anthracycline drugs on the other hand, including daunorubicin and idarubicin for example, interferes the activity of topoisomerase II. Issues related to the use of chemotherapy agents are most often caused by their effects also on healthy tissues due to their unspecific nature.¹⁵

Although chemotherapy is widely used and is often effective at inhibiting proliferation of malignant cells or even achieve complete remission, it is widely known for its toxicity and adverse effects. These include hair loss, nausea, loss of appetite, diarrhoea, fatigue, easy

bruising, and bleeding as well as an increased risk of infections due to effects on white blood cell counts. Despite of its adverse effects, chemotherapy remains an important tool in the fight against AML, with major advancements being made in developing its use together with more targeted therapies for example.¹⁶

1.1.4.2 Targeted drug therapies

Targeted therapies have been designed to target specific molecular mechanisms related to AML. As described in Section 1.1.1, AML surfaces with molecular abnormalities that can be used as targets to prevent proliferation of malignant cells.

In the fight against AML, a range of FLT3, IDH, BCL-2 and hedgehog signalling pathway inhibitors have been developed. Examples of FLT3 inhibitors used to treat AML are midostaurin and gilteritinib, which are both broad range tyrosine kinase inhibitors (TKIs) also targeting activated FLT3. In a phase 3 clinical trial, midostaurin has been shown to be effective at improving overall survivability when combined with induction chemotherapy.¹⁷ Moreover, uses of FLT3-targeting TKIs as maintenance therapy post-transplantation has shown promising results.¹⁸ However, studies on gilteritinib monotherapy in AML have shown less impressive results due to resistance accumulated due to resistance-causing mutations.¹⁹

Mutations of *IDH1* and *IDH2* interfere with normal blood cell maturation, hence playing a role in the development of AML. Ivosidenib, an *IDH1* inhibitor, can be used for AML patients who no longer respond to other treatments and as a first line treatment for patients who are ineligible for standard treatment. Enasidenib, which targets *IDH2*, can be used in patients that fit similar criteria to those receiving ivosidenib. Ivosidenib has recently been studied in *IDH1*-mutated patients ineligible for standard treatment with a median age of 76.5 years. In the trial, complete remission was achieved in over 30% of the patients, with 42.4% of the patients achieving complete remission with partial hematologic recovery.²⁰

The results are encouraging, as they give hope for making new discoveries in order to develop cures for elderly patients with a poor prognosis.

Venetoclax is a drug that has been recently approved for use in AML patients who are not suitable for chemotherapy due to high age or comorbidities. It targets the BCL-2 protein, which can enhance survival of leukaemia cells, leading to increased proliferation.²¹ A recent study conducted on patients previously untreated for AML compared a placebo group to a group of patients who were given azacitidine and venetoclax in 28-day cycles. Results showed that complete remission was achieved in more patients who received a combination of venetoclax and azacytidine, with 36.7% compared to 17.9% in the placebo group.²²

For APL specifically, all-trans retinoic acid (ATRA) is an effective targeted therapy that can lead to response rates of over 90%, although the response only last for 3 to 6 months. ATRA can also be used in combination with arsenic trioxide (ATO) are chemotherapy agents to induce an increased and more long-lasting response.²³

1.1.4.3 Stem cell transplant

Stem cell transplants, also known as bone marrow transplants, are a widely used treatment method for patients with AML. It is used to restore bone marrow function in patients who are given intensive chemotherapy, which damages the patient's own bone marrow and to eradicate remaining malignant cells through the graft-versus-leukaemia (GVL) effect.²⁴

Stem cell transplants can be used in AML patients through multiple ways. Allogeneic stem cell transplants, for example, make use of a donor's bone marrow that is transplanted to a patient. For an allogeneic transplant to be successful, the donor's tissue type must be closely matched with that of the patient. In addition to restoring the immune functions in a patient treated with high intensity chemotherapy, allogeneic transplants result in an effect

known as graft-versus-leukaemia, in which immune cells from the donor do not recognise leukemic cells as self, resulting in an attack. This can lead to further eradication of the remaining malignant cells from the body. However, allogeneic transplants do not come without costs. Graft-versus-host-disease (GVHD) is the most severe side effect resulted by the transplant, although milder adverse effects similar to those experienced during chemotherapy may occur. Due to the increased risk of severe side effects, allogeneic transplants are not given to older patients and to those whose general health condition is poor.²⁵

In patients who are ineligible for receiving an allogeneic stem cell transplant together with high intensity chemotherapy, a non-myeloablative transplant can be given. This involves leaving some of the patient's own bone marrow alive by using less intense chemotherapy methods and adding a donor's stem cells to achieve a GVL effect.²⁶

Although not used regularly, autologous stem cell transplants can be used in patients who have achieved complete remission after the first line of treatments and do not have a matched stem cell donor. In autologous transplants, the patient's own stem cells are removed from the bone marrow or blood, leukemic cells are removed, and cells are frozen prior to high-dose chemotherapy. The frozen stem cells are then retransplanted following chemotherapy. Autologous transplants are generally better tolerated by patients due to not experiencing tissue rejection, although GVL is not observed, which decreases the benefits of the transplant compared to allogeneic transplants. In addition, some leukemic cells may have escaped the purging process used to remove malignant cells from the stem cell masses, which can lead to a relapse.^{27,28}

Although stem cell transplants involve risks and can induce unpleasant side effects resulted in by graft-versus-host disease, they make it possible to eradicate cancerous cells with higher intensity chemotherapy. This can in turn lead to less residual malignant cells

remaining in the patient, allowing for decreased likelihood of relapse when monitored appropriately and combined with other therapeutic options.²⁹

1.1.4.4 Radiation therapy

Radiation therapy is not part of the standard treatment options for AML, although it is used as treatment in paediatric acute lymphoid leukaemia (ALL).³⁰ However, it is administered in rarer occasions where AML has spread from the bone marrow and blood to other parts of the body such as the brain and spine. In these cases, the use of more localised therapies is more effective, when compared to chemotherapy for example. However, interestingly, although radiation therapy is not considered a very useful tool against AML, it has been shown to increase the probability of developing AML, when given as treatment for other types of cancers.^{1,31}

1.1.4.5 Immunotherapy

The aim of immunotherapy in the context of cancer is to activate immune defence mechanisms to fight cancer while trying to leave healthy tissues unaffected. Currently, there are numerous clinical trials ongoing studying the potential of these therapies for treating both hematological and solid cancers. For AML, also a wide range of immunotherapy trials are underway, although so far only gemtuzumab ozogamicin (GO) has been approved for clinical use. Numerous strategies and targets can be utilised in designing novel immunotherapeutic therapies, leaving room for innovations in the future.³²

Antibody-based treatment options for AML aim to identify and target antigens specific to leukemic cells in AML patients to induce cancer cell death. Monoclonal antibodies take advantage of their ability to selectively target cancer cells to create cytotoxic effects, deliver drugs and boost the innate immune system. The use of monoclonal antibodies is highly dependent on the identification of AML specific antigens, a few of which have been

identified already. These include leukaemia-associated antigens such as CD33, CD47 and CD123. CD33, for example, has been found to be expressed in 85-90% of AML cases, giving rise to a promising therapeutic target.³³ However, it is worth noting that CD33 is also expressed in healthy myeloid cells, although in AML its expression is increased.³³ It is the target of GO, the first approved monoclonal antibody for the treatment of AML. In adults with *de novo* AML, GO has been shown to significantly improve the event-free survival when combined with daunorubicin and cytarabine chemotherapy.³⁴

As will be described in more detail in Section 1.2.2.3, NK cell dysfunction remains a major concern in AML patients, most notably after hematopoietic stem cell transplantation.³⁵ Bi- and tri-specific killer engager antibodies (BiKEs and TriKEs), propose a solution to this issue by augmenting NK cell function in patients with NK cell dysfunction by directing NK cells to target tumour antigens. For example, 1633 BiKE is specific to CD16 found on NK cell surface and CD33, which allows for the activation of NK cell cytotoxicity while avoiding MHC class I inhibition observed in AML cells.³⁶ Similar to 1633 BiKE, 161533 TriKE targets NK cell specific mechanisms to induce NK cell proliferation, survival and enhanced targeting of CD33⁺ AML cells, while offering slightly better outcomes than its BiKE alternative 1633. In addition to CD16 and CD33, the 161533 TriKE also targets IL-15, which has been shown to lead to enhanced NK cell function and proliferation.^{37,38}

Immune checkpoint inhibitors have been widely studied and several approved drugs exist on the market, most of which focus on solid tumours and lymphoma. Their functions are based on the inhibition of checkpoint receptors on the surface of immune cells, leading to their activation as the “off” signalling is reduced. More specifically, immune checkpoint inhibitors target for example CTLA-4 and PD-1 to induce increased T cell activation. In high-risk AML patients for example, nivolumab, a PD-1 inhibitor, following chemotherapy has been shown to enable a 12-month duration of complete remission at a 71% rate.³⁹

Adoptive cell therapies rely on the use of immune cells to kill cancer cells through immunological effects. Among these, chimeric antigen receptor (CAR) T cell therapy has been the most studied method with significant results being achieved in B cell malignancies for example.⁴⁰ Moreover, CAR T cells have been studied in combination with drug-based therapies through DSRT methods, highlighting the potentiating effects of SMAC mimetics in activating CAR T cells against malignant cells.⁴¹ In addition to CAR T cell therapies, NK cells-based therapy options have been suggested, which will be discussed later in Section 1.3.

To highlight the potential of combinatorial approaches from cancer treatment, studies show the efficacy of immunotherapy being enhanced by 20-30% when combined with conventional treatment options, including chemotherapy.⁴² This emphasises the importance of finding more effective combinatorial approaches to better utilise novel and more traditional therapy methods in the treatment of AML and other malignancies.

1.1.5 Methods to study acute myeloid leukaemia

In the study of AML, mouse models have been of great importance in the search for molecular mechanisms behind the disease. In addition, murine models have provided a platform to test a wide range of novel therapy options. Mouse models have, for example, been used to show that AML can be induced by radiation and chemicals.^{43,44} The development of transgenic mouse models has allowed the study of the effects of genetic mutations in genes related to AML. For example, the putative cellular targets of *MLL-AF9* in initiating AML have been thoroughly studied with the help of transgenic mouse models.⁴⁵ AML has also been studied in immune-compromised mice by modelling the disease by transferring patient-derived cells to animals. Through modelling AML in animals, it has been possible to study effects of different therapeutic approaches to target the malignancy, including the use of cytarabine and doxorubicin in *MLL-AF9* positive AML to reduce the residual disease burden.⁴⁶ Although murine models have been shown to be relatively

effective modelling tools to study cancers such as AML, they still fail to faithfully model the progress of the disease in humans. However, advances in biotechnology, including next generation sequencing methods, help in creating more reliable mouse models.⁴⁷

The *in vitro* study of patient-derived cell lines remains a key strategy in the study of AML and related therapy innovations. For AML, many well-defined *in vitro* models allow for the study of specific genetic mutations and other molecular abnormalities in cells that have been genetically characterised. These numerous AML models can be used for example to study effects of drugs on a cellular level and help at creating reproducible scientific experiments as the results are not specific to a patient, but rather a standardised model.

The effect of drugs and NK cells of three widely used *in vitro* AML models, MOLM-14, THP-1 and HEL will be thoroughly investigated through methods described in Section 3. The MOLM-14 cell line is an adult acute myeloid leukaemia cell line that was isolated from a 20-year-old Japanese male. It has an *MLL-AF9* (HGNC 7132) gene fusion in addition to an internal tandem duplication (ITD) of the *FLT3* gene (HGNC 3765).⁴⁸ The THP-1 cell line is an acute monocytic leukaemia cell line that was isolated from a 1-year-old male in Japan and has *KMT2A-MLLT3* gene fusion (HGNC 7136) in addition to mutations in *TP53* and *NRAS*.⁴⁹ HEL is a rarer form of AML with erythroid proliferation including mutations in *JAK2* and *TP53* genes.⁵⁰

1.2 Immunology and cancer

1.2.1 The human immune system

The human immune system has evolved to protect humans from a universe of constantly evolving pathogenic microbes, in addition to being able to eliminate toxic and allergenic substances. It comprises of the innate and adaptive immune systems, which support each other and work together to defend from foreign substances and pathogens.

The innate immune system can be considered as a series of hard-wired responses that are encoded in the human germ line. Its functions are based on recognising molecular patterns that are foreign to the human body, leading to a range of responses to eliminate the foreign structures. The innate immune system often acts as the first line of defence. However, it is less specific and does not result in as strong effects as the adaptive part of our immune system. Cells of the innate immune system include antigen independent cells such as natural killer (NK) cells, macrophages, neutrophils, mast cells, dendritic cells, basophils, and eosinophils.⁵¹

Often followed by innate immune system responses, adaptive immune system responses activate for more specific targeting of foreign structures. The adaptive immune system comprises of T and B cells, which base their function on the ability to target pathogens through somatic rearrangements of gene elements to assemble antigen-binding molecules. These antigens can bind to unique foreign structures with significant specificity, leading to highly effective target-specific responses. In addition, a key feature of the adaptive immune system is the ability to memorise target-specific responses through long-lived cells that persist in a dormant state. Upon re-exposure to an already encountered pathogen, memory cells can activate and rapidly re-express effector functions for faster pathogen elimination.⁵²

1.2.2 Role of immune system in cancer

The immune system has been shown to play a role in cancer, both in preventing it and leading to its causes. Inflammation is nowadays considered as one of the hallmarks of cancer, with at least 25% of cancers being associated with it.⁵³ Cancer-associated inflammation plays a role in different stages of tumorigenesis, with effects leading to cancer cell proliferation, genomic instability, and epigenetic modifications for example.⁵⁴ Studies have revealed the essential role of immune cells in cancer-related inflammation, including the role of macrophages, NK cells and T cells. During early stages of cancer, NK cells and

CD8⁺ T cells have been shown to eliminate immunogenic cancer cells.⁵⁵ However, as the cancer progresses, malignant cells develop ways to avoid the immune system, leading to faster proliferation and uncontrolled growth.⁵⁶

1.2.2 Natural killer cells

Natural killer (NK) cells are a lymphocyte population of the innate immune system that control infections and tumours by limiting their activity and subsequent damage to the body. As their name suggests, NK cells are naturally cytotoxic, as they do not require prior antigen exposure to mediate anti-pathogenic and anti-cancer effects, unlike T cells for example. In humans, NK cells represent 5 to 20% of the circulating lymphocyte population.⁵⁷ In addition to their unique functions, NK cell can be characterised by specific surface antigens. These include CD16, the activating Fc receptor and CD56.⁵⁸ Although being part of the innate immune system, NK cells have also been shown to have memory-like features upon activation with cytokines.⁵⁹

1.2.2.1 Development and maturation

NK cells develop mostly in the bone marrow, although evidence shows that they can also develop and mature in secondary lymphoid tissues, such as lymph nodes, although some uncertainty remains around the primary origin of NK cells and their maturation.⁶⁰ The development of NK cells begins with hematopoietic stem cells (HSCs), which differentiate into lymphoid-primed multipotential progenitor (LMPP) cells. The cluster of differentiation (CD) markers, namely CD7, CD10, CD38 and CD127, indicate transition of LMPPs to common lymphoid progenitors (CLPs). CLPs have the potential to differentiate into different innate lymphoid cells, pro-B and pro-T cells as well as NK cell progenitors (NKPs). The transition of CLPs into NK cell progenitors is indicated by the appearance of CD122, which is followed by the expression of CD56 which marks the final stage of NK cell maturation from NKPs to mature NK cells. The last stage of NK cell maturation occurs as

CD56^{bright} expression is downregulated to become CD56^{dim}, which become the dominating population of NK cells, making up over 90% of NK cells. Some evidence also argues that NKPs could directly mature into the CD56^{dim} cell population, however some questions remain unclear.⁶¹

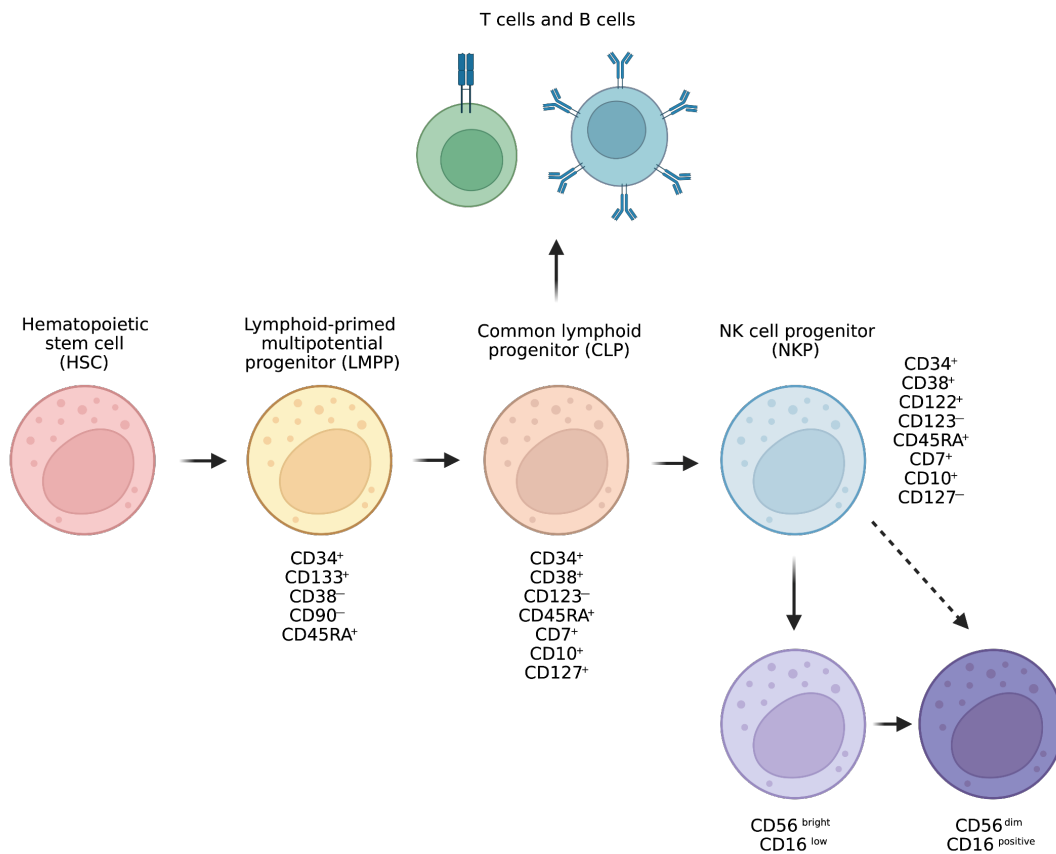


Figure 2. Mechanism of NK cell development and maturation with distinct markers related to distinct steps along the process.⁶¹ The development of NK cells starts from hematopoietic stem cells and through a set of progenitors, leads to NK cell progenitors that mature into NK cells (bottom right).

1.2.2.2 Effector functions

The effector function of NK cells relies on direct and in-direct mechanisms of action which NK cells use to clear pathogens and cancer cells from the body. Direct killing effects are based on cytotoxicity, meaning the use of cytotoxic proteins such as perforin and granzymes, stored within secretory lysosomes, to lyse malignant and infected cells. When released in the target cells, perforin polymerises, leading to pores that allow the entry of granzymes into the cell. This in turn activates caspase molecules, resulting in the induction

of apoptosis of the target cell. In addition, NK cells mediate killing of target cells through death receptor-induced apoptosis of target cells. NK cells express receptor ligands such as TNF and TRAIL, which bind to corresponding receptors on the target cell surface. The engagement of such ligands with the death receptor leads to apoptosis of the target cell through conformational changes in the death receptor and adaptor protein recruitment.⁶²⁻⁶⁴ In-direct approaches NK cells use to kill target cells are the production of inflammatory cytokines such as interferon- γ (IFN- γ), interleukin-10 (IL-10) and tumour necrosis factor- α (TNF- α), which can activate other parts of the immune system such as dendritic cells and macrophages.^{65,66}

NK cells are activated according to a "missing-self" hypothesis, that was first suggested by Karre et al. in 1986. This hypothesis suggests that NK cell activation is based on NK cell receptors' ability to recognize cells that fail to express major histocompatibility complex (MHC) class I molecules on their surface.⁶⁷ Therefore, unlike cytotoxic T cells, NK cells do not require prior antigen exposure to mediate anti-tumour effects for example. In humans, the receptors on NK cells responsible for the recognition of MHC class I molecules belong mostly to the killer immunoglobulin-like receptor (KIR) family.⁶⁸

Interleukins have been shown to have important effects on NK cell function, ranging from their role in NK cell maturation to potentiating cytotoxicity.⁶⁹ The role of interleukin (IL)-2 and IL-15 in "priming" NK cells has been well established. IL-2 can for example activate NK cells *in vitro* and can enhance responses to infections *in vivo*.^{70,71} IL-15 on the other hand, has been shown to sensitize NK cells to secondary stimuli, also referred to as "priming", which results in enhanced activation.⁷² In addition to IL-2 and IL-15, other interleukins such as IL-12, IL-18 and IL-21 have been demonstrated to strengthen NK cell cytotoxicity. IL-12, for example, have been linked with NK cell stimulating capabilities inducing higher levels of TNF- α secretion by NK cells.⁷³ A recent report has also given a more generalized description of IL-12, IL-15, and IL-18 functionality in NK cells, demonstrating that NK cells

show enhanced functionality after pre-activation with these interleukins.⁷⁴ Finally, IL-21, involved in the expression of IFN- γ through JAK1 and JAK3 activation, has been shown to promote rapid differentiation and expansion of CD16⁺CD56⁺ NK cells.⁷⁵

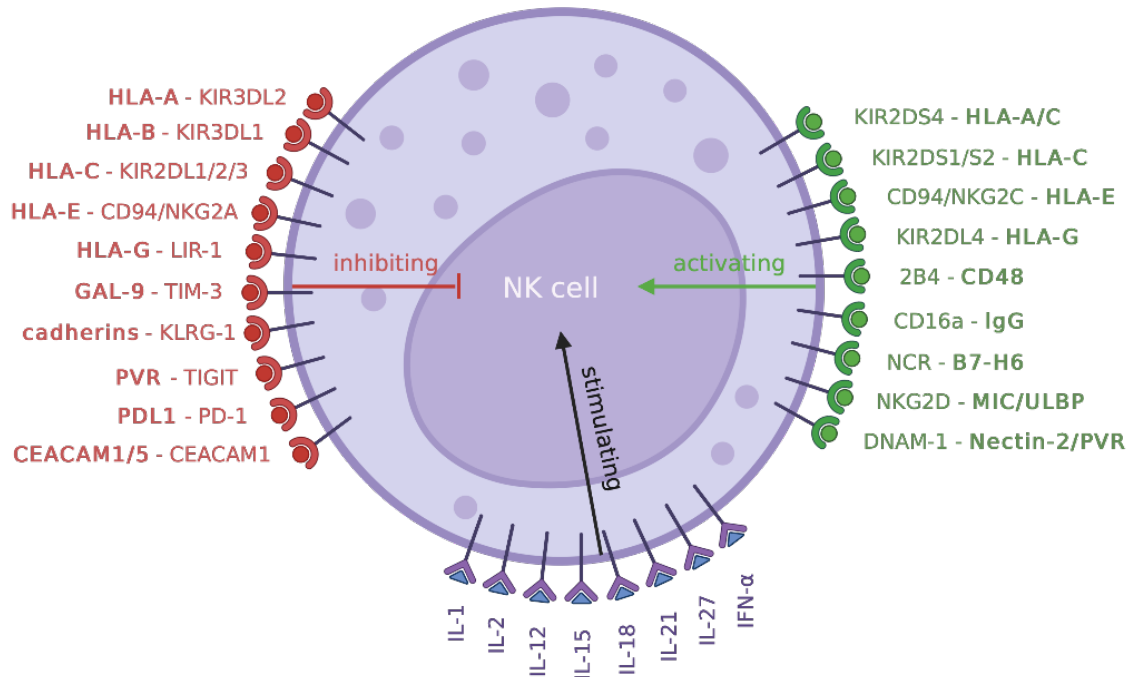


Figure 3. NK cell receptor profile and their functions on NK cell activity and cytotoxicity.⁷⁶ Receptors and their respective ligands (in bold) lead to either activating (green), inhibiting (red) or stimulating effects in the NK cell.

1.2.2.3 Role in acute myeloid leukaemia

NK cells have a wide range of function in human health and disease through their immune functions. In AML and in cancers in general, NK cells can act in destroying malignant cells through their ability to distinguish “non-self” cells that lack MHC class I molecules on the cells’ surface.⁵⁵ In addition, NK cells can target cancer cells through the release of cytokines.^{65,66} Moreover, NK cells have been demonstrated to have the ability to kill tumour cells by antibody-dependent cell-mediated cytotoxicity (ADCC), a feature mediated by the IgG Fc receptor CD16.⁷⁷

In AML, leukemic cells can escape NK cell recognition, leading to uncontrolled proliferation. In AML patients, NK cell abnormalities in inhibitory and activating receptors can lead to decreased NK cell function.⁷⁸ In addition to defects in NK cells, AML cells can also have defective ligand expression on the cell surface, that would otherwise interact with NK cells. For example, the low expression of NKG2DL ligands can render leukemic cells resistant to NK cell mediated cytotoxicity.⁷⁹ Furthermore, the effectiveness of NK cells to target malignant cells can be limited by interactions with other cells and biological compounds in the tumour microenvironment, including interactions with regulatory T cells, transforming growth factor (TGF)- β as well as myeloid-derived suppressor cells.⁸⁰

1.3 NK cell-based immunotherapy for AML

NK cell-based immunotherapy represents one of the emerging immunotherapy strategies to target various cancers. In the recent years, our understanding about the NK cell immunobiology and function in cancer has led to advancements in the development of novel treatment options taking advantage of the cytotoxic potential of NK cells against hematological malignancies. Newly developed strategies to utilise NK cells in managing hematological malignancies include adoptive NK cell transfer, chimeric antigen-receptor (CAR)-modified NK cells, cytokines, antibodies, and drug-based therapies.⁸¹ However, the use of these approaches in the management of AML remains in its early steps and much remains to be discovered.

Adoptive NK cell transfer has become a field of great interest in cancer immunotherapy due to promising results observed in allogeneic hematopoietic cell transplantation (HCT), where NK cells have shown beneficial effects due to potential alloreactivity. NK cell alloreactivity was described in more detail initially in 1999, as different donor-recipient pairs were studied in HCT receiving patients and KIR epitopes were correlated with HLA haplotype mismatch. This research suggested that NK cell alloreactivity is triggered by the mismatch between human leukocyte antigen (HLA) class I molecules on the recipient's cells

and KIRs on the donor's NK cells. The activation of NK cells resulted by alloreactions can effectively kill leukemic cells in AML through GVL effects for example.⁸²

Further to promising NK cell-based effects in HCT studies, NK cells derived from donors and expanded *ex vivo* have been transferred to AML patients in addition to HCT. NK cells can be transferred to patients after being isolated donor leukapheresis using NK cell-specific magnetic cell sorting (MACS) and expansion using cell culture methods including interleukin stimulation. A phase I study using IL-15 and IL-23 stimulated NK cells has shown lowered leukaemia progression in patients receiving patient-derived NK cells after HCT, when compared to patients receiving HCT only.⁸³ However, some drawbacks have been experienced in similar trials with cytokine release syndrome related toxicity being observed in patients receiving early NK cell transfers 6 and 9 days post-HCT.⁸⁴

Clinical trials have also investigated the use of adoptive NK cell transfer independent of HCT, the first one of which was reported in 2005 involving *in vivo* expansion of NK cells after adoptive transfer. In the study, IL-2 was used subcutaneously to induce NK cell proliferation *in vivo* in combination with chemotherapy-based treatments to activate NK cells against AML.⁸⁵ This method has been later developed, including the addition of selective NK cell purification using CD3 depletion and CD56 enrichment in addition to lower doses of IL-2 administered to reduce toxicity. Adoptive NK cell transfer in combination with chemotherapy may be an effective method of consolidation therapy, with improved prognosis for AML patients achieving complete remission as long-term recurrence is decreased, although statistical significance has not been demonstrated.⁸⁶

Increasing the number of alloreactive NK cells has been associated with better outcomes in AML patients⁸⁷ for which finding different ways to maximize the NK cell-induced alloreaction is considered important. NK cell expansions and their functionality can be, for example, significantly enhanced by co-culturing NK cells with IL-2 and IL-15 or feeding NK

cells with K562 cell line-derived feeder cells. These methods make it possible to produce larger quantities of NK cells *ex vivo* and allow them to have better functionality at targeting malignant cells.^{88,89} In addition to finding ways to meet quantity and functional demands for NK cells in AML treatment, alternative sources for such cells have been investigated to provide ways to better incorporate NK cells into clinical use. For example, the generation of NK cells from CD34 positive hematopoietic stem and progenitor cells (HSPCs) isolated from cryopreserved umbilical cord blood (UCB) has been shown to be feasible.⁹⁰ Their use in elderly AML patients has also shown to be an effective way to promote NK cell expansion and maturation *in vivo* as well as being effective at reducing minimal residual disease.⁹¹ Different methods of producing and storing expanded NK cells for later use in adoptive NK cell transfers allows for an “off-the-shelf” product that can have significant benefits for AML patients due to lowered costs, improved therapeutic potential and immediate application. Currently, numerous clinical trials are ongoing to assess the potential of using NK cell transfers as treatment for AML, also in combination with drug-based therapies.⁷⁶

In addition to adoptive NK cell transfer-based therapies, NK cells can be genetically modified to target hematological malignancies. This can be done using CAR-modified NK cells, where NK cells are modified similar to CAR-T cells in order to augment cytotoxicity and specificity of NK cells. CAR-NK therapies are being considered as alternatives to CAR-T therapy due to their lower manufacturing costs and reduced toxicity.⁹² However, it is worth noting that AML is relatively difficult to target as it shares some phenotypic markers with hematopoietic stem cells.⁹³ So far, AML-related breakthroughs in the use of CAR-NK therapies remain to be discovered, although advancements in lessons learned from their use in other cancers may help in developing the method further.

1.4 Drug sensitivity and resistance testing

Drug sensitivity and resistance testing (DSRT) has become a widely used tool as a high throughput assessment method of drug compounds against a variety of cancers and to

evaluate pharmacogenomic interactions in these malignancies. They have also paved the way for personalised medicine, allowing clinicians to find optimal doses and compounds to be used for improved effectiveness of the treatment in addition to decreased adverse effects. Although DSRT methods have been increasingly used for a variety of clinical and scientific needs, its potential to be used as a platform to investigate the synergy between immunotherapy methods and drug-based therapies has only scratched the surface.^{41,94}

Individualised systems medicine (ISM) approaches have been investigated in the treatment for AML, with focus on developing *ex vivo* drug sensitivity platforms from which findings can directly be translated back to clinical use.⁹⁴ The platform was demonstrated to be efficient at screening for effective treatment options for patients, with hopes to simultaneously de-risking the use of investigational drugs clinical testing. This study laid a firm foundation for DSRT testing combined with molecular profiling in order to fully understand drug sensitivity and resistance mechanisms, in addition to better understanding the biology behind malignancies.⁹⁴

Drug platforms used in DSRT experiments related to this study follow the design and manufacturing process described by the Finnish Institute for Molecular Medicine (FIMM) High Throughput Biomedicine Unit, which has a validated method of creating large scale drug libraries for uses in DSRT experiments.⁹⁵ The FIMM FO5A screening platform provides a high throughput model to study responses of standardised cancer cell lines and primary cells to 528 approved and investigational oncology drugs at 5 different concentrations.⁹⁵

Evaluating the effect of drugs and immunotherapy methods on cancer cells *in vitro* requires high throughput methods of measuring cell viability and proliferation for obtaining accurate quantitative data. One widely used method is the expressed luciferase viability assay (ELVA), which relies on luciferase expression of target cells for detection through luminescence measurements. Like other endogenous enzymes, luciferase is rapidly

degraded after cell death, making it a useful tool for detecting cell viability. Its bioluminescent abilities allow for luminescence measurements to be used as a tool for its detection, which can be directly related to the number of viable cells.^{96,97} The use of luciferase luminescence measurement requires, however, transduction of the cell line under investigation with luciferase constructs, which adds extra steps to the overall experimental plan.

In addition to luciferase-based viability assessment methods, other techniques evaluating the viability of cells and apoptosis exist. For example, caspase-based analytical methods allow for evaluation of apoptotic mechanisms in cells of interest.⁹⁸ In addition, flow cytometry-based methods of viability assessment could be utilised.⁹⁹ As cell viability assays only give qualitative information on drugs' ability to kill target cells or enhance proliferation, other methods such as single cell RNA sequencing can be used for determining more detailed effects induced by drugs.

Future approaches for high throughput DSRT include computational models, which would allow for testing and optimising drug compounds to different biological targets *in silico*. This minimizes the need for expensive laboratory experiments as well as speeds up the time it takes for obtaining results, which may turn out crucial in the study of acute malignancies in clinical settings.

1.5 Combinatorial approaches to improve immunotherapy

Due to the complexity of cancers and their varying pathophysiology, effective cancer treatments are rather a combination of targeted strategies to counteract the malignancy than one universal miracle therapy that would solve the puzzle. This idea also applies to immunotherapy methods, to which combining other more conventional treatment options may prove beneficial for improved anti-cancer effects.

Chemotherapy, a widely used and effective cancer treatment also used to treat AML, can target biological mechanisms that can help potentiate immune responses towards cancer. They can, for example, inhibit immunosuppressive pathways developed by mutated cancer cells or increase immunogenicity of malignant cells for more effective immunological responses. Although these effects can occur, they are rarely the primary mode of action of chemotherapy drugs.¹⁴ Therefore, more in-depth studies into their potential as immunotherapy potentiators are increasingly more important with immunotherapy options being introduced for clinical use. Studies focusing on discovering chemotherapy drug-related effects on the immune system have reported findings that support their use in combination with immunotherapy methods. Cyclophosphamide chemotherapy has been associated with restoration of NK and T cell function in patients with advanced cancer.¹⁰⁰ In addition, 5-fluorouracil has been shown to promote NK cell recruitment in murine models of pancreatic carcinoma.¹⁰¹ NK cell recruitment in human cancers has also been shown to be a secondary effect of gemcitabine.¹⁰²

Similar to chemotherapeutic agents, targeted anti-cancer drugs have also shown to affect the immune system. In relation to NK cells, imatinib has been shown to favour NK cell expansion in chronic myeloid leukaemia (CML) patients, in addition to IFN- γ production activation in NK cells in patients suffering from gastrointestinal stromal tumours.¹⁰³ Furthermore, dasatinib has been shown to result in effect similar to those seen with imatinib in CML patients.¹⁰⁴ NK cell function has also been shown to be affected by JAK inhibitors, which block the effect of IFN- γ , resulting decreased MHC class I molecule expression on cells' surface, leading to stronger activation of NK cells.¹⁰⁵ However, not only potentiating effects have been reported. For example, MAPK inhibitors have been shown to upregulate the expression of MHC class I molecules, which lead to increased antigenicity and hence decreased NK cell cytotoxicity.¹⁰⁶

Interestingly, although specific underlying biological mechanisms of individual oncology drugs have been investigated, relatively little is known about combining NK cells with drug-based treatment options using high throughput methods. In addition, drugs have primarily been studied with models of their intended cancer target, without evaluating their potential in treating myeloid malignancies such as AML. By combining high throughput DSRT methods with NK cell co-cultures, we hope to find clues to better understand the potential of NK cells in targeting AML.

2. Aims of the Thesis

In this thesis and in the larger project connected to it, we aim to evaluate the potential of approved and emerging investigational oncology drugs to enhance NK cell-based immunotherapy in the treatment of AML. In addition, we hope to increase our biological understanding of underlying cellular mechanisms behind NK cell function in its capabilities to kill tumorous cells. Furthermore, we hope to find drug compounds and targets that may adversely affect the function of NK cells so that in the future, if NK cells are made available in the oncology clinics, these compounds could be avoided in conjunction with NK cell immunotherapy. Finally, our aim is to discover drug compounds that sensitize cancer cells to immune cell-mediated apoptosis and finding compounds that synergize with NK cells to induce strong cytotoxic effects.

3. Materials and methods

3.1 Cell culture related methods

3.1.1 Cell lines

All cancer cell lines were obtained from commercially available sources, including also the Finnish Red Cross' Blood Service. Buffy coats used to obtain NK cells were received from the Finnish Red Cross, where samples were taken from healthy donors with whom necessary agreements have been signed for the use of their samples in research. In addition, for NK cells used in single-cell sequencing experiments, buffy coats from donors with additional agreements for their genetic material to be used and analysed for research purposes were obtained from the Finnish Biobank.

3.1.2 Cell culture

Cell culture media, later referred to as R10, was prepared beforehand by adding 5 mL of penicillin-streptomycin (10,000 $\mu\text{L}/\text{mL}$ penicillin, 10,000 $\mu\text{L}/\text{mL}$ streptomycin, Lonza), 5 mL L-glutamine (200 mM in 0,85% NaCl solution, Lonza) and 57 mL heat inactivated FBS (Gibco) to 500 mL of RPMI-1640 cell culture media (without L-glutamine, Lonza). R10 media was used in culturing cancer cell lines, where cells were kept at approximately 0.50×10^6 cells/mL concentration.

NK cells were cultured in cell culture media containing IL-2, later referred to as NKEM. NKEM was prepared by adding IL-2 (10 $\mu\text{g}/\text{mL}$) 1 μL to each mL of R10 to obtain a 10 $\mu\text{g}/\text{mL}$ IL-2 concentration.

3.1.3 NK cell isolation and expansion

3.1.3.1 Irradiating K562 cells

10.0×10^6 K562 CSTX002 cells obtained from Kiadis Pharma were thawed in 13 mL R10 and a pellet of cells was recovered after centrifugation at 300g for 5 mins. The media was removed, and cells were washed with 12 mL PBS, following centrifugation at 300g for 5 mins. After washing, PBS was removed, and cells were resuspended in R10 to obtain a concentration of 5.0×10^5 cells/mL in a T75 (with filter, Greiner) flask.

Cells were kept in culture for 14 days, during which they were passaged every 3 days. At the end of the 14 day culture, 2.0×10^9 cells were collected and prepared for irradiation by changing the media and transferring to two T75 flask at 10.0×10^6 cells/mL concentration with 100 mL of cell suspension in each flask. Cells were then placed into an OB29/4 (Cs-137 isotope, Braunschweig, Germany) gamma irradiator and given a 100 Gy dose of radiation by irradiating them for 5078 s. Dose calculations can be found from Supplementary Materials, Equation 1.

3.1.3.2 NK cell expansion from buffy coat

A buffy coat was obtained through The Finnish Red Cross and taken from a healthy donor through leukapheresis. To start the expansion, the buffy coat was placed in 50 mL Falcon tubes and diluted in a 1:1 ratio with PBS in sterile conditions. After dilution, 30 mL of the diluted buffy coat was layered on top of 20 mL of Ficoll-Paque solution (GE Healthcare) following centrifugation for 20 mins at 300g. Once layered, peripheral blood mononuclear cells (PBMCs) were recovered from the plasma interface using a glass pipette. The recovered PBMCs were then washed three times with PBS and centrifuged each time for 5 mins at 300g. Once washed, cells were counted using a Bio-Rad automated cell counter.

The NK cell expansion was then started (day 0) by seeding 5.0×10^6 of PBMCs with 10.0×10^6 irradiated K562 CSTX002 cells in 40 mL of NKEM in a T75 cell culture flask, which was placed upright in an incubator set to 37°C and 5% CO₂. On days 3 and 5 of the protocol, cells were recovered by centrifuging the suspension for 5 mins at 300g. Half of the supernatant was removed and replaced with fresh R10, following the addition of 10 ng/mL of IL-2. On day 7 of the expansion protocol, NK cells were counted and an equal number of irradiated CSTX002 cells were added together with NKEM in order to obtain a 2.5×10^5 total cells/mL concentration. On days 10 and 12, the entire media was changed to fresh NKEM and cell suspensions were diluted to 5.0×10^5 cells/mL. On day 14, the expansion was finished by purifying the cell suspension and separating NK cells.

NK cells were purified from the expanded PBMCs using a Miltenyi NK cell isolation kit (Miltenyi Biotec, catalogue number 130-092-657). 50 million PBMC cells were first centrifuged for 5 mins at 300 g and the supernatant was removed. 200 µL of a buffer solution containing PBS with 2 mM EDTA and 0.5% BSA was added to tube and the cells were resuspended in it. Into the resuspended cell suspension, 50 µL of NK Cell Biotin-Antibody Cocktail was added and carefully mixed, following a 5 min incubation at 4°C. After incubation, 150 µL of the buffer solution and 100 µL of NK Cell MicroBead Cocktail were added and carefully mixed, following a 10 min incubation at 4°C. An LS column (Miltenyi Biotec) was placed in a MACS Separator (Miltenyi Biotec), which was rinsed with 3 mL of buffer solution. The cell suspension was applied onto the column and the flow-through was collected, leading to other cells being left into the column. The column was washed with 2 mL of buffer and the effluent was combined with the first flow-through. Collected cells were counted and checked for purity.

3.1.3.3 NK cell analysis with flow cytometry

Samples containing 10.0×10^6 cells of the NK cell expansion were frozen on day 0 of expansion and on day 14 after isolation. On the day of flow cytometry analysis, both

samples were thawed in 14 mL of PBS containing 2 mM EDTA and 0.5% BSA. After thawing, cell suspensions were centrifuged at 300g for 5 mins and supernatant was discarded. Cells were counted and viabilities were recorded. The cell suspensions were diluted to obtain a cell concentration of 10.0×10^6 cells/mL using PBS.

A master mix of markers was prepared by combining 60 μ L CD3 PerCP-Cy5.5, 24 μ L CD 45 APC-H7, 24 μ L CD8 BV510, 60 μ L CD56 BV421 and 24 μ L PBS. After combining the markers, the mixture was vortexed and 9,5 μ L of the master mix was pipetted into labelled FACS tubes according to Tables 2 and 3. Following the same table, other markers were added to tubes. To tubes labelled 5, only 2 μ L CD3 APH-H7, 2 μ L CD56 BV510, 5 μ L CD57 BV421, 5 μ L PerCP-Cy5.5 CD19 and 5 μ L PerCP-Cy5.5 CD14 were added. Tubes labelled 8 and 9 were left without markers.

100 μ L of the NK cell suspensions were added to tubes with different marker contents and the contents were allowed to incubate for 15 mins at room temperature. After incubation, 1 mL of PBS was added to all tubes which were then centrifuged for 5 mins at 300g. Tubes 5 and 9 were set aside and 100 μ L of 2% PFA was added following a 15 min incubation at room temperature. 100 μ L of PBS was added to all other tubes, which were then vortexed, covered with aluminium foil and left in room temperature.

After 15 mins of incubation, 1 mL of PBS was added to tubes 5 and 9, which were then centrifuged for 5 mins at 300 g. Cells in tubes 5 and 9 were then permeabilized by adding 100 μ L of 0.05% Triton-X in PBS and incubating the samples for 15 mins at room temperature. Samples were then washed by adding 2 mL of PBS and centrifuging for 5 mins at 300 g, after which the supernatant was removed, and the procedure repeated another time. To tube 5, 2 μ L FITC Fc ϵ R1gamma, 3 μ L APC Syk, 3 μ L PLZF PeCy7 and 3 μ L EAT2 FITC were added. Both tubes 5 and 9 were then left to incubate for 30 mins at room temperature in a dark box. After incubation, 1 mL of PBS was added to tubes and

they were centrifuged for 5 mins at 300g, after which the supernatant was removed. Following this, 180 μ L of PBS was added and samples were vortexed, covered with aluminium foil and left in room temperature.

After the preparation of all samples, they were analysed using the FACSVerse (BD Biosciences) flow cytometer with pre-set parameters. The data was then interpreted to verify the purity of NK cells.

3.1.4 Transducing cell lines with luciferase constructs

All cell lines used in the DSRT experiments were transduced to express luciferase for viability measurements. MOLM-14 and THP-1 cells were transduced with pLenti PGK V5-LUC Neo lentivirus (Addgene, luc-neo) prior to being used in this study. Specifically for this project, the HEL cell line was transduced using EF1a-Luciferase (firefly)-2A-GFP (puro) lentivirus (Amsbio, LVP437). The general protocol for both viruses is the same, however differences in the number of cells used in the transduction differs between lentiviruses.

Cells were first thawed 6 days prior to starting the transduction experiment and passaged once on day 3 after thawing. Cell suspensions were then moved to a BSL2 facility. For cell lines transduced using LUC Neo, 1.50×10^6 cells were centrifuged, the supernatant was removed and replaced by 400 μ L R10 in which cells were resuspended. 200 μ L of the cell suspension was placed in two separate wells of a 48-well flat-bottom plate (Corning). To one (control well), 50 μ L of R10 and 0,25 μ L polybrene (Sigma-Aldrich, 8 mg/mL) were added. To the other well, 50 μ L of concentrated (175x) luc-neo virus suspension and 0,25 μ L polybrene were added.

For cell lines transduced using LVP437 virus, 0.40×10^5 cells were centrifuged, the supernatant was removed and replaced by 100 μ L R10 in which cells were resuspended. 50 μ L of the cell suspension was placed in two separate wells of a 96-well flat-bottom plate.

To one (control well), 50 μL of R10 and 0.10 μL polybrene (Sigma-Aldrich, 8 mg/mL) were added. To the other well, 50 μL of LVP437 virus suspension and 0.10 μL polybrene were added.

Independent of the virus used, cell-containing plates were centrifuged for 2h at 800g (Multifuge 3SR+, Thermo Scientific). Following centrifugation, the supernatant was aspirated, and cells were moved resuspended in media and transferred to new plates. For transductions involving 750,000 cells/well, the cells were resuspended in 1 mL of R10 and moved to 12-well plates. For cells transduced using LVP437 virus, cells were resuspended in 100 μL R10 and moved to a 96-well plate (Corning).

Cells were then cultured for 14 days, with media change after every 3 days. On the 13th day of cell culture after transduction, the supernatant was removed after centrifugation at 300g for 5 mins, following 2 washes with PBS. Cells were then resuspended back in appropriate amount of R10 to obtain a 1.50×10^6 cells/mL concentration. On the 14th day after transduction, cell suspensions were centrifuged and 1 mL of supernatant was set aside for replication competent virus (RCV) testing, which was performed by the Biomedicum Virus Core. Once cleared by the RCV test, the cell suspensions were moved to a BSL1-level laboratory facility, tested for luciferase and frozen.

3.1.5 Selection of transduced cell lines – THP-1 and MOLM-14

Clones that were successfully transduced were first tested for luciferase levels by diluting the cell suspension to 0.80×10^6 cells/mL concentration and then pipetting 25 μL of the suspension into a row of wells of a sterile 384 well plate. The samples were then incubated at 37°C for 24h, after which 25 μL of ONE-Glo™ reagent was added and the luciferase levels were measured according to the method described in Section 3.2.2.3. In the case of MOLM-14 and THP-1 cell lines, the luciferase level measured for 20,000 cells after 24h of incubation was 600 or over, meaning that the cells can be used in the drug screenings

without the need for further sorting. However, in the case of the HEL cell line, the luciferase levels were not high enough, requiring further refinements that are described in the next section.

3.1.6 Post-transduction single cell sorting of HEL cell line

The HEL cell line was thawed 6 days prior to the sorting and passaged once to obtain enough viable cells for the experiment. Before the sorting, the cell culture media was changed to fresh R10 and cells were diluted to 2.0×10^6 cells/mL concentration. Cells were placed in a 15 mL Falcon tube (Corning), placed on ice and transported to the cell sorting facility. To sort the cells, a Sony SH800S cell sorter was used. The sorter was set to pick single cells at high GFP levels and place them into wells of a 96 well round-bottom plate (Corning), where one cell was placed in each well containing 100 μ L of R10.

Single cell sorted cells of the HEL cell line were let to grow in a 96 well round-bottom plate containing 100 μ L R10 for 10 days. The wells were then checked under a microscope to see which cells had started to divide and to check for bacterial infection. Those clones of the HEL cell line were selected which had started to grow efficiently and showed no bacterial infection in the form of a cloudy microscope image. Selected clones were suspended in their culture media and moved to a 48 well plate to the wells of which 100 μ L of R10 was added. Cells were allowed to grow for 3 days, after which 100 μ L of media was removed from each well and another 100 μ L of fresh R10 was added. As more cells were grown, the clones were moved to larger well plates and more R10 was added.

After 21 days of culture and 7 passages, 8 clones of 20,000 cells/well were plated onto a 384 well plate (low flange, Corning) and suspended in 25 μ L of R10 media. These clones were placed in culture for 24 h to later check for luciferase levels. After 24h of incubation, the HEL clones were tested for luciferase levels according to the method described in Section 3.2.2.3. Out of all the clones tested, the HEL D8 clone was selected due to its high

viability and high luciferase level of approximately 6000 compared to 3000 of the second-best clone.

3.1.7 Freezing and thawing

Cells were frozen by suspending cells into cold FBS containing 10% DMSO and placing 1 mL of the cell suspension into cryotubes. Cryotubes were then placed in a freezer set to -80°C for a day, after which they were moved to a -150°C cryogenic freezer for long-time storage.

For thawing cells, 12 mL of R10 was pre-heated to 37°C in a 15 mL Falcon tube. Cells were taken up from the cryogenic freezer (37°C) and placed in a water bath at 37°C for 1 min. The cryogenic tubes containing the cells were then moved to room temperature and allowed to thaw for a further 2 mins. Once all the content was in a liquid state, cells in the freezing media were taken from the cryogenic tubes and added to Falcon tube containing R10. The contents of the tube were then carefully mixed by turning the tube upside down and centrifuged for 5 mins at 300g (Universal 320, Hettich). After centrifugation, the media was removed using suction and the cell pellet was resuspended in 12 mL sterile PBS (Corning). The cell suspension in PBS was then centrifuged for 5 mins at 300g. After centrifugation, the PBS was removed using suction and the cell pellet was resuspended in 2 mL R10 by thorough mixing by pipetting up and down with a 1000 µL micropipette. Cells were then counted by mixing 10 µL of cell suspension with 10 µL of 0,4% Trypan blue (Gibco) and placing 10 µL of the mixture into a TC10 counting slide (BioRAD). The counting slide was placed in a TC20 automated cell counter (BioRAD) for counting cells and the cell count and viability was recorded. The cell suspension was then diluted with R10 to obtain 0.5×10^6 cells/mL concentration. The cell suspension was then placed in a cell culture flask with a filtered cap and placed in a cell incubator (37°C, 5% CO₂).

3.2 Drug screening

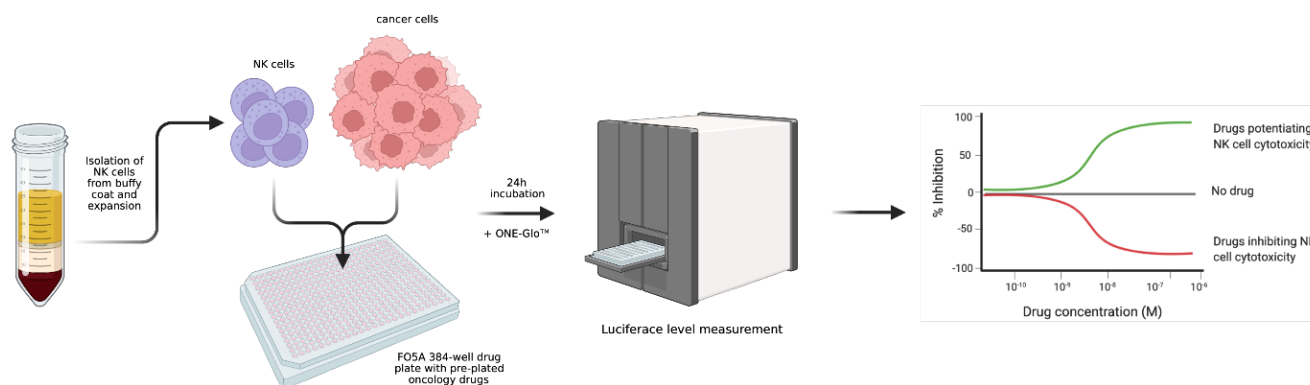


Figure 4. Representation of main experimental methods to study the combinatorial effects of oncology drugs and NK cells. Overall experimental set-up to study the effects of drugs using a high-throughput method.

3.2.1 Optimisation

Prior to applying high-throughput drug screening methods, the killing effect of NK cells was evaluated to enable the study of the effects induced by drugs in both directions, leading to either the enhanced or decreased killing of cancer cells. This was achieved by testing different NK cell to target cell ratios with the aim of finding a ratio that would lead to 50% of target cells being killed by NK cells alone.

Selected target cells and expanded NK cells (day 14 of expansion) were thawed 3 days prior to the optimization experiment and placed in appropriate culture media to allow for recovery. After 3 days of culture, target cells were placed into 50 mL Falcon tubes and centrifuged. Media was removed and cell pallets were resuspended in 2 mL of R10. Cells were then counted by mixing 10 μ L of cell suspension with 10 μ L of 0.4% Trypan blue (Gibco) and placing 10 μ L of the mixture into a TC10 counting slide (BioRAD). The counting slide was placed in a TC20 automated cell counter (BioRAD) for counting cells and the cell count and viability was recorded. The cell suspension was then diluted with R10 to obtain 0.80×10^6 cells/mL concentration. 25 μ L of the target cell solution at the appropriate

concentration was then plated into wells of a 384-well plate (low flange, Corning) according to a plating map of the 24h optimization plates. The same amount of the target cell suspension was then added into a separate 384-well plate that was used as a 0h control.

NK cells were also placed in Falcon tubes and centrifuged to change the media. Cells were counted and diluted to 4.00×10^6 cells/mL concentration. A serial dilution was then made from the NK cell suspension by first placing 2 mL of the 4.00×10^6 cells/mL suspension into one well of a 6-well plate. 1 mL of R10 was then added into the remaining wells and 1 mL of the 4.00×10^6 cells/mL suspension was added to one of the R10 containing wells and thoroughly mixed using a pipette. 1 mL of the diluted solution was then moved to the adjacent well and the same process was applied to the rest of the wells until 6 wells with 4.00×10^6 cells/mL, 2.00×10^6 cells/mL, 1.00×10^6 cells/mL, 0.50×10^6 cells/mL, 0.25×10^6 cells/mL, 0.125×10^6 cells/mL concentrations were obtained.

Once the serial dilutions of NK cells were made, 25 μ L of the NK cell suspension of different concentrations were added to the wells containing the target cells according to the plating map. In addition, 25 μ L of R10 was added into no-NK wells and the 0h control plate. Once plated, 24h plates were placed in an incubator and the 0h control plate was tested for luciferase levels according to the method described in Section 3.2.2.3.

3.2.2 DSRT method

3.2.2.1 Drug plates

FO5A drug plates, containing 528 approved and investigational oncology drugs at 5 concentrations were purchased from the Finnish Institute for Molecular Medicine (FIMM) High Throughput Biomedicine Unit. The drugs included in the FO5A plates, their targets and approval status can be found from Supplementary Materials, Table 1.

3.2.2.2 DSRT experiment

Both NK cells and target cells were thawed 3 days prior to the experiment and placed in appropriate media at 0.50×10^6 cells/mL concentration. From optimization data, the appropriate effector-target ratio was determined, and on the day of the experiment, cell suspensions were prepared accordingly as demonstrated in Table 3. The old cell culture media was first removed and fresh R10 was added to get appropriate concentrations. Once diluted, cells were counted three times for accurate counts and the R10 volume was adjusted if necessary. Cell suspensions at final concentrations were placed in 250 mL screw top bottles and stored in an incubator set to 37°C.

Table 3. Cell suspension concentrations of cancer cell lines and NK cells.

Target cell line	Effector-target ratio	Target cell concentration	NK cell concentration
MOLM-14	1:1	$2,00 \times 10^6$ cells/mL	$2,00 \times 10^6$ cells/mL
THP-1	1:1	$2,00 \times 10^6$ cells/mL	$2,00 \times 10^6$ cells/mL
HEL	1:1.5	$2,00 \times 10^6$ cells/mL	$1,33 \times 10^6$ cells/mL

R10 was warmed to 37°C and 200 mL of it was placed in a 250 mL screw top bottle. Two sets of pre-made drug plates (FO5A, Finnish Institute for Molecular Medicine) were retrieved from storage and 5 µL of R10 was plated into each well of the 384 well-plates containing drug compounds using a BioTek multi-mode dispenser (Multiflo FX with stacker, 5 µL RAD™ cassette). The drug plates were then centrifuged for 1 min at 1000 rpm, following 10 mins of shaking in a plate shaker set to 450 rpm at variable setting (Perkin Elmer, DELFIA® PlateShake). Meanwhile, 15 µL of R10 was also added to one column of a 384 well plate (low flange, Corning) which was used as a 0h control plate.

Next, target cells were taken from the incubator, a magnetic stirrer bar was added to the suspension and the bottle was placed on a magnetic stirrer set to minimum mixing setting. Plates were placed back in the dispenser and 10 µL of the cell suspension was pipetted into

each well (20,000 cells/well). 10 μ L of the cell suspension was also added to the column containing R10 of the 0h plate. At this point, the two sets of drug plates were separated, and one was assigned to be the control set and the other was referred to as the NK cell set.

After plating target cells, the dispensing cassette was washed and 10 μ L of R10 was added to wells of the drug plate set that was set to not contain NK cells (control set). The NK cell set was then placed into the dispenser and 10 μ L of R10 was also added to the control wells. After plating R10, the NK cell suspension was mixed by pipetting it rigorously and a magnetic stirrer bar was added. The bottle was then placed on the magnetic stirrer set to its lowest setting and 10 μ L of the NK cell suspension was plated on the appropriate wells of the drug plates. The plating plan used to plate cells and media can be found from Supplementary Materials, Table 1.

Once all components were plated into the drug plates, the plates were covered with lids and shaken for 5 mins at 450 rpm. After shaking, the plates were placed into an incubator set to 37°C and 5% CO₂ for 24 h. Instead of incubation, the 0h control plate was measured for luciferase levels as described in the following section.

3.2.2.3 Luciferase bioluminescence measurement

200 mL of ONE-Glo™ luciferase assay solution (Promega, E6130) was thawed in a water bath and placed in a 250 mL screw top bottle covered in aluminum foil. Once the ONE-Glo™ solution was prepared, plates containing cells or drugs and cells were placed in a BioTek multi-mode dispenser and 25 μ L of the ONE-Glo™ solution was pipetted into each well. After this, plates were covered with aluminum foil covers and placed in a shaker (Perkin Elmer, DELFIA® PlateShake) set to 450 rpm for 10 mins, following centrifugation for 5 mins at 1000 rpm.

After applying the ONE-Glo™ solution, luciferase levels were measured using a PHERAstar FSX microplate reader with a pre-made reading protocol specifically designed for this experiment.

3.3 Single cell RNA sequencing using hashtag oligos

3.3.1 Drug dilutions

Drug solutions at 10 mM concentration, including ruxolitinib, daporinad, midostaurin, pictilisib, pevonedistat and quizartinib were aliquoted by FIMM High Throughput Biomedicine Unit into aliquots of 50 µL. Drugs were diluted by first adding 40 µL of H₂O, and from then on different amounts of solution containing H₂O with 20% DMSO. More detailed descriptions on the dilutions can be found from Supplementary Materials, Figure 2.

3.3.2 Pre-hashing optimisation

Both NK cells and MOLM-14 cells were thawed 3 days prior to the experiment. On the day of plating the cells, they were first counted and diluted to 2.00×10^6 cells/mL in R10. First, 10 µL of MOLM-14 cell suspension was plated according to the plating plan into two 384 well plates (low flange, Corning), one being the 0h plate and the other being the 24h plate. Once MOLM-14 cells were plated, a serial dilution was made of the NK cells in a 6 well plate (Corning), starting with 2 mL of NK cell suspension at 2.00×10^6 cells/mL concentration. 1 mL of R10 was added to all wells apart from the one containing the cell suspension, after which 1 mL of the NK cell suspension was systematically transferred from higher concentration to a well only containing R10, hence ending up with suspensions at 2.00×10^6 cells/mL, 1.00×10^6 cells/mL, 0.50×10^6 cells/mL, 0.25×10^6 cells/mL, 0.125×10^6 cells/mL concentrations. When combined with target cells, these dilutions would lead to effector-target ratios of 1:1, 0.5:1, 0.25:1, 0.125:1 and 0.0625:1 respectively. One well was left with only R10 without the addition of NK cells.

Once NK cell dilutions were made, 10 μL of the suspensions of different concentrations were plated according to the plating plan. For wells with no NK cell suspension added, 10 μL of R10 was added instead. Following the plating of NK cell suspensions, 5 μL of drug solutions were added to relevant wells according to the plating plan. After all components had been plated, the plates were centrifuged for 1 min at 1000 rpm, placed in a shaker for 5 mins at 450 rpm and placed in an incubator set to 37°C and 5% CO_2 . The luciferase level measurement was then performed on the 0h plate. After 24h incubation of the 24h plate, luciferase levels were also measured following the addition of ONE-Glo™ and relevant steps described in Section 3.2.2.3.

3.3.3 Hashing experiment and preparation for single cell RNA sequencing

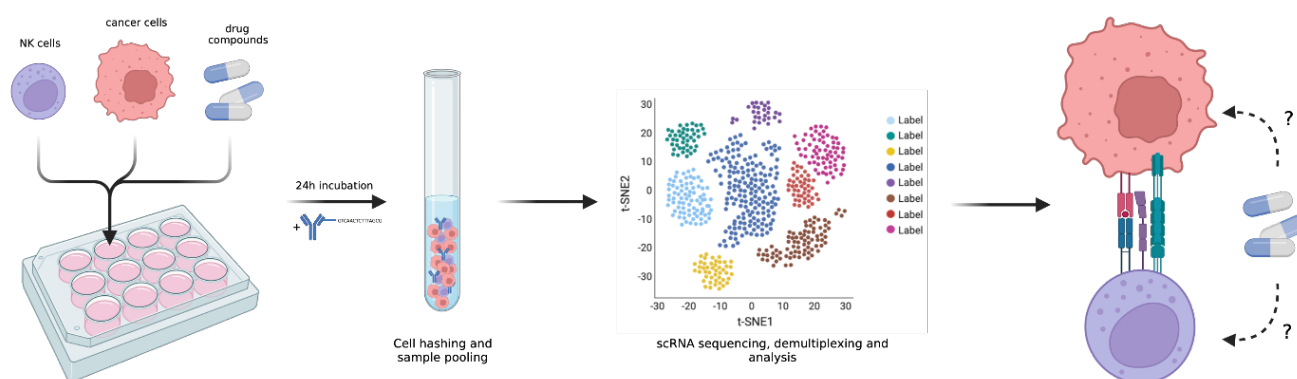


Figure 6. Experimental method for hashing experiment in preparation to scRNA sequencing.

Experimental set-up of hashing scRNA sequencing experiment following the selection of drugs using high-throughput DSRT.

Cells were thawed 3 days prior to plating the cells into co-culture with NK cells having 10 ng/mL IL-2 added to the media. Based on the pre-hashing optimization experiment, a 1:4 effector-target ratio was selected. On the day of plating, old media was discarded, MOLM-14 cells were resuspended in R10 to obtain a 2.00×10^6 cells/mL concentration and NK cells were also resuspended in R10 to a 0.50×10^6 cells/mL concentration. 250 μL of MOLM-14 cell suspension was then plated according to the plating plan into appropriate wells of four 24 well plates (Corning), leading to two duplicate plates of two different conditions. 250 μL

of NK cell suspension was then added to appropriate wells and the contents were mixed with a pipette.

After plating all cells, drugs were combined with R10 by adding 5 μL of the pre-diluted drug solution into either 495 μL or 745 μL of R10. For each drug, four 750 μL drug and R10 solutions were made in 1 mL Eppendorf tubes in addition to two 500 μL solutions per drug. A 20% DMSO solution was also made by combining 200 μL of DMSO (99,9%, Sigma-Aldrich) and 800 μL H_2O . 5 μL of the 20% DMSO solution was then added to 8 Eppendorf tubes containing 745 μL of R10 and four tubes containing 495 μL of R10. Once all drug solutions and DMSO solutions were ready, they were added into appropriate wells according to the plating plan. The contents of each well were thoroughly mixed by pipetting and placed into an incubator set to 37°C and 5% CO_2 for 24h.

After 24 h incubation, one plate of each condition was taken out of the incubator and the contents of each well were moved to separate 15 mL Falcon tubes containing 10 mL of cold PBS (4°C). The cells were mixed with PBS, following centrifugation of 5 mins at 300g. After centrifuging the samples, the supernatants were removed, and all samples were washed another two times with 10 mL of cold PBS. After the last wash, as much of the PBS was removed from each tube as possible using a micropipette.

After removing the excess PBS, 10 μL of Fc blocking reagent (FcX, BioLegend) was added to FACS tubes assigned to each sample. Following this, cells were resuspended in 100 μL of staining buffer (BioLegend) and transferred to assigned FACS tubes. Tubes and their contents were mixed using a vortex mixer and left to incubate at 4°C for 10 mins. After incubation, 2 μL of a unique Cell Hashing antibody was added according to Tables 2 and 3. Samples were then mixed using a vortex mixer and left to incubate at 4°C for 30 mins. In the meantime, a 0,04% BSA solution in PBS was prepared by mixing 19,92 mL of PBS with 0,08 mL BSA (10%, Sigma-Aldrich). After incubating the cells with the hashtag

antibodies, each sample was washed five times with 3 mL staining buffer including a 300g centrifugation at 4°C for 5 mins between each wash to remove the staining buffer.

After the last wash, 100 µL of staining buffer was added to each tube and cells were resuspended. Once in suspension, all cells from different tubes within each condition were combined into one tube and centrifuged for 5 mins at 4°C in 300g. The staining buffer was then removed, and cells were resuspended in 3 mL of PBS with 0.04% BSA and the suspension was transferred into a 15 mL Falcon tube. Cells were then counted, and the concentration of the suspension was adjusted by adding more of the PBS with 0.04% BSA to obtain a final concentration of 1.50×10^6 cells/mL. Finally, 1 mL of the final product was placed in a 1.5 mL Eppendorf tube and transported on ice to the sequencing facility for further analysis.

Table 4. Hashtags used in sequencing sample 1. Hashtag oligonucleotides with respective sequences and co-culture conditions to which they bound in the sequencing sample consisting of activating drugs.

Hashtag	Sequence	Sample / Condition	Catalogue number
1	GTCAACTCTTTAGCG	Daporinad + NK	394601
2	TGATGGCCTATTGGG	Ruxolitinib + NK	394603
3	TTCCGCCTCTCTTTG	Pevonedistat + NK	394605
4	AGTAAGTTCAGCGTA	Daporinad + MOLM-14	394607
5	AAGTATCGTTTCGCA	Ruxolitinib + MOLM-14	394609
6	GGTTGCCAGATGTCA	Pevonedistat + MOLM-14	394611
7	TGTCTTTCCTGCCAG	Daporinad + MOLM-14 + NK	394613
8	CTCCTCTGCAATTAC	Ruxolitinib + MOLM-14 + NK	394615
9	CAGTAGTCACGGTCA	Pevonedistat + MOLM-14 + NK	394617
10	ATTGACCCGCGTTAG	NK in 0,1% DMSO	394619
12	TAACGACCAGCCATA	MOLM-14 in 0,1% DMSO	394621
13	AAATCTCTCAGGCTC	MOLM-14 + NK in 0,1% DMSO	394623

Table 5. Hashtags used in sequencing sample 2. Hashtag oligonucleotides with respective sequences and co-culture conditions to which they bound in the sequencing sample consisting of inhibiting drugs.

Hashtag	Sequence	Sample / Condition	Catalogue number
1	GTCAACTCTTTAGCG	Pictilisib + NK	394601
2	TGATGGCCTATTGGG	Quizartinib + NK	394603
3	TTCCGCCTCTCTTTG	Midostaurin + NK	394605
4	AGTAAGTTCAGCGTA	Pictilisib + MOLM-14	394607
5	AAGTATCGTTTCGCA	Quizartinib + MOLM-14	394609
6	GGTTGCCAGATGTCA	Midostaurin + MOLM-14	394611
7	TGTCTTTCCTGCCAG	Pictilisib + MOLM-14 + NK	394613
8	CTCCTCTGCAATTAC	Quizartinib + MOLM-14 + NK	394615
9	CAGTAGTCACGGTCA	Midostaurin + MOLM-14 + NK	394617
10	ATTGACCCGCGTTAG	NK in 0,1% DMSO	394619
12	TAACGACCAGCCATA	MOLM-14 in 0,1% DMSO	394621
13	AAATCTCTCAGGCTC	MOLM-14 + NK in 0,1% DMSO	394623

3.3.4 Single cell sequencing using hashtag oligos

Sequencing of the MOLM-14 sample containing hashtags was performed by the Single-Cell Analytics Unit of the Finnish Institute for Molecular Medicine. Single cell gene expression profiles were studied using 10x Genomics Chromium Single Cell 3'RNAseq platform. The Chromium Single Cell 3'RNAseq run and library preparation were done using the Chromium Next GEM Single Cell 3' Gene Expression version 3.1 Dual Index chemistry. The Sample libraries were sequenced on Illumina NovaSeq 6000 system using read lengths: 28bp (Read 1), 10bp (i7 Index), 10bp (i5 Index) and 90bp (Read 2). The TotalSeq™-A Antibodies and Cell Hashing with 10x Single Cell 3' Reagent Kit v3 or v3.1 (Single Index) protocol from BioLegend® was used.

3.4 Data analysis

3.4.1 Analysis of DSRT data

DSRT data was analysed with a purposefully designed script on R that uses a validated systematic algorithmic solution to calculate differential drug sensitivity scores for each drug. This relies on reading data from luciferase measurements to calculate scores and create inhibition curves. The analysis incorporates both NK and no-NK conditions for comparison.¹⁰⁷

Raw Data (LUM plus)

	1	2	3	4	5	6	7	8	9	10	11	12	13	14	15	16	17	18	19	20	21	22	23	24
A	198	3	56	148	528	106	1	6	21	5	11	170	63	124	197	196	243	79	194	181	97	37	1	2
B	272	254	194	212	463	198	4	24	232	4	34	210	177	168	209	3	194	55	212	203	204	199	5	213
C	232	272	238	260	474	180	83	81	207	26	214	160	341	235	221	200	237	86	246	245	225	230	9	252
D	305	263	294	204	189	203	265	221	271	69	241	233	215	222	194	211	218	242	240	190	217	227	197	221
E	245	242	264	261	383	268	224	214	260	195	237	250	226	233	240	163	206	215	214	212	241	273	227	231
F	222	204	222	241	306	140	171	219	245	3	2	260	14	250	236	210	17	47	94	219	202	209	198	238
G	295	175	261	276	524	2	175	270	245	156	32	61	221	217	3	206	163	82	208	0	221	281	78	280
H	237	200	226	251	527	192	176	247	187	160	143	73	223	221	8	210	202	190	213	132	208	194	222	198
I	261	258	250	257	603	225	223	215	187	184	244	48	233	229	47	263	192	224	240	218	276	195	247	224
J	201	266	264	229	538	216	218	250	217	216	301	255	234	2	137	203	276	257	217	253	258	214	244	245
K	280	228	279	274	368	227	220	234	266	206	224	236	240	263	199	223	249	261	243	259	3	187	235	214
L	261	261	223	429	271	243	270	291	223	225	90	272	126	247	250	242	238	245	225	206	194	240	241	285
M	233	274	146	10	273	231	291	247	270	232	54	262	13	281	258	285	286	202	246	224	308	294	279	238
N	263	291	137	586	313	248	233	224	210	210	2	154	3	183	250	223	208	203	259	236	198	259	236	248
O	300	235	137	661	296	238	183	216	187	329	11	97	242	51	272	297	52	4	199	250	177	207	260	229
P	240	203	218	625	193	123	19	157	201	248	0	77	0	10	258	117	18	96	196	52	139	260	5	0



Matching readouts with appropriate drug and NK cell condition

Comparing cell viability to controls and calculating drug sensitivity scores

Curve fitting for inhibition curves

ID	DRUG_NAME	ANALYSIS	IC50	SLOPE	MAX	MIN	Min.C	Max.C	IC50_std_error	D1	D2	D3	D4	D5	GRAPH	DSS	sDSS	DSSnot	D1_noNK	D2_noNK	D3_noNK	D4_noNK	D5_noNK
Prexasertib	Prexasertib	IC50	87.1	2.5	94.7	0	1	10000	0.9	1.6	-22.9	56.1	79.3	94.7		23.8	23.8	0	2.5	-8.5	69.8	87.1	-42.4
Daporinad	Daporinad	IC50	5.8	0.7	59.6	0	0.1	1000	0.9	16.2	6.4	37.5	52.8	59.6		14.9	14.9	0	-14.3	-35.9	8.6	-14.3	-16.4
Letrozole	Letrozole	IC50	3.1	2.5	32.7	0	1	10000	331.3	0.4	32.7	22.1	28.9	23.6		14	13.1	0.9	5.9	14.4	-11.2	11.4	13.1

Figure 7. Processing and analysis of DSRT data, starting with bioluminescence readouts. Data was computationally matched to specific conditions. These values were used to calculate drug sensitivity scores, and the results between NK only and NK with drug conditions were compared to determine differential drug sensitivity scores.

3.4.2 Analysis of scRNA sequencing data

Data processing and analysis were performed by the FIMM Technology Center using 10x Genomics Cell Ranger v5.0.1 pipelines. Cell Ranger includes several pipelines of which the “cellranger mkfastq” was used to produce raw data files and “cellranger count” to perform

alignment, filtering and UMI counting. Mkfastq was run using the Illumina bcl2fastq v2.2.0 and alignment was done against human genome GRCh38. Cellranger aggr pipeline was used to combine data from multiple samples into an experiment-wide gene-barcode matrix and analysis. Count matrix for hashtag oligonucleotides (HTO) was generated using the CITE-seq-Count-tool.¹⁰⁸

Further analysis including quality control, normalization, data correction and clustering were performed using the Seurat package (version 4.0) according to the Current Best Practices in Single-Cell RNA-seq analysis.¹⁰⁹ Further analysis and exploring of the data was done using R scripts kindly provided by MD Olli Dufva with functions and added features created by MD Jani Huuhtanen. The analysis consisted of packages such as SingleR and clusterProfiler. After merging data from both scRNA sequencing samples, these computational tools were used to study the NK cell and MOLM-14 cell populations separately to investigate cell-specific changes in response to drug co-culturing with NK cells. Additional figures related to the scRNA sequencing data can be found from the Supplementary Materials, Figures 3-5.

4. Results

4.1 Effector-target optimisation of different cell lines and different donor effects

Prior to performing drug screenings with cells of interest, target cell and NK cell ratios were optimised as target cells differ in sensitivity to NK cells, in addition to donor-dependent differences in NK cells' ability to kill target cells. Hence, target cells and NK cells were co-cultured for 24 hours to study the effect of NK cells on cancer cells without the addition of drug compounds. Differences between different effector-target ratios were studied with the goal of obtaining approximately a 50% inhibition of the cell viability by exposing target cells to a given number of NK cells. The 0.5 viability has been selected as the condition at which target cell viability can show changes in both inhibiting and activating directions when drugs are applied.

For MOLM-14, a 1 to 1 ratio of target cells and NK cells showed inhibition of the target cell viability by 50%. This result was observed by comparing the condition in which only target cells were cultured in R10 to the condition in which the luciferase luminescence was halved to that of the control. Similarly, for THP-1 and HEL cell lines, effector-target ratios of 1 to 1 and 1 to 1.5 were determined respectively.

In the optimisation data for the HEL cell line, increases in viabilities are observed as small numbers of NK cells are co-cultured with the target cell. As seen in Figure 8, at 1:16, 1:8 and 1:4 effector-target ratios, HEL cells proliferate more compared to the condition in which no NK cells are added, which could imply that NK cell may interfere with the luciferase level measurements. In addition, small errors in cell counts may have led to such effects being seen despite of small numbers of NK cells being added.

Interestingly, the effector-targets required to reach a 50% decrease in viability were notably higher compared to unpublished previous measurements made on MOLM-14. In a previous experiment performed in our group, a 1 to 4 effector-target ratio was required, shedding light on donor-dependent differences in the effects of NK cells on the targeted cancer cell line. This finding emphasized the importance of a validation experiment when changing to NK cells expanded from a different donor.

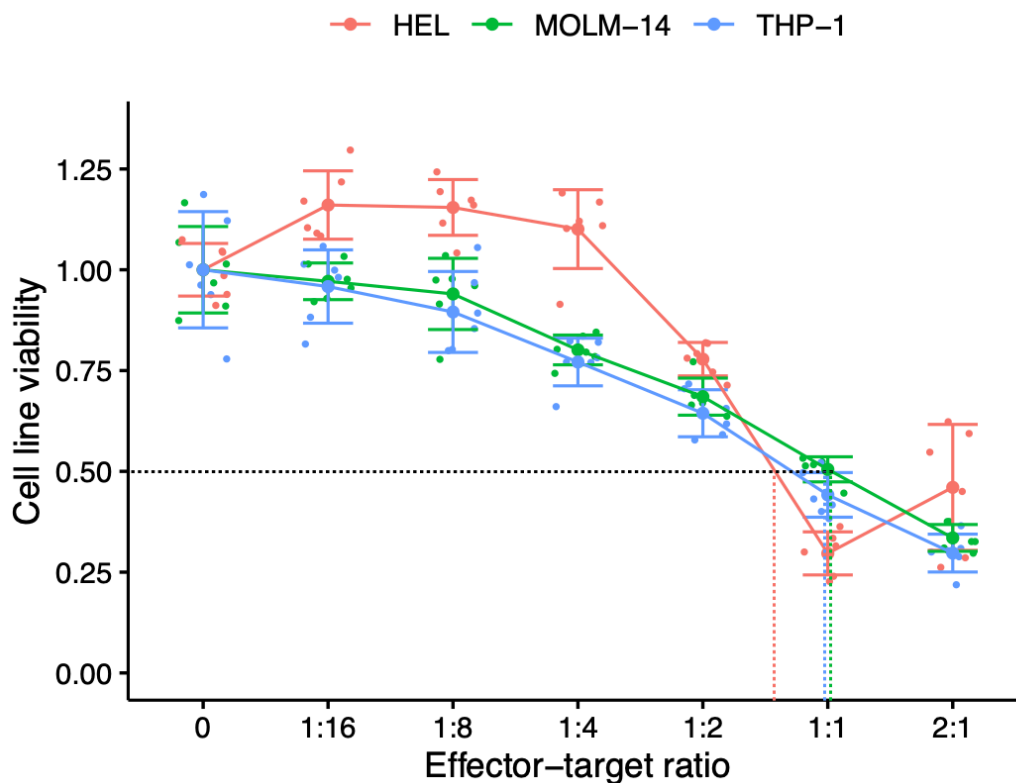


Figure 8. Cell viability curves with respect to ratio of effector cells to target cells. This gives indication of appropriate effector-target ratio to be used in later experiments to reach 50% inhibition with NK cells alone.

4.2 DSRT results

High-throughput drug sensitivity and resistance testing was used to obtain qualitative information on the capability of different oncology drugs to synergise with NK cell for effects on cytotoxic capabilities against AML cell lines. Out of hundreds of drugs, the most potential NK cell cytotoxicity-enhancing compounds, in addition to those limiting their

effect, were studied further using single-cell methods for deeper understanding about the underlying mechanisms of action.

In principle, comparison between target cell cultures with added drug or drug and NK cells was performed using computational methods. Drug sensitivity scores (DSS) and differential drug sensitivity scores (sDSS), obtained from the computational analysis, were studied in detail to determine the effects of drugs and NK cells on target cell lines. Although the computational model used for analysis works well in general, it fails to consider errors within the raw screening data, for which viability curves, also provided by the computational method, must be gone through to determine meaningful results from compounds giving a significant sDSS score.

To determine whether a drug shows meaningful results in the DSRT, a cut-off sDSS score was used. Generally, for a drug to have been considered as being significantly NK cell-activating, the sDSS score had to be over 7.5, although exceptions exist. When analysing inhibitory effects, sDSS of -10.0 and below were generally considered significant and worth investigating further. In addition, the drug concentrations at which the drug showed meaningful activity was taken into consideration, as compounds with significant inhibitory effect only achieved at high concentrations were considered less effective and meaningful, due to not necessarily being achievable *in vivo*. All differential drug sensitivity scores describing the relative inhibition between conditions with only NK cells and NK cells with drugs can be found from Supplementary Materials, Table 1.

In this section, DSRT data from significant compounds for each cell line will be analysed. Overall, this covers only a small minority of all compounds used in the drug screenings, which consisted of 528 oncology drugs. In the following assessment of results, it is important to note that inhibition of target cells reflects their decreased viability, and hence their killing.

4.2.1 Data quality

The DSRT data quality was evaluated as part of computational data analysis for each experiment to evaluate the validity of findings in a high throughput setting. Data quality was analysed primarily through the Z-prime value, which evaluates the quality of high-throughput screening data by studying positive and negative controls. Z-prime values between 0.5 and 1.0 are considered as indicator of good quality data. Data quality measures for different cell lines can be seen in Table 6, with average Z-prime values provided, taken from individual screening plate's Z-prime values.

The Z-prime value can be calculated using the following equation,

$$Z' = 1 - \frac{3(\sigma_p + \sigma_n)}{|\mu_p - \mu_n|}$$

where means (μ) and standard deviations (σ) of positive (p) and negative (n) controls are used as parameters. Using this equation, mean Z-prime values can be calculated for sets of drug plates used to study each cell line (Table 6).

Table 6. Average Z-prime values of all drug plates for respective cell lines' drug screenings.

Cell line	Z-prime value
MOLM-14	0.61
THP-1	0.76
HEL	0.82

4.2.2 Most activating drugs

4.2.2.1 MOLM-14

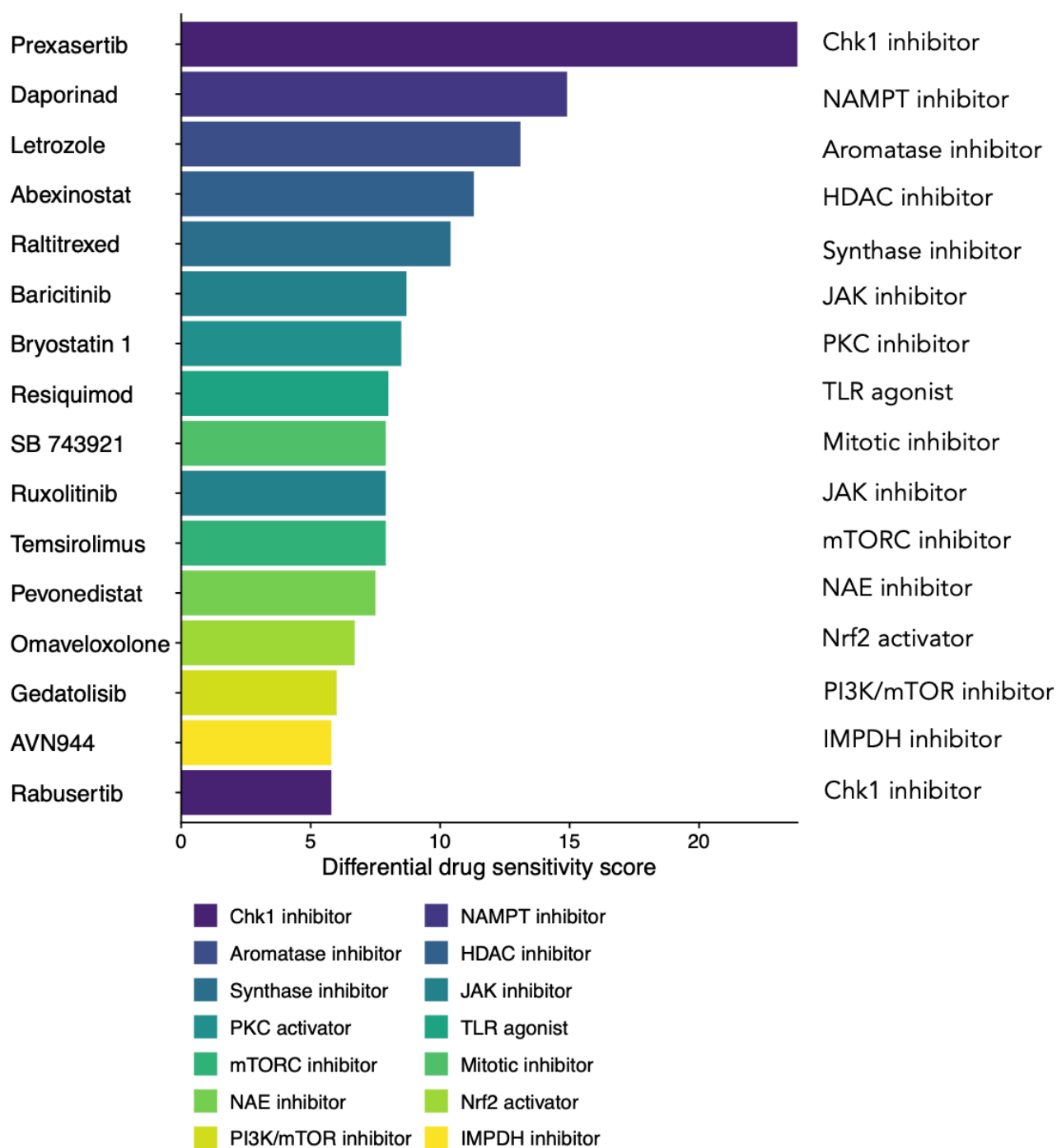


Figure 9. Bar plot of top activating drugs in MOLM-14.

Out of the DSRT data of MOLM-14, 12 compounds had an sDSS score of over 7.5, which are shown in Figure 9. Although prexasertib gives the highest sDSS score, the analysis of

its inhibition curve reveals what would seem to be a measurement error at 1000 nM drug concentration, for which the result is interpreted as insignificant. The analysis of inhibition curves of abexinostat, bryostatin 1 and SB 743921 also reveals errors in the measurement of viabilities at individual drug concentrations, which has an increasing effect on the sDSS score.

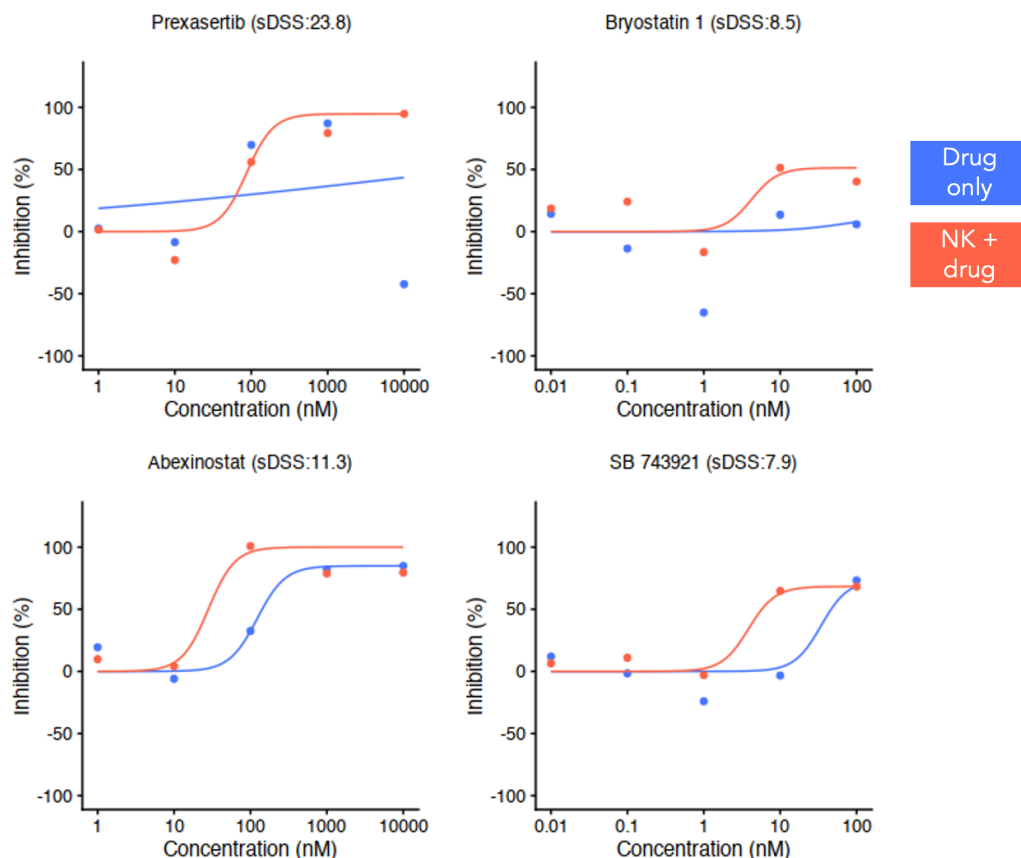


Figure 10. Inhibition curves of prexasertib, bryostatin 1, abexinostat and SB 743921 in MOLM-14.

The blue line represents the condition in which only MOLM-14 cells are cultured with the drug, whereas the red line is representative of MOLM-14 cells combined with NK cells and the drug.

Interesting findings are seen for eight other drug compounds, which seem to synergise with NK cells to create an increased inhibitory effect. Daporinad gives a high sDSS score of 14.9 and data indicates no effect of the drug alone on target cells. However, with NK cells present, the inhibition increases to 37.5% at 10 nM drug concentration, rising to 59.6% at 1000 nM. Similar effects are also observed in drugs belonging to the family of JAK inhibitors such as baricitinib and ruxolitinib. In these drugs, increased inhibition in the presence of

NK cells is observed at higher concentrations, rising to 45.3% and 60.0% in baricitinib and ruxolitinib respectively. Furthermore, pevonedistat shows increase in inhibition at 100 nM drug concentration, although the effect of combining drugs with NK cells is diminished at higher drug concentrations. Resiquimod also shows a 50% difference in inhibition when comparing the drug only to NK cells with drug conditions, which can, however, only be seen at higher concentrations.

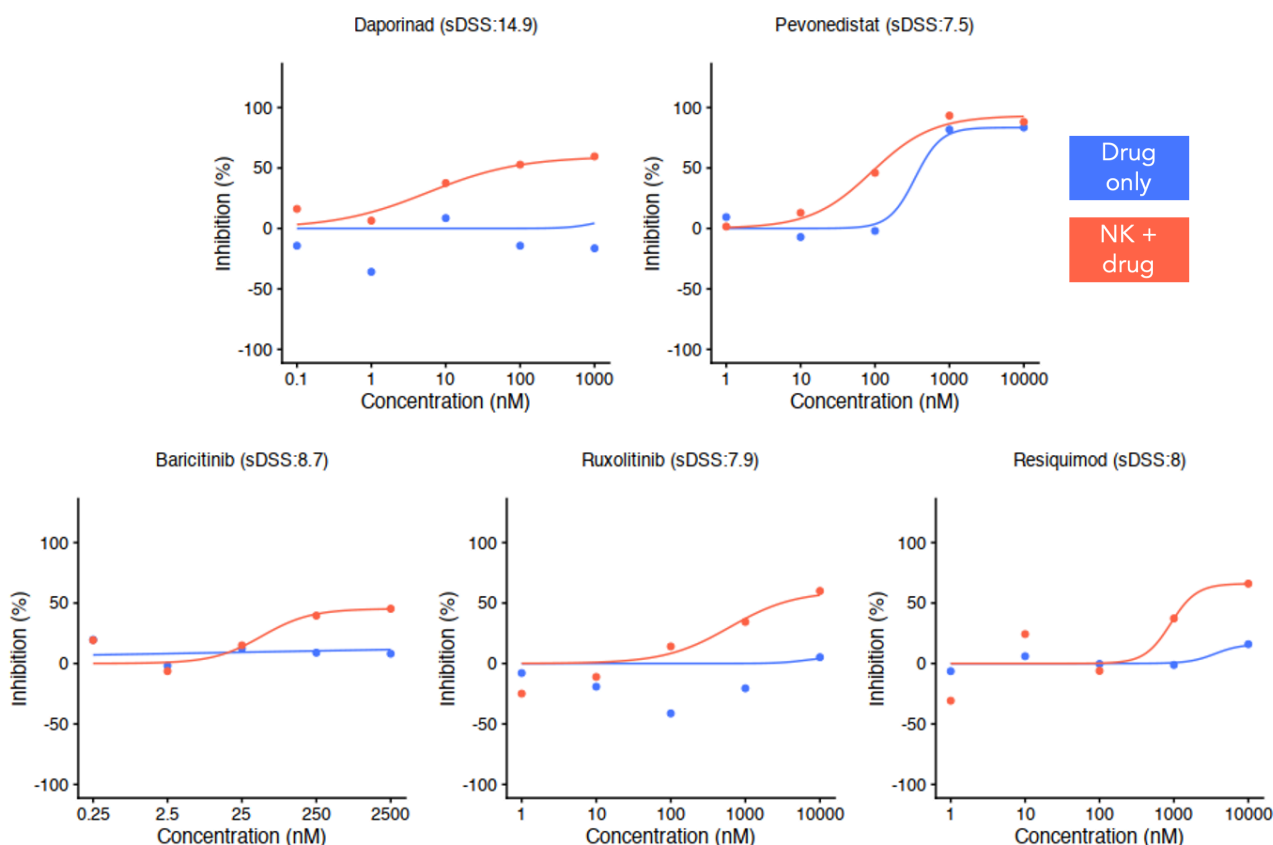


Figure 11. Inhibition curves of daporinad, pevonedistat, baricitinib, ruxolitinib and resiquimod in MOLM-14. The blue line represents the condition in which only MOLM-14 cells are cultured with the drug, whereas the red line is representative of MOLM-14 cells combined with NK cells and the drug.

Smaller NK cell induced increases in inhibition are noted in drugs such as letrozole, raltitrexed, and temsirolimus. In the case of temsirolimus, the drug itself has a relatively good inhibitory effect on the cancer cells and adding NK cells to the picture does not significantly increase the inhibitory effect. In the other drugs with small increases in inhibition, small differences exist across all drug concentrations which, however, remain relatively minor.

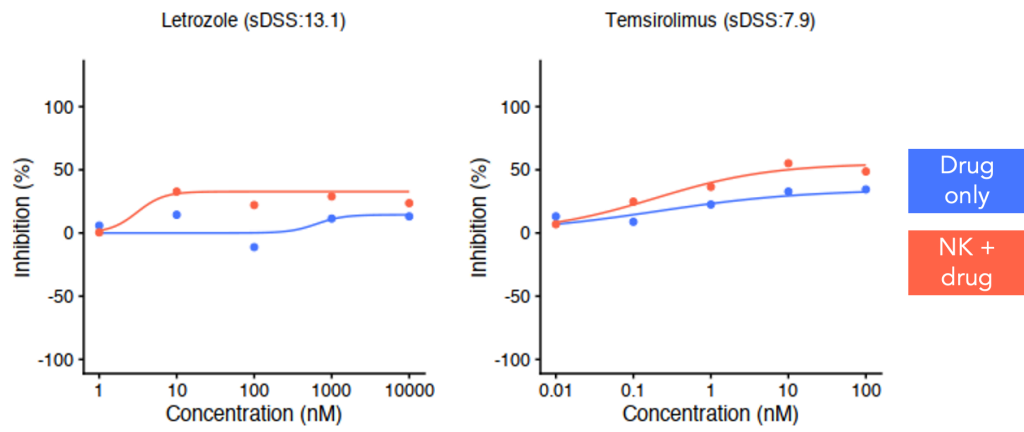


Figure 12. Inhibition curves of letrozole and tamsulosin in MOLM-14. The blue line represents the condition in which only MOLM-14 cells are cultured with the drug, whereas the red line is representative of MOLM-14 cells combined with NK cells and the drug.

4.2.2.2 THP-1

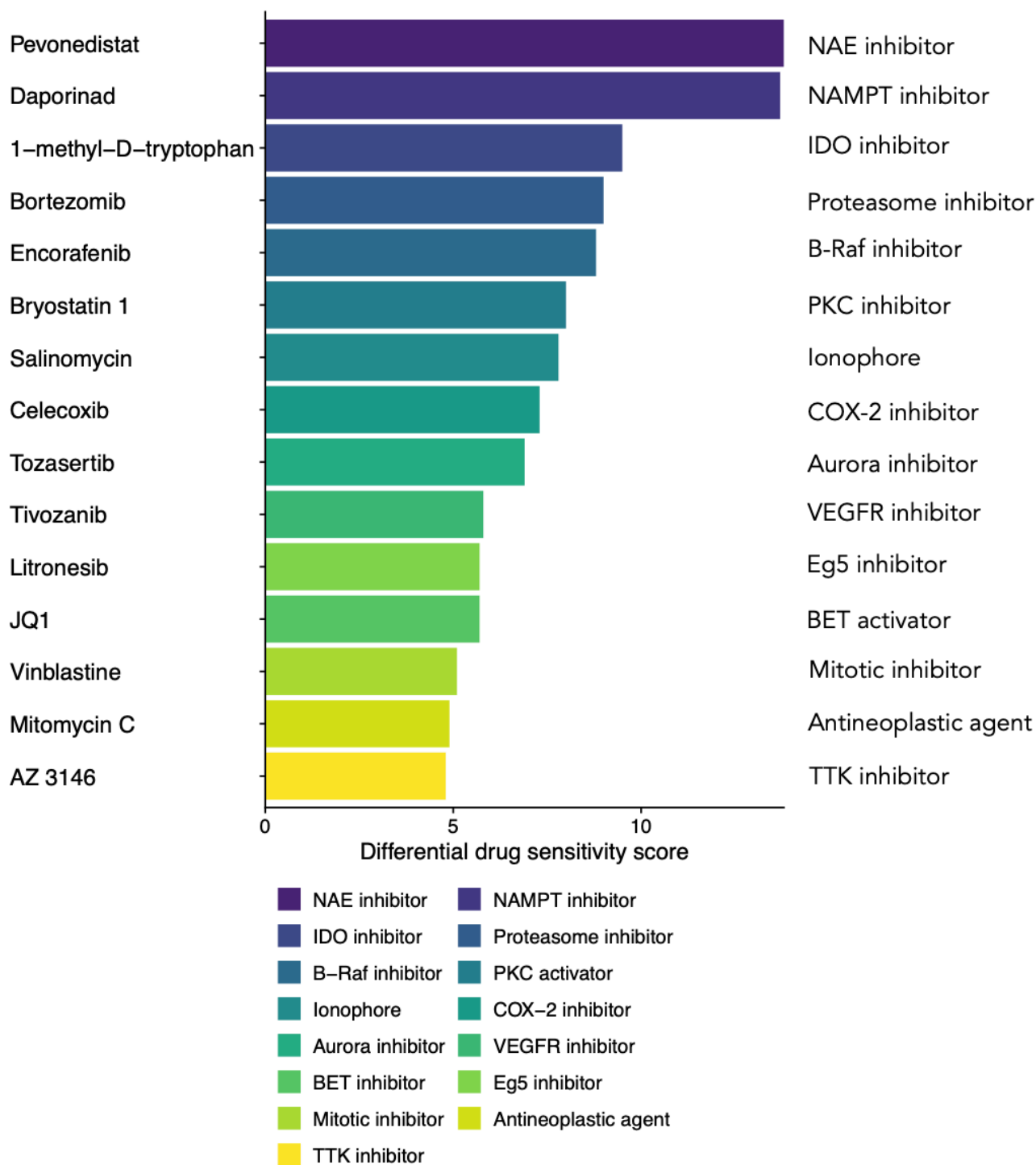


Figure 13. Bar plot of top activating drugs in THP-1.

THP-1 data shows fewer activating drug compounds when compared to MOLM-14 as only seven compounds reach the 7.5 sDSS threshold. However, similar to MOLM-14, pevonedistat and daporinad both give a strong sDSS score of 13.8 and 13.7 respectively.

In the case of pevonedistat, the drug itself reaches a 37.4% inhibitory effect at 1000 nM concentration. Notably, the effect is increased when NK cells are co-cultured with target cells, reaching 90.0% inhibition at 1000 nM and 94.6% at 10,000 nM concentration. Daporinad, on the other hand, has no effect on the target cell line on its own. With NK cells, however, a notable inhibitory effect is observed with an inhibition of 53.1% at 100 nM drug concentration.

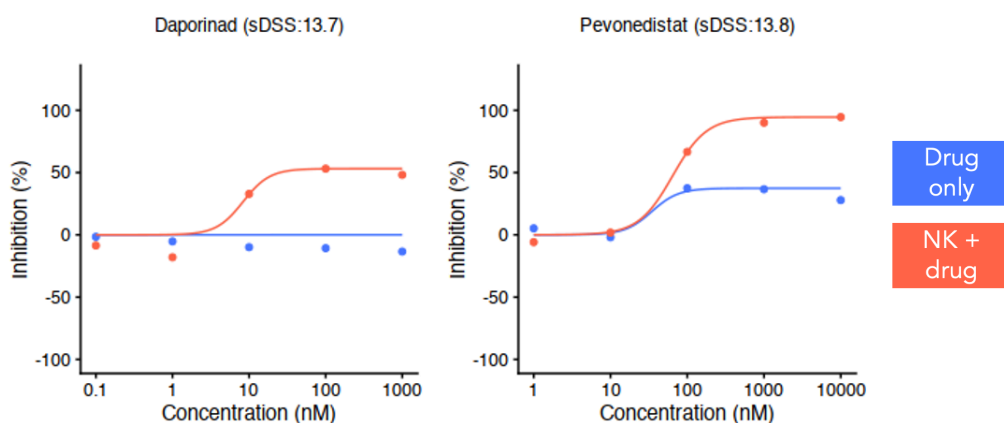


Figure 14. Inhibition curves of daporinad and pevonedistat in THP-1. The blue line represents the condition in which only THP-1 cells are cultured with the drug, whereas the red line is representative of THP-1 cells combined with NK cells and the drug.

Less significant activating effect are seen when NK cells are combined with 1-methyl-D-tryptophan, bortezomib, encorafenib, bryostatin 1 and salinomycin. Out of these, the effect of 1-methyl-D-tryptophan on the target cells is increased by approximately 24% across all concentrations when NK cells are used. The inhibitory effect of bortezomib increases from 19.0% to 57.8% at 10 nM drug concentration when NK cells are co-cultured with target cells. However, bortezomib has also a good effect alone at 100 nM and 1000 nM drug concentration, and NK cells do not seem to give an advantage over the “drug only” condition at these concentrations. Encorafenib, bryostatin 1 and salinomycin in NK co-cultures show small improvements over “drug only” conditions, however the effect is not large enough to be considered significant at any concentration.

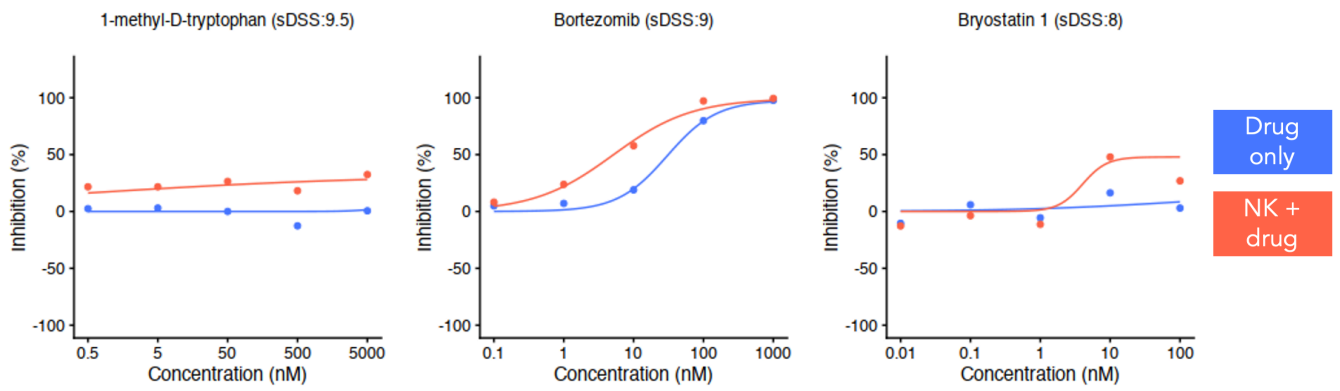


Figure 15. Inhibition curves of 1-methyl-D-tryptophan, bortezomib and bryostatin 1 in THP-1. The blue line represents the condition in which only THP-1 cells are cultured with the drug, whereas the red line is representative of THP-1 cells combined with NK cells and the drug.

4.2.2.3 HEL

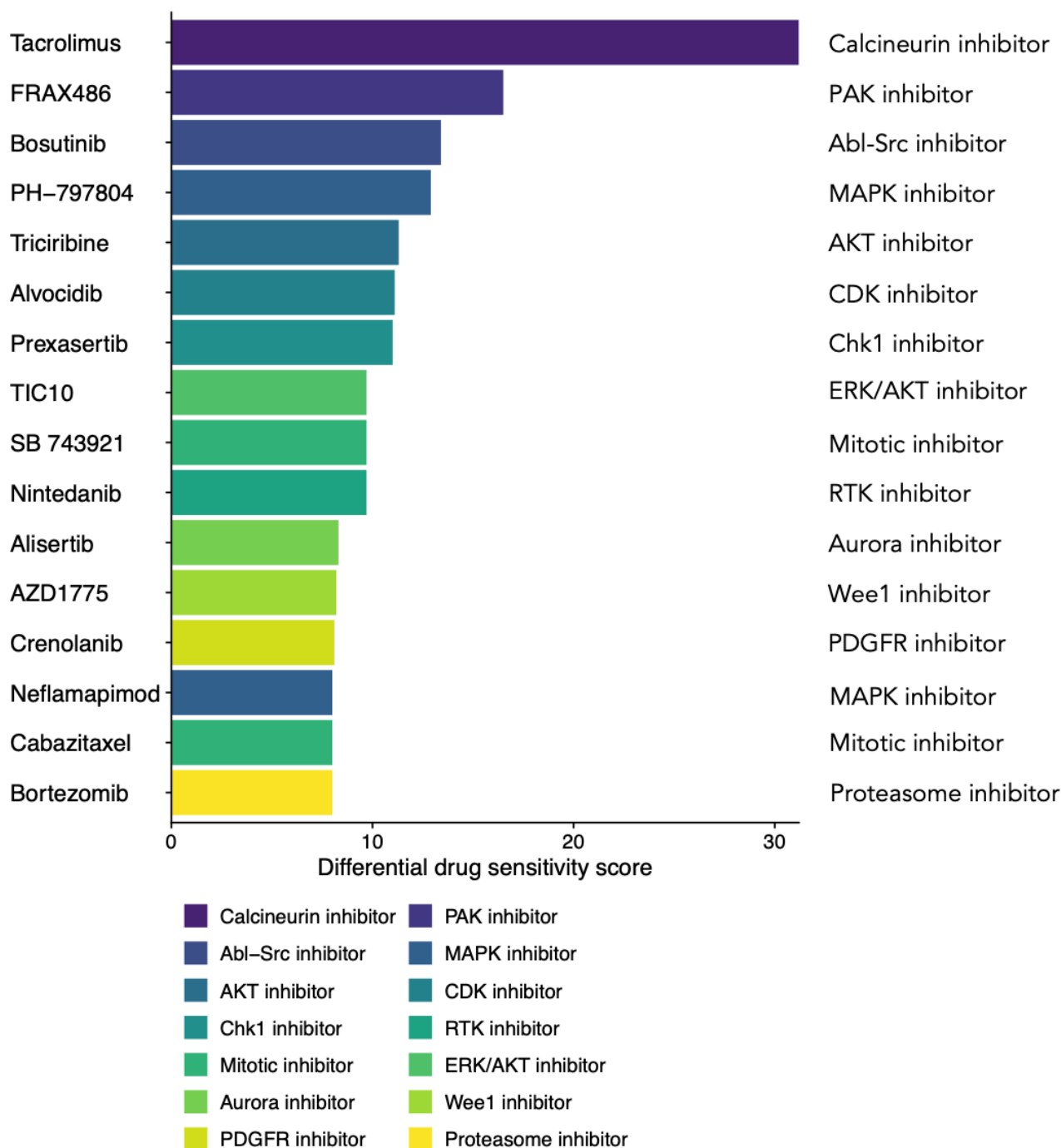


Figure 16. Bar plot of top activating drugs in HEL.

Results for the HEL cell line gave rise to 16 drug compounds that have an sDSS score of 7.5 or over. All compounds with significantly positive sDSS scores had a clear inhibition curve, and as the data was of good quality, none of the drug compounds had to be discarded due to errors.

The most notable activating result was observed in tacrolimus, the results of which showed a consistent inhibiting effect of 60% to 70% at concentrations ranging from 10 nM to 10,000 nM drug concentration in the condition involving NK cells. The drug alone had no significant effect on the target cell line and the “no NK” DSS score was analysed to be zero. A similar effect was observed in the results for FRAX486, however the higher inhibitory effect of the NK cell-including condition was only observed at higher drug concentrations of 500 nM and 5000 nM.

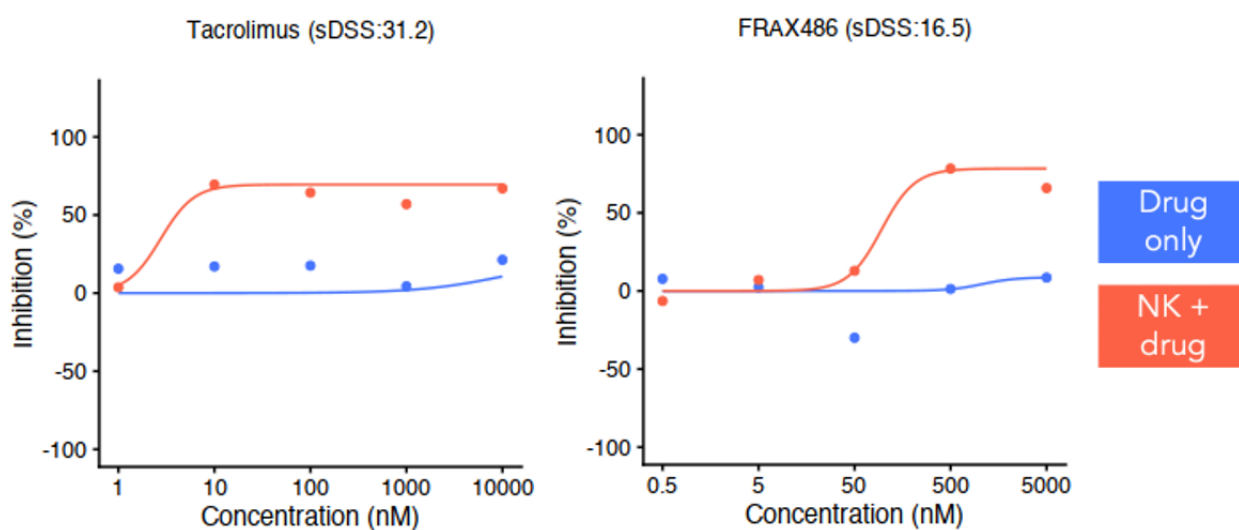


Figure 17. Inhibition curves of tacrolimus and FRAX486 in HEL. The blue line represents the condition in which only HEL cells are cultured with the drug, whereas the red line is representative of HEL cells combined with NK cells and the drug.

Bosutinib, prexasertib, nintedanib, AZD1775, crenolanib and bortezomib all showed increased inhibition of the target cells at one or two drug concentrations, although at the highest drug concentration point the drug alone achieved the same effect. In addition, TIC10 reached the same inhibitory effect at the highest drug concentration tested, although a 20% to 30% increase in inhibition was observed at all lower concentrations when NK cells were involved. Cabazitaxel and neflamapimod, on the other hand, had a slight improvement in inhibition in the NK cell-containing condition at higher drug concentrations

when compared to “drug only”. However, the difference in inhibition between the two conditions was only approximately 15%.

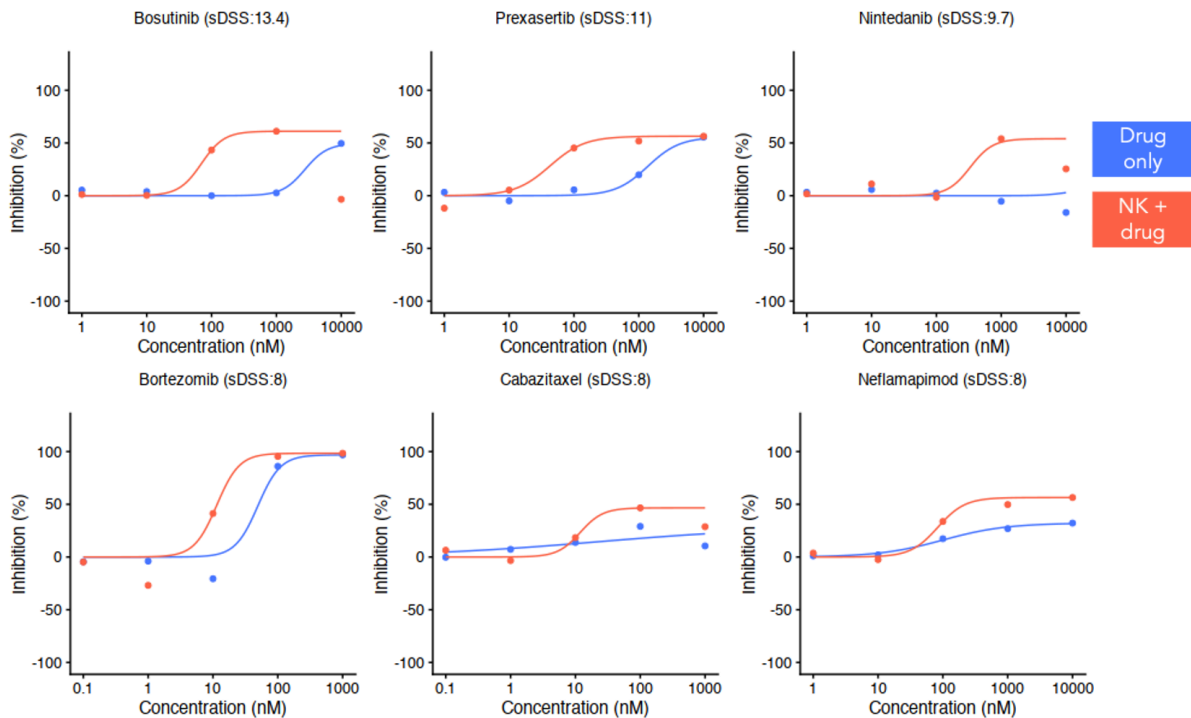
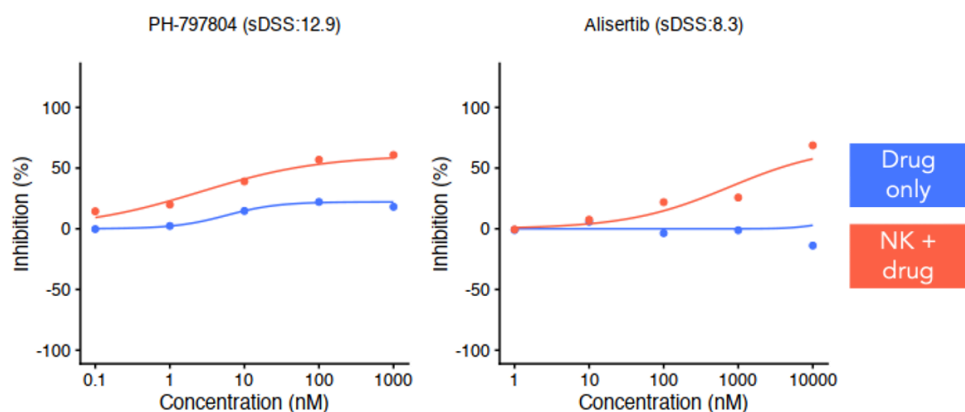


Figure 18. Inhibition curves of bosutinib, prexasertib, nintedanib, bortezomib, cabazitaxel and neflamapimod in HEL. The blue line represents the condition in which only HEL cells are cultured with the drug, whereas the red line is representative of HEL cells combined with NK cells and the drug.

PH-797804, triciribine, alvocidib, SB743921 and alisertib all showed an increase in inhibition across all drug concentrations when co-cultured with NK cells. The most significant improvements in target cell inhibition were seen in PH-797804 and alisertib. PH-797804 reached inhibition of 60.8% with NK cells compared to 18.1% without at 1000 nM drug concentration and alisertib had an inhibitory effect of 68.7% with NK cells compared to -13.9% with drug alone at 10,000 nM concentration.

Figure 19. Inhibition curves of PH-797804 and alisertib in HEL.



4.2.3 Most inhibiting drugs

4.2.3.1 MOLM-14

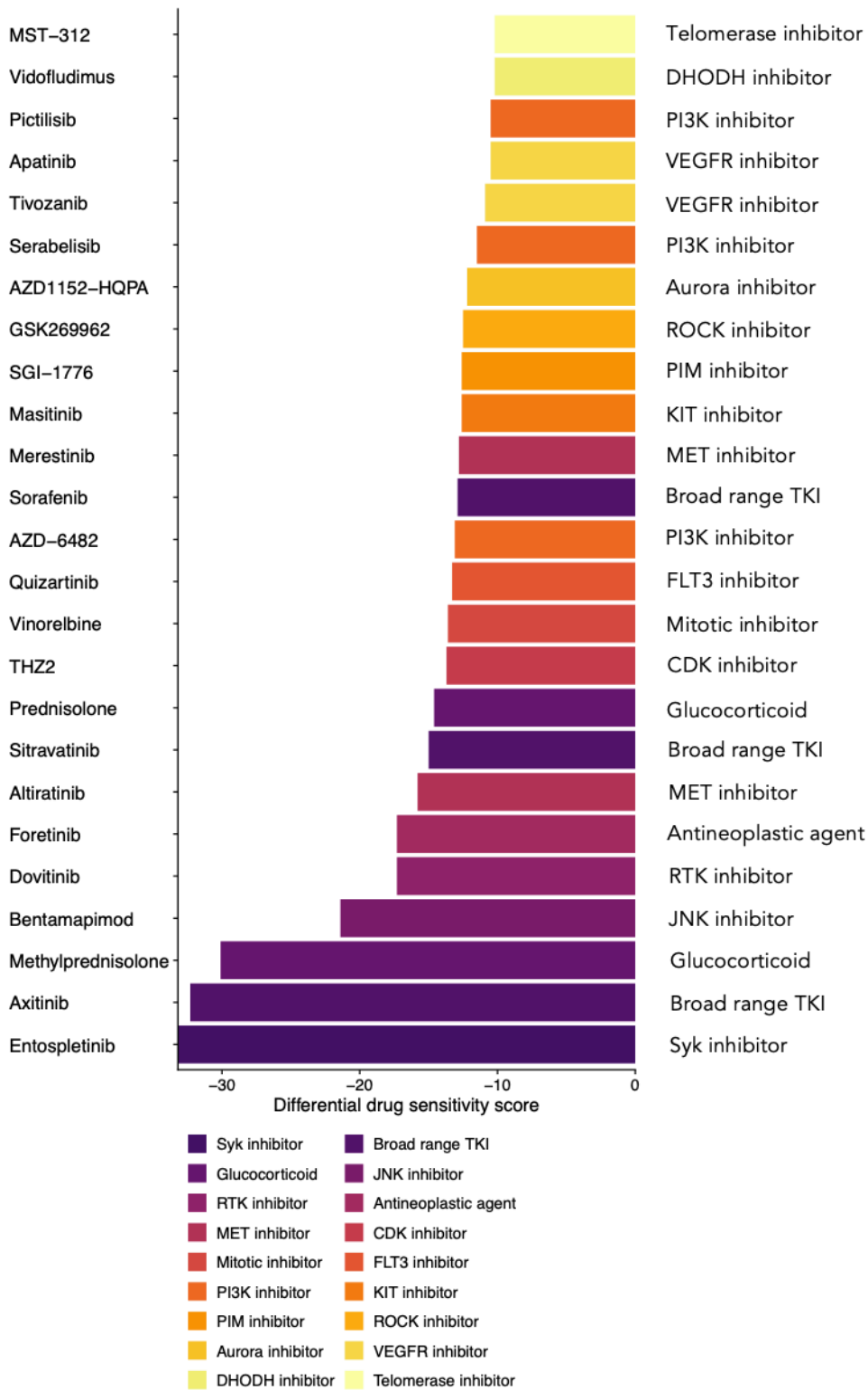


Figure 20. Bar plot of top inhibiting drugs in MOLM-14.

NK cells have an inhibitory effect of -10.0 sDSS on 27 drug compounds in the screening. However, many of these can be discarded due to errors on the data that can be observed by analysing the individual inhibition curves. A more thorough overview of the drugs that were considered as having been significantly inhibited by NK cells are displayed in Figure 20.

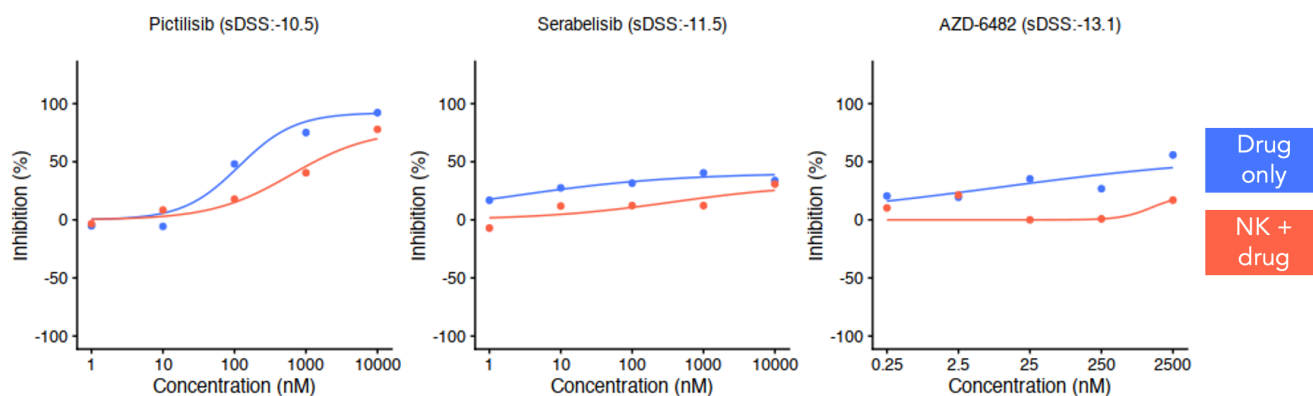


Figure 21. Inhibition curves of pictilisib, serabelisib and AZD-6482 in MOLM-14. The blue line represents the condition in which only MOLM-14 cells are cultured with the drug, whereas the red line is representative of MOLM-14 cells combined with NK cells and the drug.

Many of the drugs that are found to be inhibited by NK cells have a high inhibitory effect on the cancer cells on their own, which is decreased when NK cells are co-cultured with the target cells. Notable groups of compounds being adversely affected by NK cells include PI3K inhibitors, FLT3 inhibitors, and more broad range tyrosine kinase inhibitors. Pictilisib shows a decrease of 30% to 35% at 100 nM and 1000 nM concentrations respectively. Quizartinib for instance shows a decrease in inhibition of 10% to 20% across all concentrations in co-culture. Midostaurin is most significantly affected at 10 nM concentration, where a negative difference of 54.1% is observed when NK cells are combined with the drug.

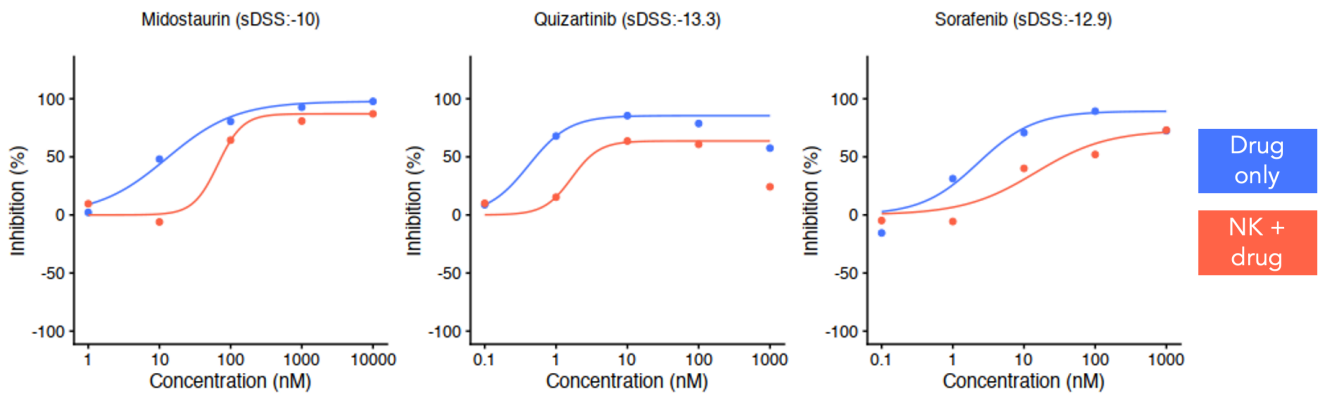


Figure 22. Inhibition curves of midostaurin, quizartinib and sorafenib in MOLM-14. The blue line represents the condition in which only MOLM-14 cells are cultured with the drug, whereas the red line is representative of MOLM-14 cells combined with NK cells and the drug.

4.2.3.2 THP-1

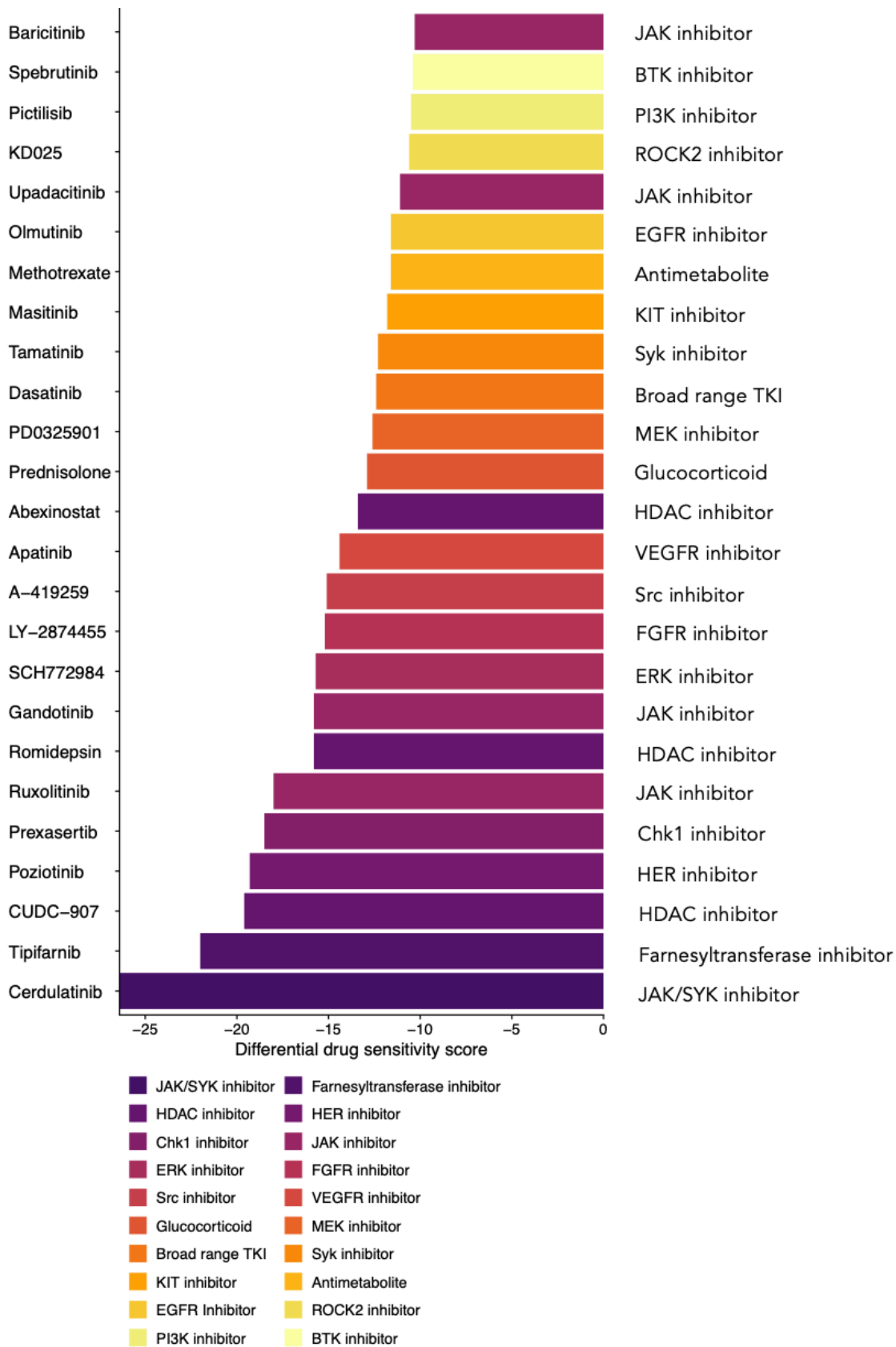


Figure 23. Bar plot of top inhibiting drugs in THP-1.

Out of 528 drugs screened for THP-1, 27 show a significantly negative sDSS score of -10.0 or lower. However, more detailed analysis of the findings reveals several drugs having abnormalities in the data, suggesting decreased reliability of the findings in these specific compounds.

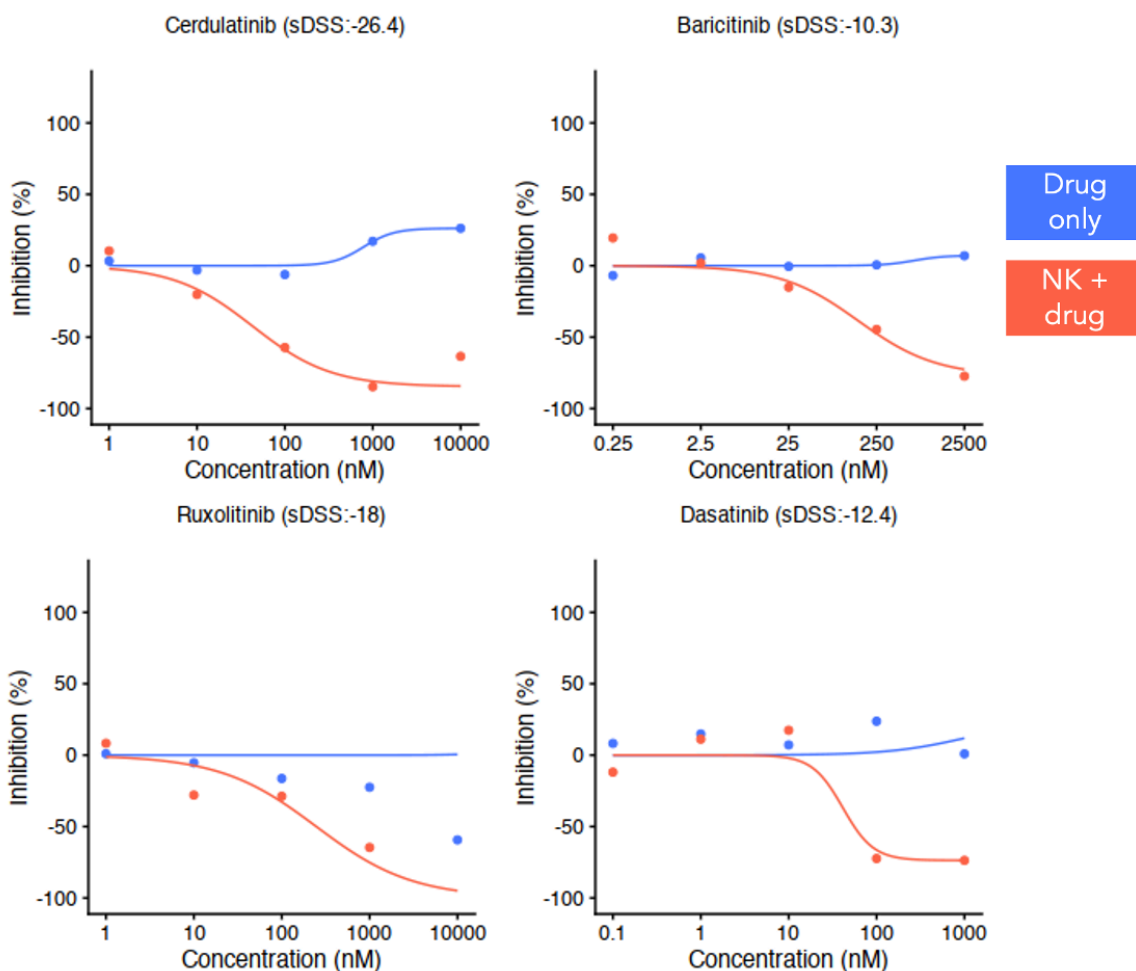


Figure 24. Inhibition curves of cerdulatinib, baricitinib, ruxolitinib and dasatinib in THP-1. The blue line represents the condition in which only THP-1 cells are cultured with the drug, whereas the red line is representative of THP-1 cells combined with NK cells and the drug.

The compounds with inhibiting effects in THP-1 can be divided into two distinct groups based on the way in which they seem to interact with NK cells to give a negative sDSS score. In one distinct group, including JAK inhibitors such as cerdulatinib, ruxolitinib and baricitinib, the drug alone has no effect on the target cells. However, in co-culture conditions the target cells seem to proliferate, which appears as a negative inhibition curve.

In addition to JAK inhibitors, A-419259, dasatinib, tamatinib, olmutinib, and spebrutinib show similar effects.

In the other group of drugs, the drug itself has an inhibiting effect on the target cells. When NK cells are added to the picture, the inhibiting effect of the drug is decreased, portraying as a shielding effect created by NK cells. This group of drugs include prexasertib, LY-2874455, PD0325901, methotrexate, pictilisib, selumetinib, and cobimetinib.

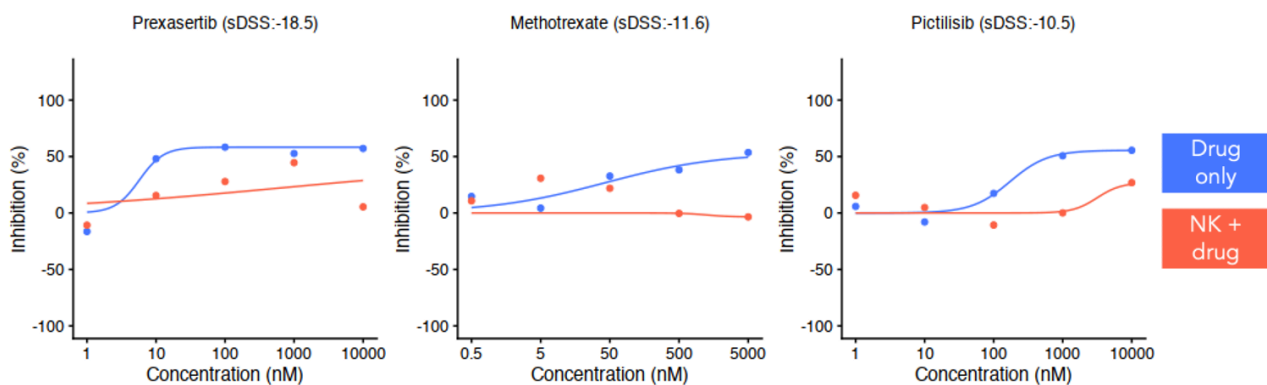


Figure 25. Inhibition curves of prexasertib, methotrexate and pictilisib in THP-1. The blue line represents the condition in which only THP-1 cells are cultured with the drug, whereas the red line is representative of THP-1 cells combined with NK cells and the drug.

4.2.3.3 HEL

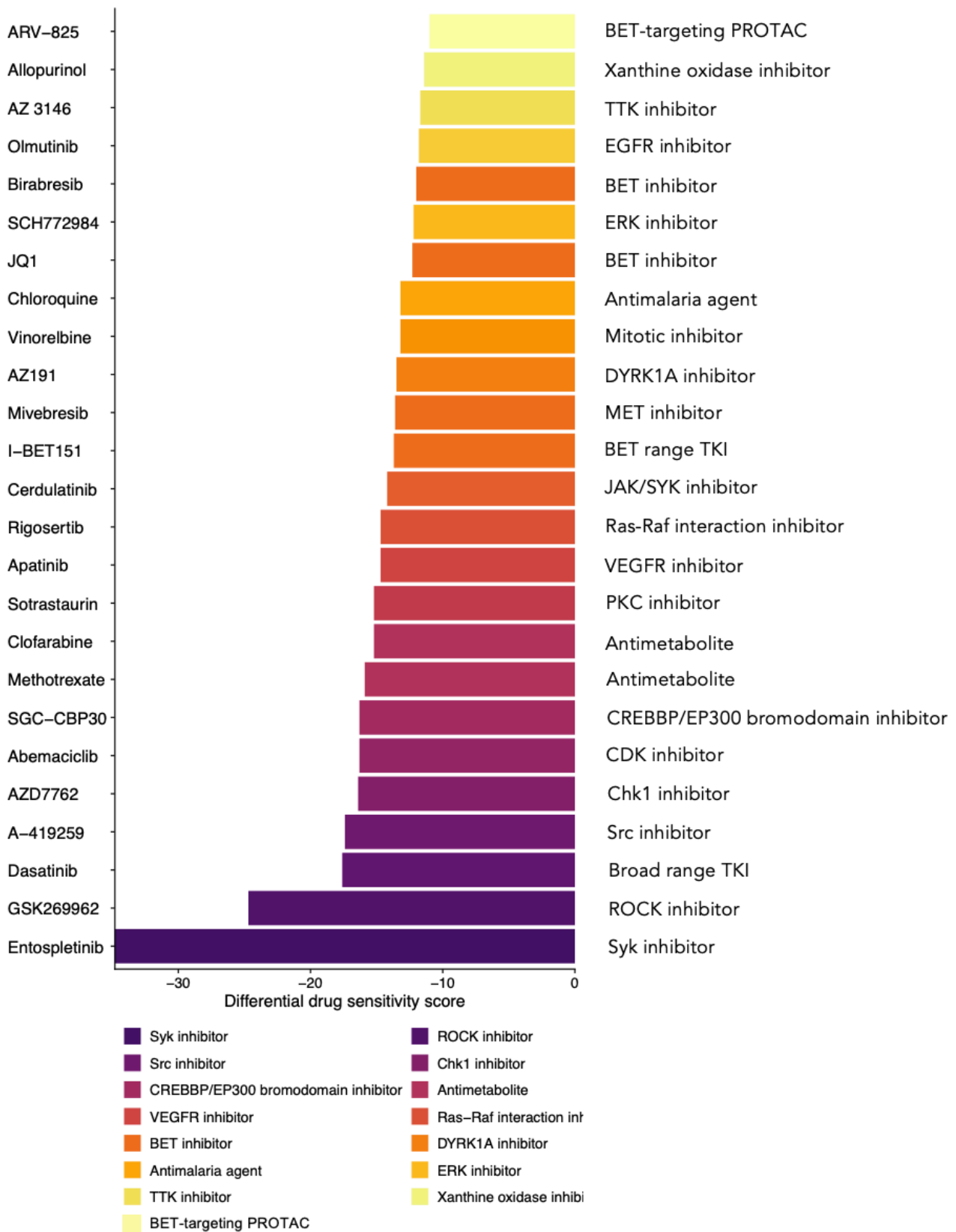


Figure 26. Bar plot of top inhibiting drugs in HEL.

Overall, 35 compounds give sDSS scores of -10.0 and below, although the analysis of inhibition curves reveals errors in how they have been determined, mostly due to measurement errors seen at individual conditions. Data from entospletinib misses data points in the “drug only” condition completely, in addition to the extremely low negative inhibition points. Similarly for ARV-825, the condition without NK cells is reported as exactly zero across all concentrations, which is unlikely to be the case. Clofarabine also shows some irregularities in both NK and no-NK conditions, for which the reliability of the data is hard to assess. In addition, apatinib is falsely reported with a highly negative sDSS score of -14.7, although the closer study of the data reveals significantly negative inhibitory effects at higher concentrations in the condition without NK cells, which are similar to the findings in the NK cell-containing condition. The same is observed in the case of rigosertib, vinorelbine, SCH772984, milciclib and dBET1.

More significant findings are seen in the case of GSK269962, dasatinib, AZD7762, chloroquine, olmutinib, AZ3146, fingolimod and palbociclib which have no effect on target cells on their own but following co-culture with NK cells induce proliferative activity seen as a strongly negative inhibition curve.

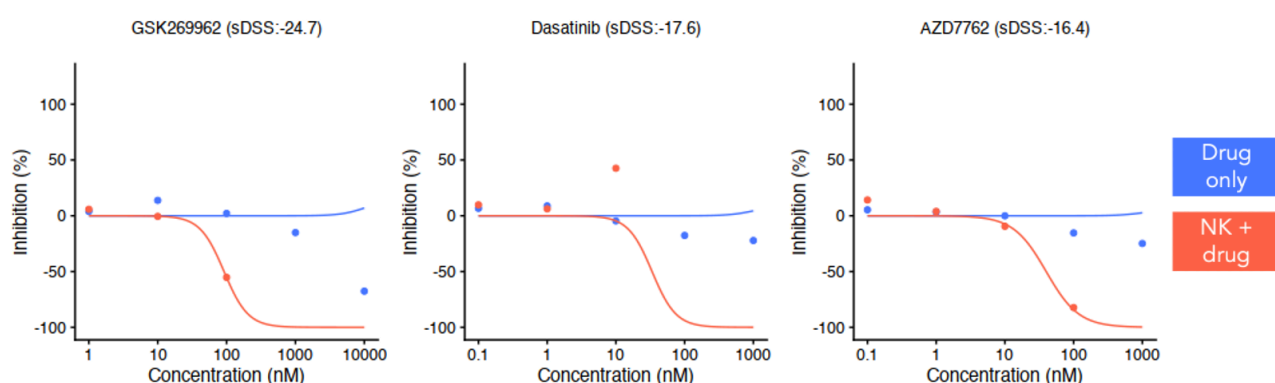


Figure 27. Inhibition curves of GSK269962, dasatinib and AZD7762 in HEL. The blue line represents the condition in which only HEL cells are cultured with the drug, whereas the red line is representative of HEL cells combined with NK cells and the drug.

Another group of drugs have some inhibiting effects on target cells, however co-culture with NK cells reverses anti-proliferative effects on target cells, leading to maintained or increased target cell viability. These drugs include abemaciclib, methotrexate, sotrastaurin, cerdulatinib, I-BET151, JQ1, birabresib, allopurinol and paclitaxel. In these drugs, we hypothesise that cytokines produced by NK cells may interfere with the mechanisms of action of these drugs, leading to unwanted proliferative activity. Mivebresib, on the other hand, shows high inhibitory effect when administered to HEL cells on its own, but NK cells seem to shield target cells from its function, leading to a decreased inhibitory effect.

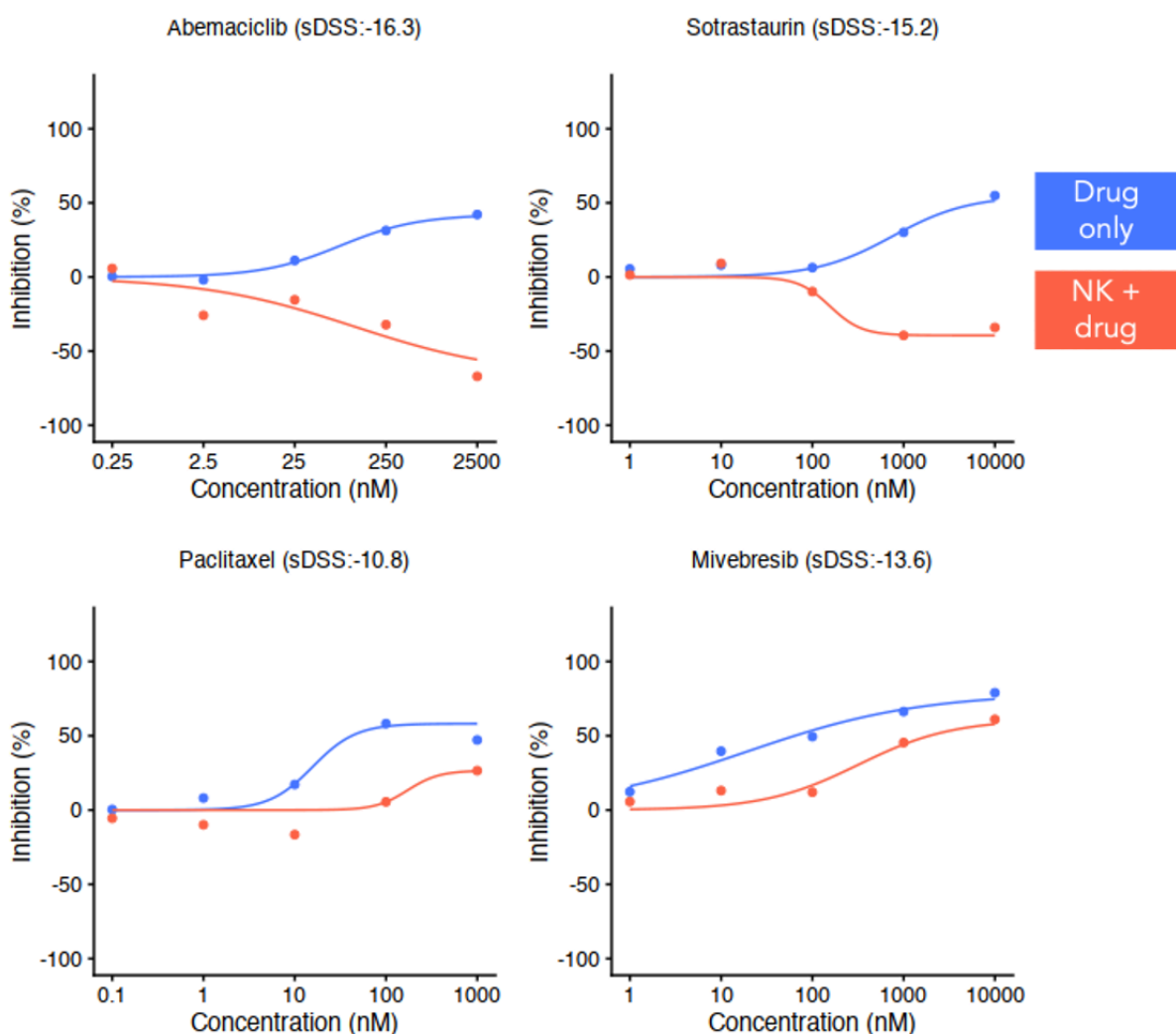


Figure 27. Inhibition curves of abemaciclib, sotrastaurin, paclitaxel and mivebresib in HEL. The blue line represents the condition in which only HEL cells are cultured with the drug, whereas the red line is representative of HEL cells combined with NK cells and the drug.

4.3 Single cell RNA sequencing of MOLM-14

To add more information on what was observed in high-throughput DSRT, single cell RNA sequencing (scRNA seq) was performed on the MOLM-14 cell line. ScRNA seq was hoped to reveal biological mechanisms affected by interactions between NK cells, target cells and drugs.

4.3.1 Drug selection for transcriptomic analysis and validation experiment

Based on DSRT results, daporinad, pevonedistat, ruxolitinib, midostaurin, pictilisib and quizartinib were selected for further analysis using scRNA seq methods combined with oligo-tagged antibodies, enabling multiplexing and improved doublet detection. In the drug screening data, daporinad and pevonedistat both showed significant increases in MOLM-14 killing when co-cultured with NK cells, a finding shared with THP-1. These strong effects shared across different cell lines was considered significantly important for further investigation. Ruxolitinib, forming part of a number of JAK inhibitors having an activating effect over NK cells, was selected due to its wider use in clinical settings as compared to other compounds of the same family such as baricitinib. On the side of inhibitory effect-inducing drugs, pictilisib was chosen out of several PI3K inhibitors to study the effect of such compounds on NK cell cytotoxicity. Midostaurin and quizartinib were chosen for further investigation due to their shared target, FLT3. We hypothesised that, due to the *FLT3-ITD* mutation present in MOLM-14, the drugs are effective at targeting this pathway to induce a killing effect, but the target cells can be shielded by NK cells from their effect. Quizartinib, a more FLT3 affinitive compound was chosen to give further details on the specific role of FLT3, whereas midostaurin, a more widely used broad range tyrosine kinase inhibitor, was chosen due to its wider clinical application.

Prior to proceeding to single cell experiments with drug compounds of interest, findings from drug screenings were validated and effector-target ratios were revised to compensate for the change in donor of expanded NK cells used in the experiment. Co-cultures with

target cells and the new set of NK cells, followed by viability measurements, revealed an effector-target ratio of 1 to 4 capable of achieving 50 percent inhibition of target cell viability. This confirmed the change from the originally used 1 to 1 effector-target ratio to a 1 to 4 ratio for the single cell experiment to make sure there are enough cells for the sequencing. In addition to revising the effector-target ratio, the viability measurements with target cells, NK cells and drugs confirmed the findings from screenings, indicating that daporinad, pevonedistat and ruxolitinib increase target cell killing when in co-culture with NK cells. In addition, the experiment confirmed the inhibitory effects of pictilisib, quizartinib and midostaurin on NK cell cytotoxicity towards target cells.

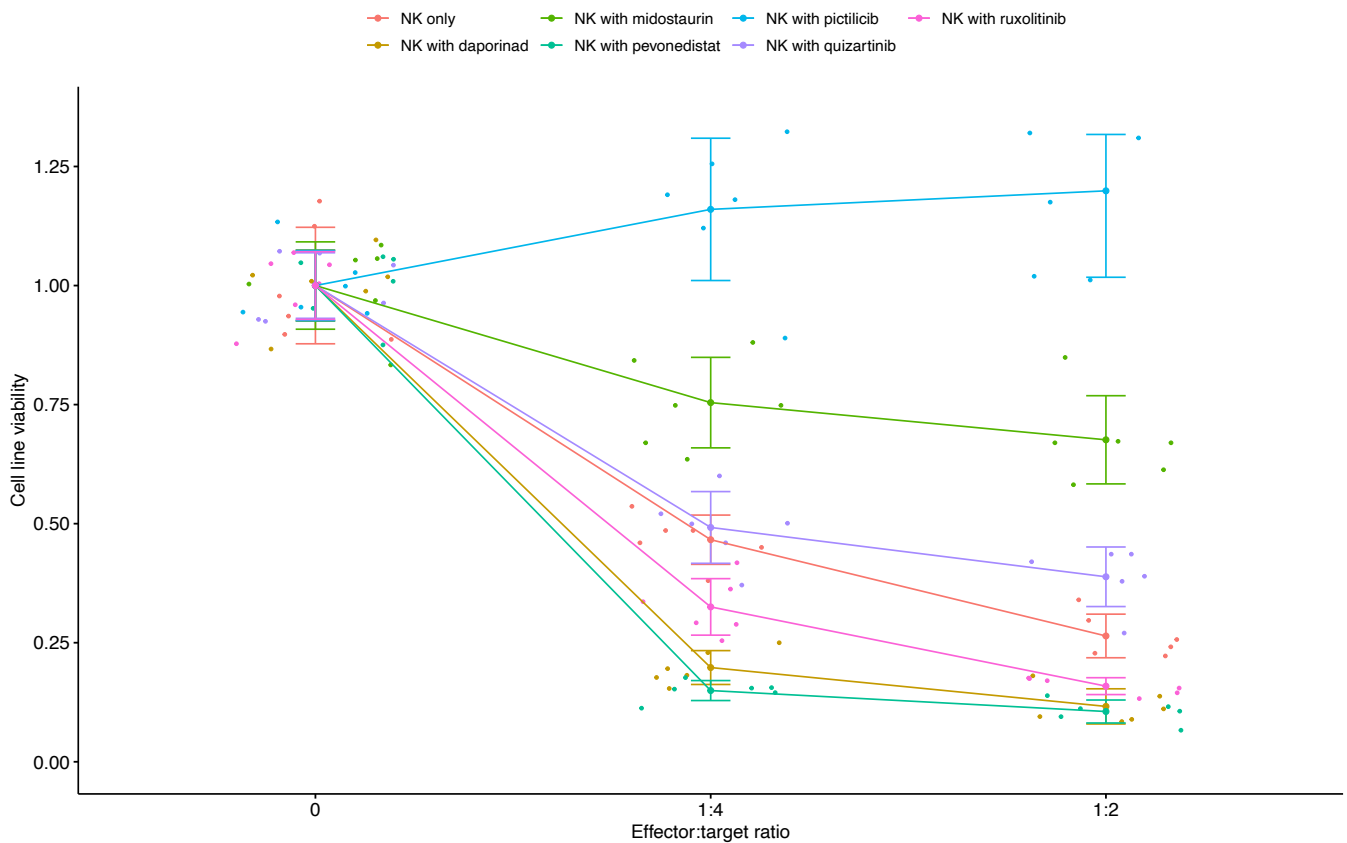


Figure 28. Inhibition curves of pre-hashing optimisation experiment. At 1:4 effector-target ratio, the inhibition with NK cells is 50%. In addition, the results confirm findings from DSRT, where in MOLM-14 daporinad, pevonedistat and ruxolitinib enhance target cell killing, whereas pictilisib, midostaurin and quizartinib have reduced effects when co-cultured with NK cells.

4.3.2 MOLM-14 scRNA data analysis

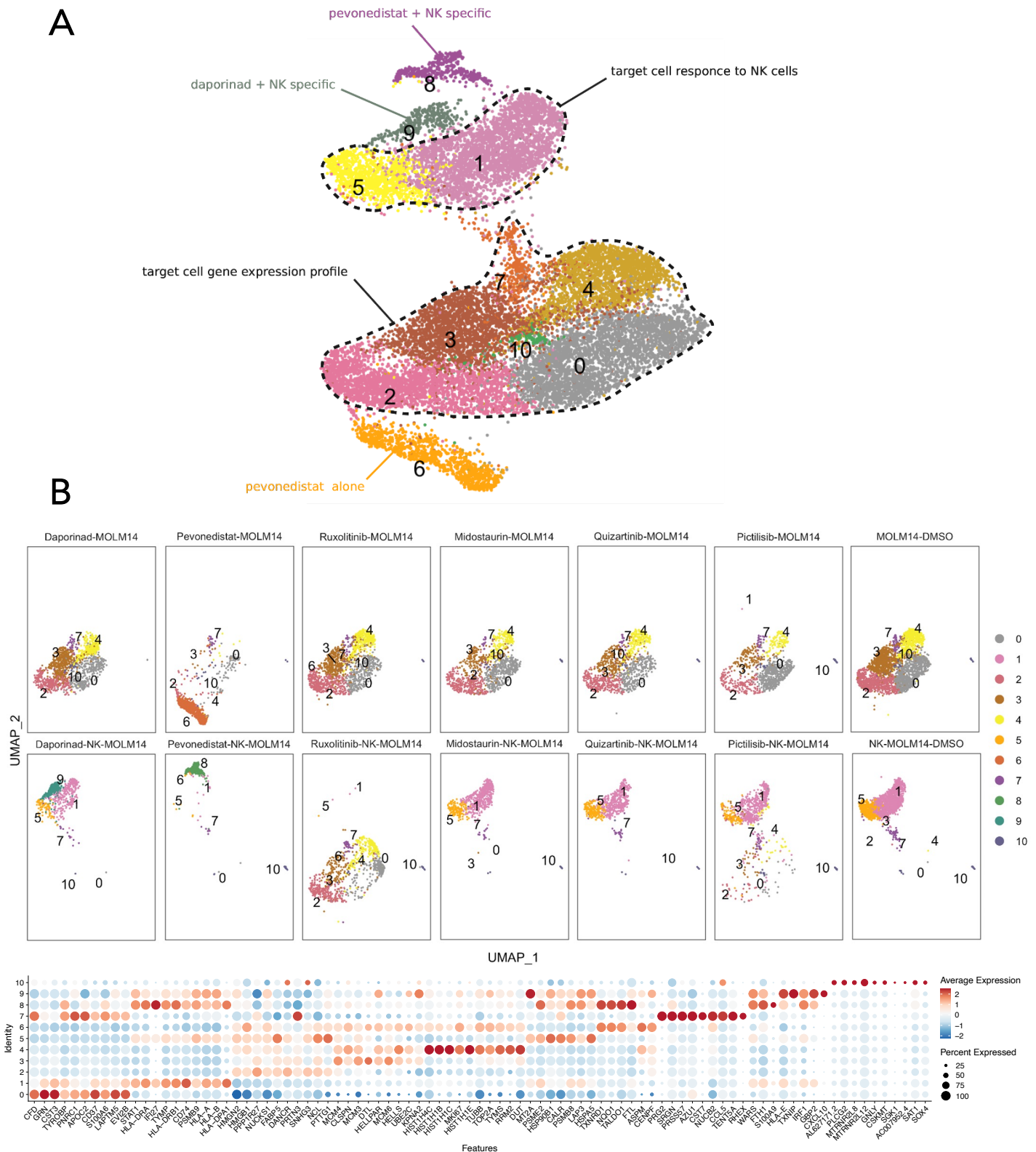


Figure 28. Analysed scRNA sequencing data of MOLM-14 cells. UMAP of MOLM-14 cells based on the condition to which the cells were cultured in (A). The transcriptomic profile can also be compared between drugs and controls (B), where distinct changes occur in daporinad, pevonedistat and

ruxolitinib. Differential gene expression in different clusters can reveal why changes in target cell viability occur when co-cultured with NK cells and drugs (C).

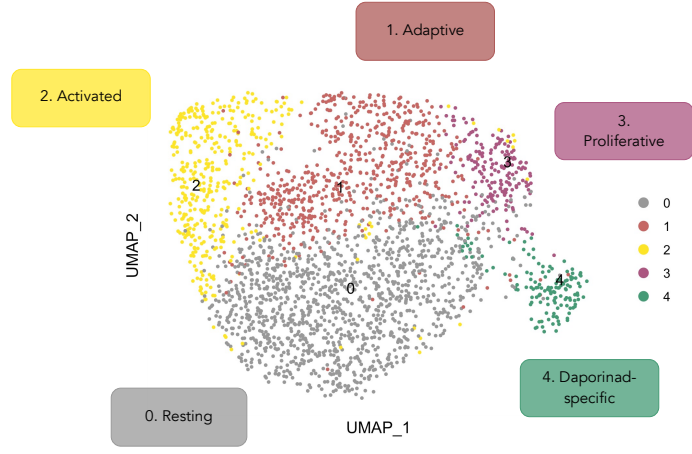
To effectively study the transcriptomic data and changes occurring due to interactions with drugs and NK cells, the single cell data was divided into two groups – NK cells and MOLM-14 cells. This allowed for detailed analysis of the transcriptomic landscape and the specific effects seen in the different cell types. As a consequence, separate clustering and UMAPs were created for NK cells and MOLM-14 cells and the differential gene expression was calculated by comparing cell-specific clusters. As described in Figure 28, a range of difference arise as different drugs are applied to target cells. These differences become increasingly more apparent as NK cells are co-cultured with target cells in the presence of selected drug compounds.

Generally, when drugs are administered to MOLM-14 cells alone, the transcriptomic profile remains very similar across all drugs. However, pevonedistat is an exception to these as some differences already occur when it is administered to MOLM-14 cells without NK cell co-culture. In this condition, genes such as *TXNRD1*, *NQO1* and *TALDO1* are increasingly expressed in most cells, and relatively little of the normal transcriptomic profile, seen in the control condition with target cells only, remains. In the control condition with MOLM-14 cells and DMSO only, cells form smaller clusters depending on the activated genes of different cells within the group of MOLM-14 cells. These represent characteristic features of the target cell line, with proliferation related genes such as *GRN* and *MKI67* being increasingly expressed. In addition, *CD37*, a leukaemia-related gene is also highly expressed in the major cluster within MOLM-14 cells.

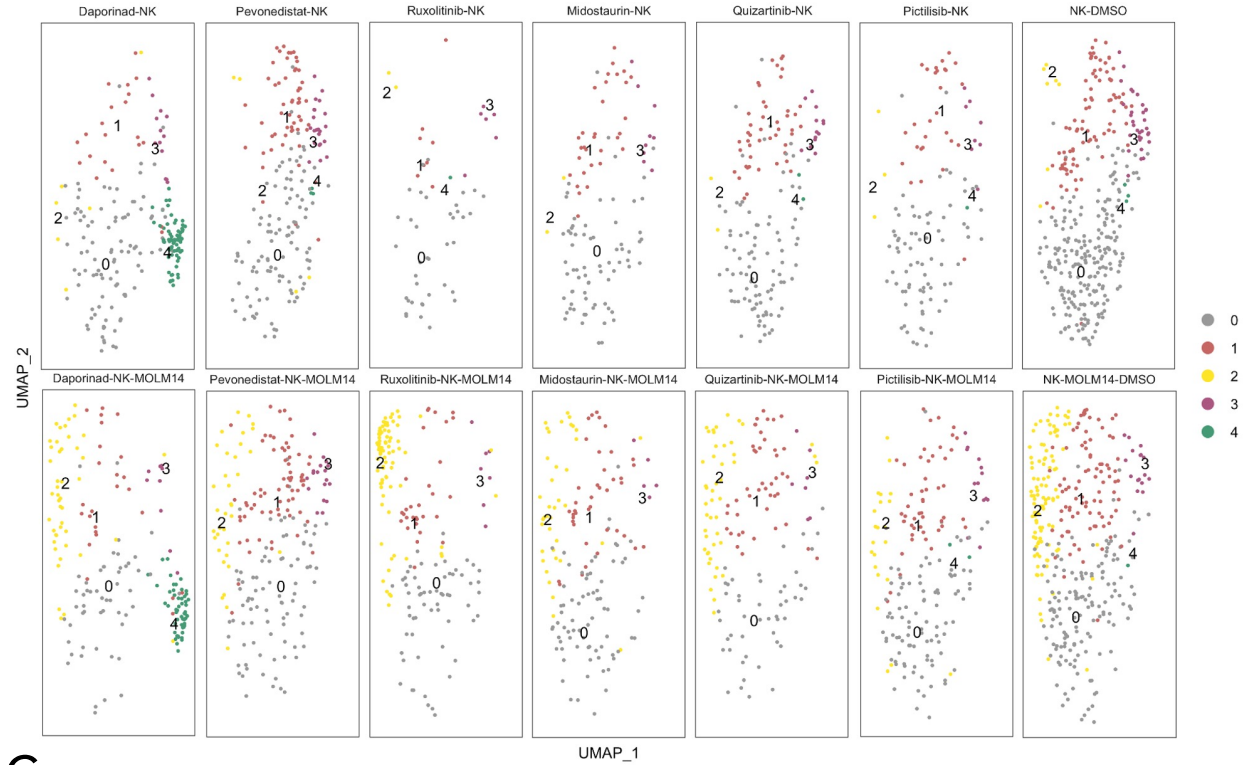
The addition of NK cells into culture with target cells results in a change in the genetic expression of MOLM-14 cells. Co-culture of target cells with NK cells results in an increase in expression of HLA-encoding genes, lysozyme-encoding *LYZ* gene, Heat Shock Protein (HSP) family protein-encoding genes as well as *PTTG1*. A similar effect is observed with the addition of midostaurin, pictilisib or quizartinib, where a signature consisting of clusters 1,

5 and 7 form the NK cell activated MOLM-14 gene expression profile. Compared to midostaurin and quizartinib, pictilisib has a less significant effect on the target cell gene expression as some cells remain in their natural form. The addition of daporinad into the co-culture of NK cells and MOLM-14 cells also changes the transcriptional profile to form clusters 1, 5, 7 and 9. Cluster 9, a daporinad-specific cluster of genes is created in response, with upregulated *CXCL10*, *HLA-E*, *MT2A*, *TXNIP*, *IRF1* and *CBP2*. Like daporinad, pevonedistat also results in a significantly different genetic expression profile when added into co-culture conditions. In pevonedistat-specific clusters 6 and 8, genes such as *IFI27*, *TXNRD1*, *NQO2*, *TALDO1*, *FTL*, *GCLM*, *S100A9*, *WARS*, and *FTH1* are upregulated. Unlike other drugs, ruxolitinib does not induce a major change in gene expression when added into co-culture with NK cells and MOLM-14 cells. Its co-culture gene expression profile is very similar to that of MOLM-14 alone, and comparable to that of ruxolitinib with MOLM-14 alone.

A



B



C

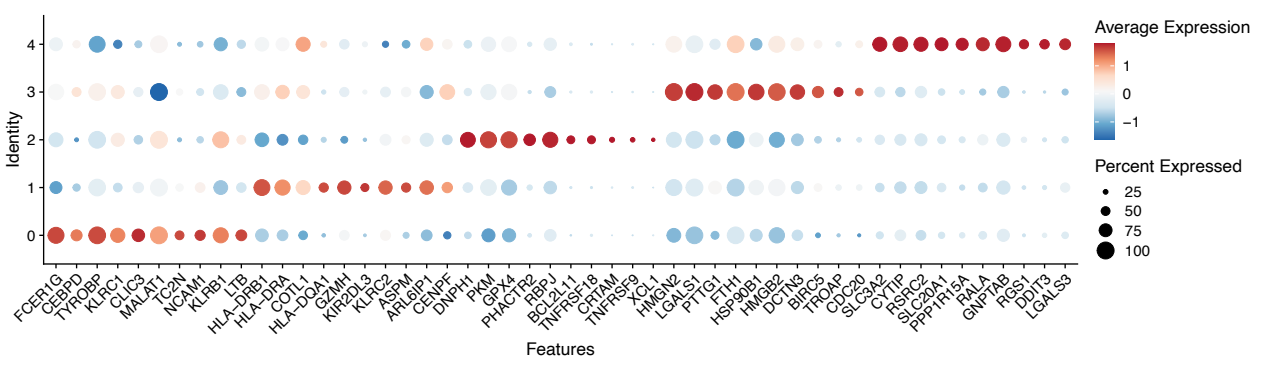


Figure 29. Analysed scRNA sequencing data of NK cells. UMAP of NK cells can be divided into sections based on the gene expression (A). The transcriptomic profile can also be divided according to NK-only and NK-MOLM-14 co-culture conditions (B), where distinct changes occur in daporinad as a

daporinad-specific cluster is formed. Differential gene expression in different clusters can reveal why changes in target cell viability occur when co-cultured with NK cells and drugs (C).

According to the transcriptional profile, the NK cell gene expression profile can be broken down into clusters representing certain populations of NK cells (Figure 29). *KLRC1* and *KLRB1* genes mark for NK cells in resting state and are described as cluster 0, whereas cluster 1 includes adaptive NK cells, with *KLRC2* as well as different KIR and HLA-related genes. *TNFRSF18*, *TNFRSF9* and *BCL2L11* upregulation in cluster 2 indicate an activated NK cell population, with activated cytokine signalling pathways. Despite of phase correction at analysis phase, cluster 3 reflects a distinctly proliferative NK cell population with *LGALS1* and *BIRC5* upregulation being indicators of this effect. Notably, cluster 4 represents a daporinad-specific transcriptional profile, with strong *CYTIP* upregulation indicating activated NK cells.

The most notable effect in NK cell transcriptional profile is seen in daporinad-including cultures, where a distinctive cluster appears. This daporinad-specific transcriptional profile is expressed in both daporinad-NK and daporinad-NK-MOLM14 conditions, indicating daporinad's effects on the NK cell population. Moreover, upon addition of target cells into co-culture conditions, a cluster appears, indicating NK cell activation including the transcription of genes such as *TNFRSF18*, *TNFRSF9* and *BCL2L11*.

Pevonedistat, on the other hand, has a transcriptional profile relatively similar to the NK control condition, with increase of activated NK cells when target cells are introduced. Ruxolitinib alone, appears to have anti-proliferative effects on NK cells, which can be noted as the decreased cell count when administered to NK cells alone. However, high numbers of NK cells are activated when co-cultured with target cells, leading to decrease of target cell viability. Midostaurin, pictilisib and quizartinib all have a very similar transcriptional profile across the board, with slight activation of NK cells being observable when co-cultured with target cells.

4.4 Drug-specific effects and further analysis

DSRT data reveals specific compounds and drug targets which give rise to significant effects in target cell inhibition and proliferation. Combining this with transcriptomic data analysis and existing knowledge on the drugs' functions can help determine the underlying mechanisms of action in addition to revealing potential enhancers of NK cell cytotoxicity in NK cell-based immunotherapy approaches.

4.4.1 Pevonedistat activates NK cell mediated killing in both MOLM-14 and THP-1

Pevonedistat, also known as MLN4924, is a NEDD8-activating enzyme (NAE) inhibitor, which works by promoting apoptosis of dividing cells through deregulating S-phase DNA synthesis.¹¹⁰

In DSRT data, pevonedistat shows a high sDSS score, indicating that the drug, when applied to the target cells together with NK cells, has an improved killing effect on the cancer cells. Although the drug itself already has an inhibitory effect on the target cell proliferation and function, when combined with NK cells the effect is significantly larger. The effect is even more significant in THP-1, with which the full inhibitory effect is only seen when NK cells and the drug are applied together. This effect could be explained by the TNF- α that is generally known to be released by NK cells, although its levels were not measured as part of this study. It has been shown that TNF- α synergises with pevonedistat to induce apoptosis, which could lead to effects observed in our findings. Therefore, it could be considered that NK cells themselves do not result in the increased killing of the target cells, but rather the compound released by them to activate apoptosis-inducing signalling pathways.

Gene differential expression analysis from scRNA sequencing highlights that an activating effect is observed in NK cells when co-cultured with MOLM-14 cells, although the effects

are similar when pevonedistat is not added to the culture. However, the transcriptomic landscape of target cells is more significantly affected, with significant changes observed when compared to the normal target cell transcriptomic profile. Pevonedistat alone, when administered to MOLM-14 cells, significantly upregulates the transcription of *NQO1*, *TXN*, *TXNRD1* and ferritin-related genes such as *FTL* and *FTH1*. In addition, the monocyte specific *LYZ* gene is notably downregulated. In co-culture with NK cells, pevonedistat induces significant downregulation of *MYC* proto-oncogene, which could serve as an explanation to the inhibitory effect observed in DSRT. In addition, the *FLT3-ITD* mutation occurring in MOLM-14 seems to become a target when NK cells are co-cultured with MOLM-14 cells, as *FLT3* is downregulated by the addition of pevonedistat when compared to control conditions.

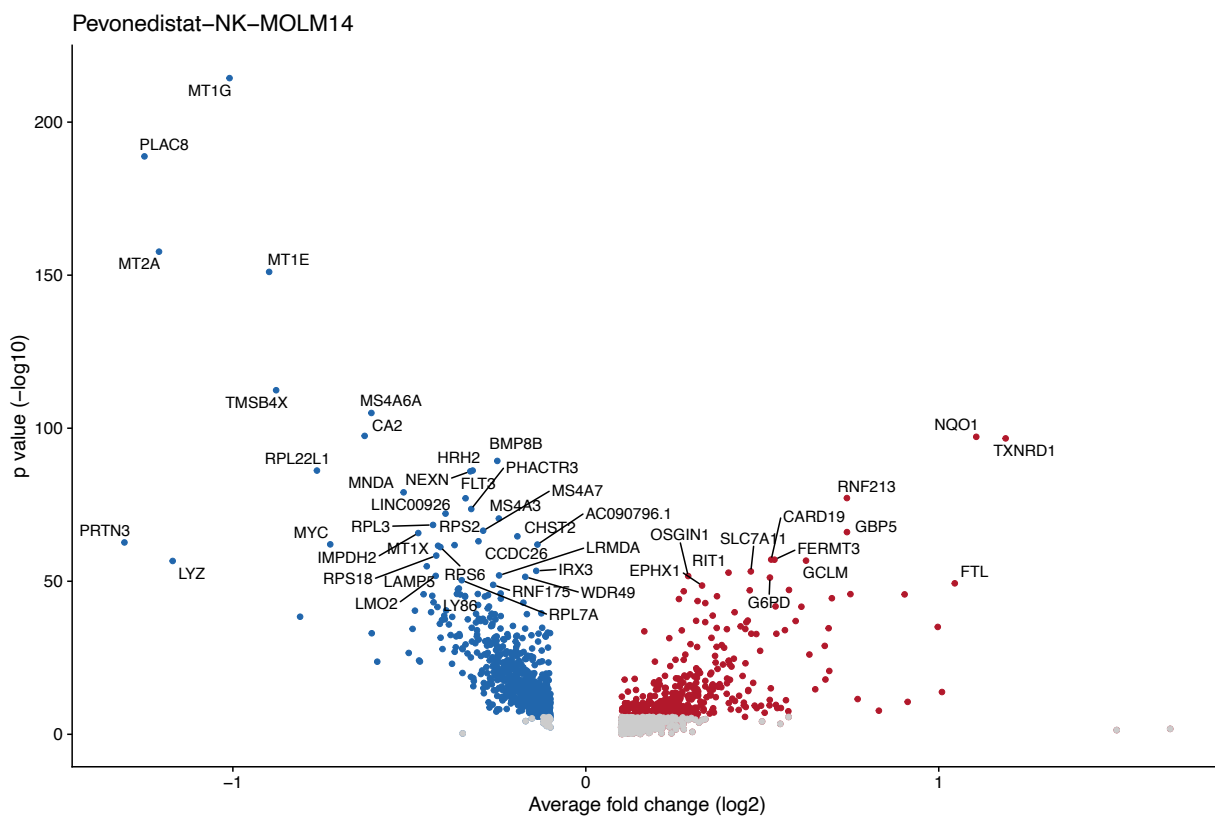


Figure 30. Volcano plot representation of differentially expressed genes in pevonedistat-NK-MOLM-14 co-culture. Comparison of NK-MOLM-14-DMSO control condition versus pevonedistat-NK-MOLM-14 co-culture to highlight effects of pevonedistat on the MOLM-14 transcriptome.

4.4.2 Daporinad enhances NK cell cytotoxicity in MOLM-14 and THP-1

Daporinad is a small molecule drug that targets the nicotinamide phosphoribosyltransferase (NMPRTase). By inhibiting NMPRTase, it inhibits the biosynthesis of niacinamide and nicotinamide adenine dinucleotide (NAD⁺), which in turn can deplete the energy reserves of metabolically active tumour cells, leading to apoptosis. In addition to these effects, daporinad has potential antineoplastic and antiangiogenic activities.¹¹¹

In the DSRT results, daporinad can be seen to enhance NK cell induced cytotoxicity in both MOLM-14 and THP-1 cell lines. In both cell lines, the drug itself does not seem to influence the cancer cells but when co-cultured with NK cells, the inhibition rises to 50% at 100 nM drug concentration. However, no effects are seen in the HEL results, which implicates that the effect is not extended to acute leukaemias of erythroid origin. This could suggest that MOLM-14 and THP-1 cell lines are more sensitive to changes in the energy levels within the cells and are therefore more prone to NK cell induced killing. Single cell RNA sequencing reveals interesting findings in the transcriptomic data, supporting the DSRT findings by shedding light on daporinad-specific gene regulation.

The transcriptomic data suggests that daporinad does not affect MOLM-14 cell on its own, but its inhibiting activity requires NK cells. This can be seen as a MOLM-14 transcriptomic profile relatively similar to control conditions when only daporinad is added to the culture. However, daporinad alone with NK cells creates changes in the gene expression by upregulation of *CYTIP*, *GNPTAB*, *SLC3A2* and *RSRC2*. In addition, when NK cells are co-cultured with MOLM-14 cells together with daporinad, a separate cluster appears in both NK cell and target cell transcriptional profiles presented as UMAPs. In co-culture conditions, NK cells show activation-related transcriptomic changes through the upregulation of *BCL2L11* and *TNFRSF9* for example, in addition to upregulated genes already observed in NK cells cultured with daporinad alone. Moreover, in MOLM-14, daporinad upregulates the gene expression of *HLA-E*, in addition to *CXCL10* known for its role in NK cell

chemoattraction and activation as response to IFN- γ . In addition, tumour suppressor genes such as *TXNIP* and *IRF1* are also upregulated in response to daporinad and NK cells.

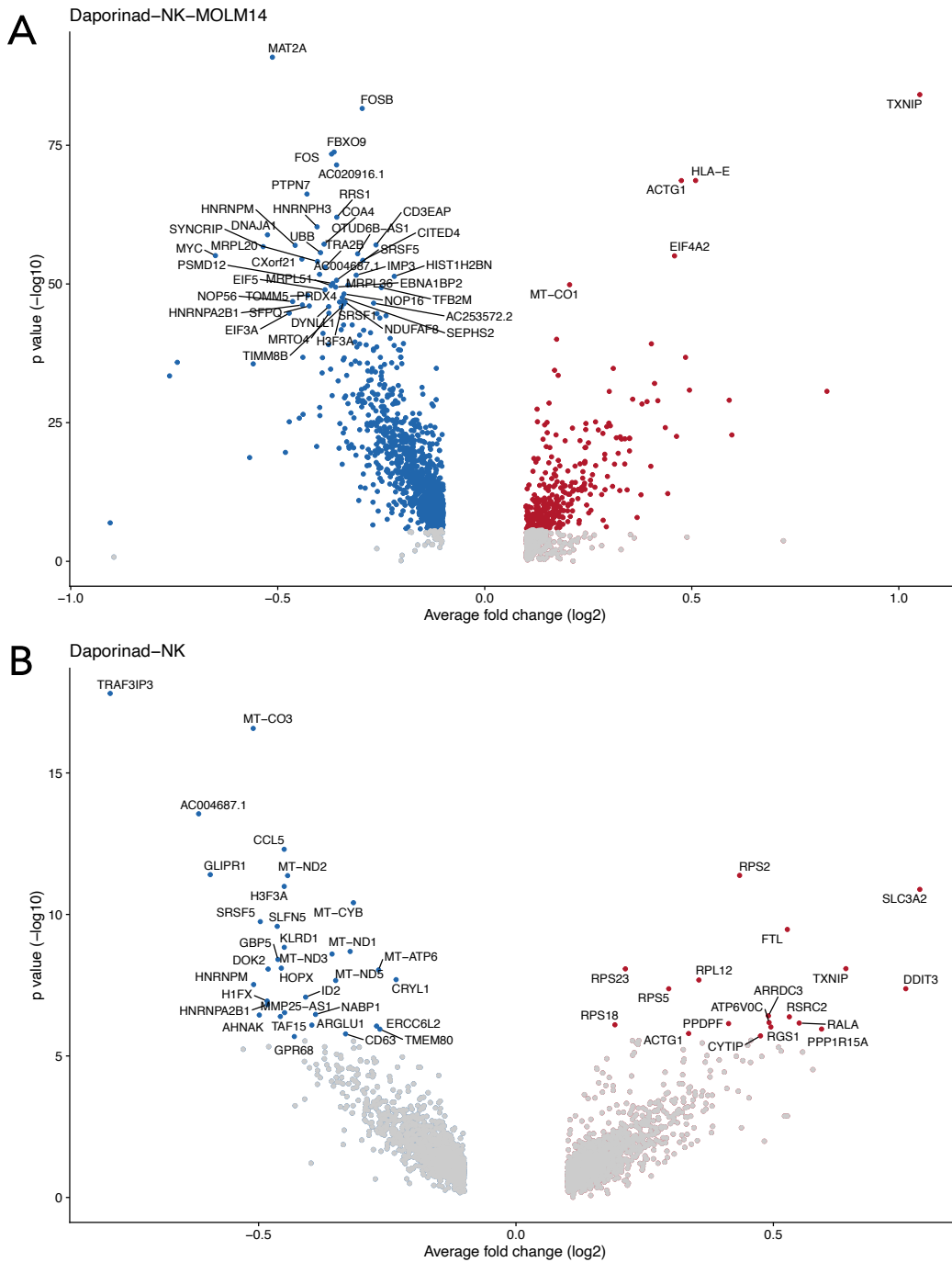


Figure 31. Volcano plot representation of differentially expressed genes in MOLM-14 and NK cells after co-culture with daporinad. Comparison of NK-MOLM-14-DMSO control condition versus daporinad-NK-MOLM-14 co-culture to highlight effects of daporinad on the MOLM-14 transcriptome (A). NK cell transcriptome shows also effects when comparing NK-DMSO to NK-daporinad co-culture (B).

4.4.3 Effect of JAK inhibitors are cell line dependent

Janus kinase (JAK) inhibitors such as baricitinib, ruxolitinib and tofacitinib function by interfering with the JAK/STAT signalling pathway through inhibition of the activity of one or more of the JAK enzymes. More specifically, baricitinib and ruxolitinib target JAK 1 and 2, whereas tofacitinib targets JAK 1 and 3.¹¹²

In the DSRT testing, JAK inhibitors have a varied effect depending on the cell line. In MOLM-14, the drug alone has no effect but when cultured with NK cells, a killing effect is observed at higher drug concentrations. However, in THP-1 the effect is opposite, with negative sDSS scores as low as -18.0 in the case of ruxolitinib. With all drugs, no effect is observed with the drug alone, but when cultured with NK cells the target cells seem to proliferate increasingly. In the case of HEL, a similar killing effect is observed both with and without NK cells, with DSS scores as high as 14.4 in the case of ruxolitinib, although the sDSS score is only 0.3 with the same drug. This can be explained by the genetic profile of the HEL cell line, where a *JAK2* mutation is present. By inhibiting the JAK/STAT signalling pathway in HEL, a killing effect can be observed, which is not affected by NK cells.

Single cell RNA sequencing was hoped to give more information on how ruxolitinib affects NK cells and MOLM-14 cells to enhance target cell killing. However, compared to daporinad and pevonedistat, no distinct transcriptional changes were observed, when looking at the overall transcriptional profile of MOLM-14 and NK cells in co-culture conditions. Nevertheless, NK cell activation was observed in NK cell co-cultures with MOLM-14 including ruxolitinib, with differential gene expression analysis showing significant downregulation of *IFI27*, *IRF1* and HLA class I-encoding genes when compared to control conditions. This finding supports findings made in previous studies, where JAK signalling pathways have been shown to play a role in MHC class I receptor expression.¹¹³ More specifically, IFN- γ signaling has been shown to result in activation of JAK and STAT signaling pathways, which are in turn critical at regulating MHC class I molecule expression,

which is crucial for NK cell recognition. By blocking the JAK/STAT pathway, target cells fail to express HLA class I molecules on the cells' surface, leading to "non-self" recognition by NK cells. However, this hypothesis does not support the findings in THP-1, for which specific scRNA sequencing experiments should be performed.

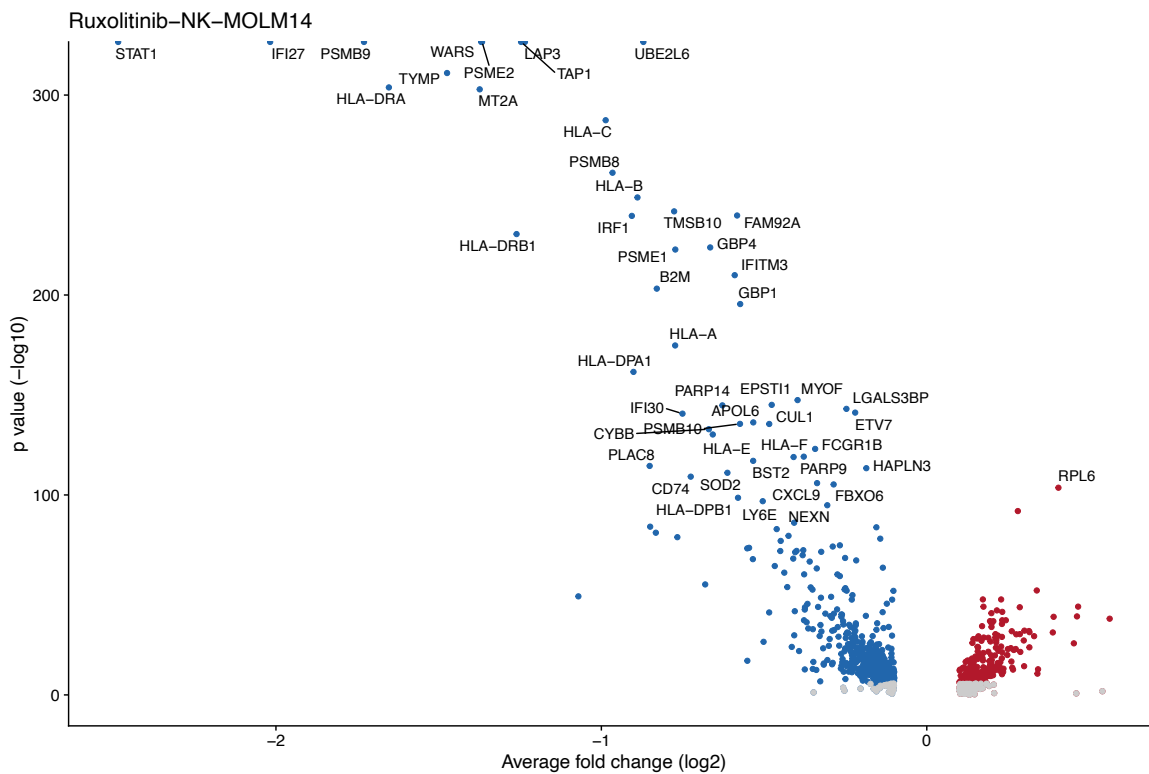


Figure 32. Volcano plot representation of differentially expressed genes in MOLM-14 after co-culture with ruxolitinib. Comparison of NK-MOLM-14-DMSO control condition versus ruxolitinib-NK-MOLM-14 co-culture to highlight effects ruxolitinib on the MOLM-14 transcriptomic profile.

4.4.4 Tacrolimus strongly activates NK cell cytotoxicity in HEL cell line

Previous studies combining CAR-T therapy and oncology drugs has shown tacrolimus to be highly inhibiting with regards to CAR-T activity.⁴¹ However, in the case of NK cell in combination with tacrolimus in targeting HEL cells, the effect is the opposite, with 50 percent inhibition achieved only with the combination of the drug and NK cells. However, no effects are seen in other cell lines, indicating that the effect is specific to erythroleukemia. As scRNA sequencing was only performed on MOLM-14 at this stage, the

transcriptomic data cannot be investigated to get a better picture of the underlying mechanisms.

4.4.5 PI3K inhibitors have an inhibitory effect on NK cell cytotoxicity in MOLM-14

DSRT results reveal that NK cells inhibit the effect of phosphoinositide 3-kinase (PI3K) inhibitors such as pictilisib, serabelisib and AZD-6482 in MOLM-14. PI3Ks signal downstream of G protein coupled receptors and GTPases to control cellular functions such as proliferation and metabolism. In MOLM-14, the drugs alone have a higher effect on the cancer cells than when cultured together with NK cells.

In THP-1, pictilisib has a similar effect with an sDSS score of -10.5. However, other PI3Ks do not seem to affect the cell line anti-proliferatively and hence NK cells do not seem to affect their function. A similar effect is seen in HEL with pictilisib, although the sDSS score is only negative at -5.0, which may not be interpreted as a significant finding.

Prior to scRNA sequencing, we hypothesised that NK cells may be shielding target cells from PI3K function, therefore resulting in a decreased inhibitory effect by the drug. Although differential gene expression analysis, when comparing the drug-NK-MOLM-14 condition to NK-MOLM14-DMSO, revealed moderate upregulation of *RPL5*, *RPL13* and *RPL14* in addition to downregulation of *WARS* and *IFI27* genes, these fail at providing a clear answer to protective effect NK cells seem to have at keeping target cells shielded from the drug.

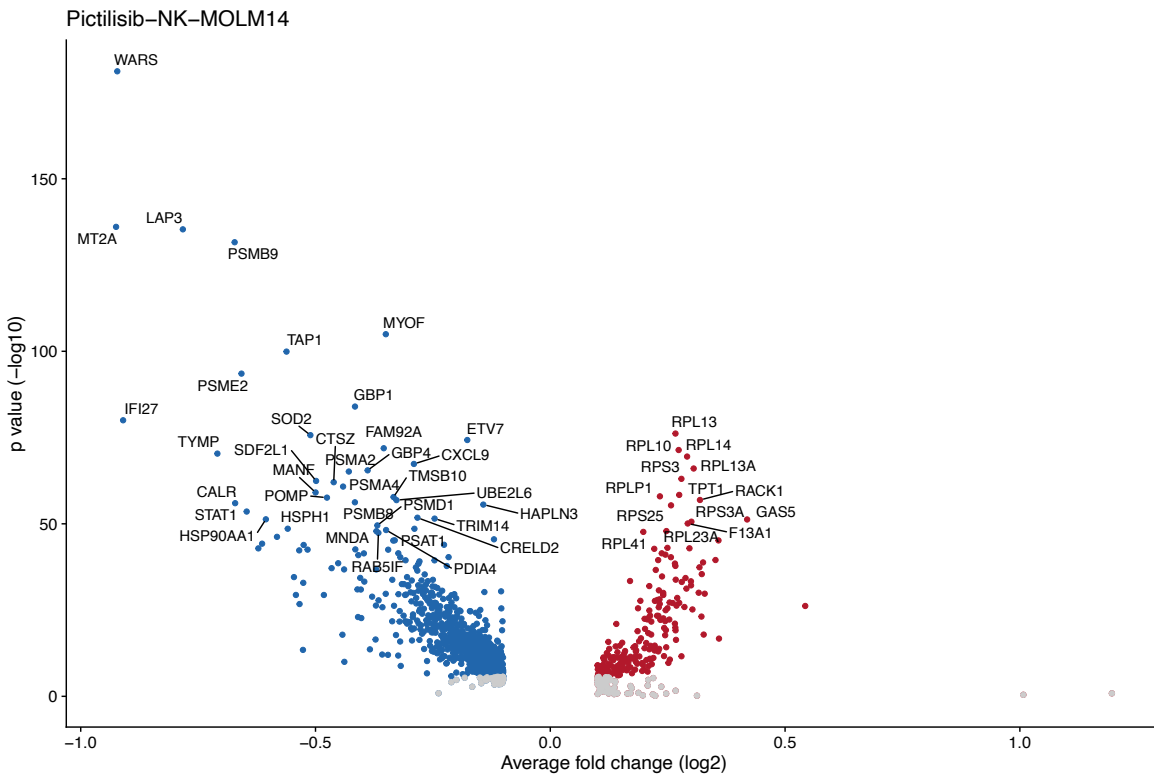


Figure 33. Volcano plot representation of differentially expressed genes in MOLM-14 after co-culture with pictilisib. Comparison of NK-MOLM-14-DMSO control condition versus pictilisib-NK-MOLM-14 co-culture to highlight effects pictilisib on the MOLM-14 transcriptomic profile.

4.4.6 Effect of FLT3 inhibitors and other broad range TKIs is decreased by NK cells

Tyrosine kinase inhibitors (TKIs) work by inhibiting the function of tyrosine kinases, which can, in the case of cancer, be mutated leading to unregulated cell growth. DSRT results show that the effect of TKIs targeting the *FLT3* mutation in MOLM-14 cells is effectively decreased when co-cultured with NK cells. This effect can be seen for example with quizartinib, which is more specific to *FLT3* as compared to other broader range TKIs. Effects related to TKIs were not observed in neither THP-1 nor HEL, which could be explained by different genetic profiles lacking *FLT3* mutations.

Similar interest in studying the shielding effect of NK cells to decrease the effect of TKIs on MOLM-14 was the primary interest in wanting to investigate the transcriptomic profile through scRNA sequencing. Our primary hypothesis was similar to that we had with PI3K inhibitors, which led us to believe NK cells can limit the effect of such drug by interacting

with the target cell. Investigations into the transcriptomic data provided by the scRNA sequencing revealed increases in *HLA-A* and *HLA-E* transcription in both midostaurin and quizartinib co-cultures with NK cells. This could in part, explain the inability of NK cells to target MOLM-14 cells to induce apoptosis. However, the closer inspection of transcriptomic changes when comparing the drug condition to the control does not reveal distinctive features that would explain the shielding effect observed in the DSRT results.

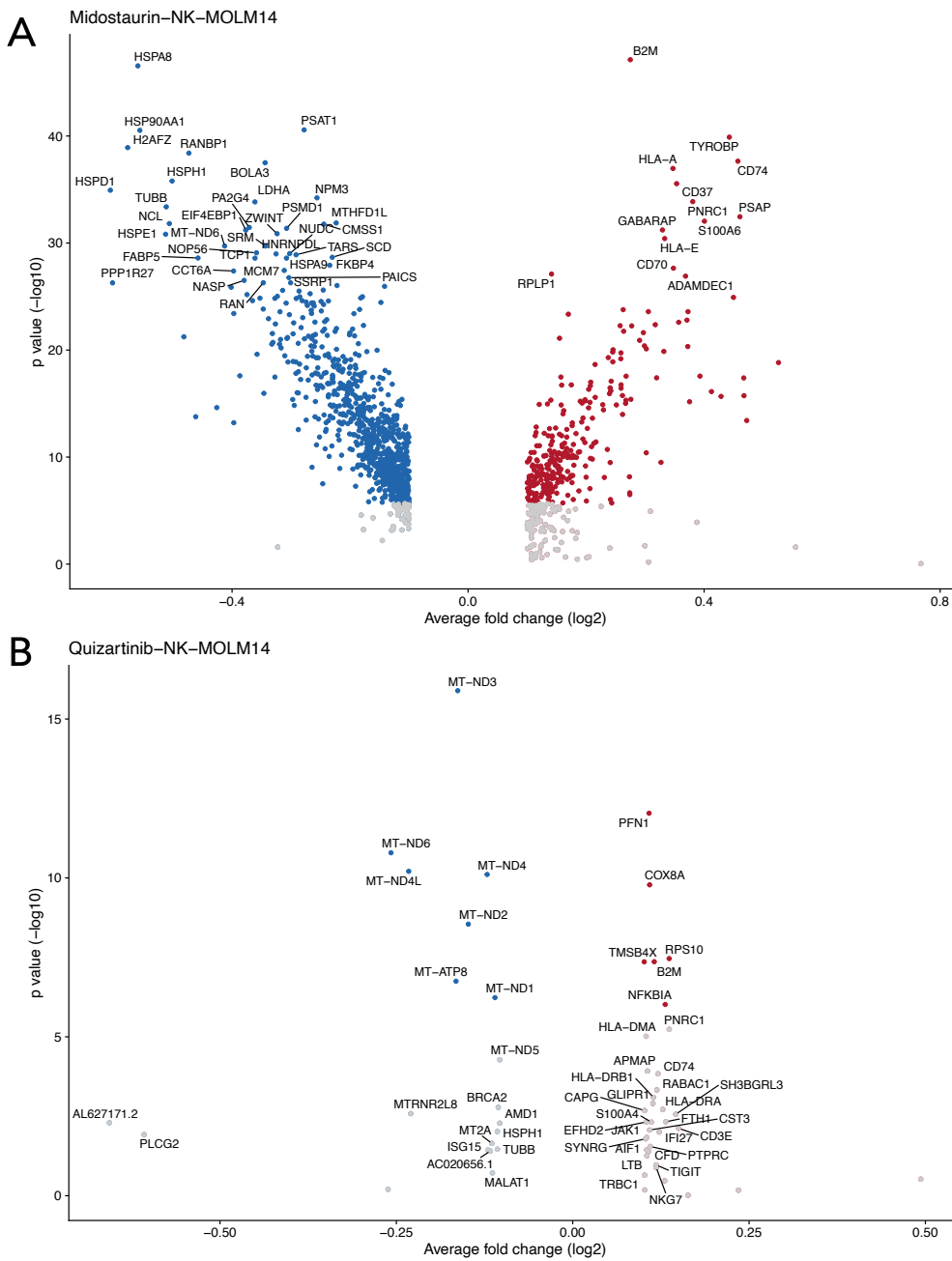


Figure 34. Volcano plot representation of differentially expressed genes in MOLM-14 after co-culture with midostaurin and quizartinib. Comparison of NK-MOLM-14-DMSO control condition versus midostaurin-NK-MOLM-14 (A) and quizartinib-NK-MOLM-14 (B) co-cultures.

5. Discussion

In this study, the effect of different approved and investigational oncology drugs on NK cell cytotoxicity against AML cell lines was evaluated, with the hopes of finding compounds capable of synergising with NK cells for improved activity against malignant cells.

5.1 Significant findings and their potential implications

Most significant findings were related to the potentiating effects observed with the use of daporinad and pevonedistat in combination with expanded NK cells. In DSRT results, both showed significant improvements in the inhibition of MOLM-14 viability, although the importance and significance of these effects were only confirmed after interpretation of scRNA sequencing data.

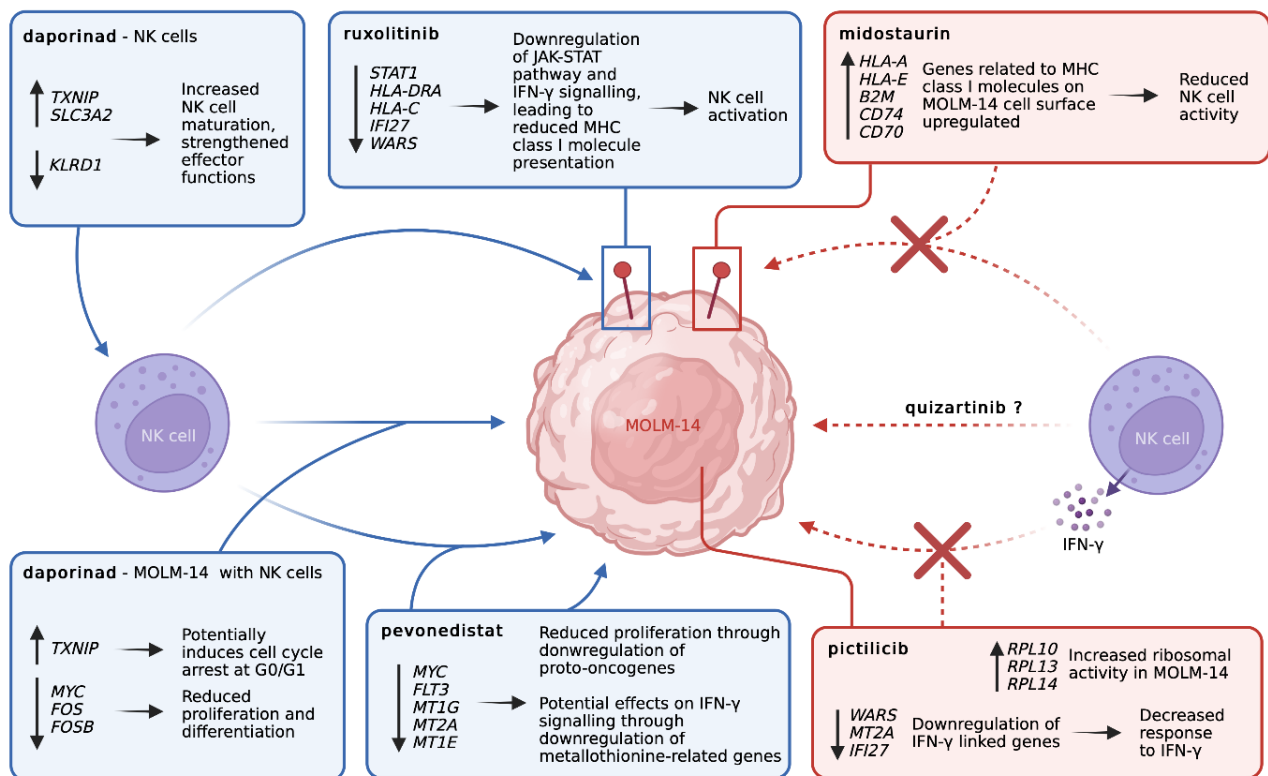


Figure 35. Summary of key findings on the effects of drugs on NK cell cytotoxicity. Daporinad affects both the NK cell transcriptome and MOLM-14 gene expression when co-cultured with NK cells. Pevonedistat has direct effects on MOLM-14 cells and induces changes in the NK cell activity. Ruxolitinib is hypothesised to affect MHC class I molecule presentation on the target cell surface. Midostaurin and pictilisib give rise to effects in MOLM-14 gene expression that can explain the reduced effects of NK cells. The effects of quizartinib remain unclear.^{113–121}

Daporinad showed significant differences compared to control samples in its transcriptomic landscape, with distinct genes being up- and downregulated as it was used in combination with NK cells. In co-culture conditions, daporinad interacted with NK cells to create a completely new type of transcriptomic profile for NK cells, resulting in effect in the target cells as well. Previous studies and literature fail at giving explanatory answers to the findings, which further emphasises the unique nature of investigating NK cell function in combination with oncology drugs for enhanced anti-tumour effects. Based on the transcriptomic profile, however, some conclusions can be made to describe the potential reasoning behind effects observed in the scRNA seq findings. One possible explanation is that in target cells, daporinad downregulates *MYC* transcription, which is a proto-oncogene known for its role in controlling cell cycle progression, apoptosis, and cellular transformation. This could lead to more vulnerable leukemic cells, that are more likely to suffer from NK cell cytotoxicity. In addition, upon administration of daporinad, NK cells significantly upregulate *TXNIP*, a gene with potential tumour suppressor activities as its over expression has been linked with cell-cycle arrest, which could explain the promotion of the killing effect by NK cells.¹¹⁸ *TXNIP* is also upregulated in the NK cell population, which could be another explanation to the enhanced cytotoxic capabilities induced by daporinad.¹¹⁸ In NK cells, its expression has been linked with increased maturation which, together with the upregulation of *SLC3A* and downregulation of *KLRD1*, could lead to strengthened effector functions.^{114,120} However, further investigation into the underlying mechanism of action is required before being able to make any further conclusions.

Similar findings were made with the use of pevonedistat, although effects were more focused on target cell activity and NK cell activation. In the case of pevonedistat, the transcription of *MYC* was also significantly downregulated, suggesting that it may play a key role in determining the fate of MOLM-14 cells. In addition, in the case of pevonedistat, *IFI27* upregulation is significant, indicating IFN- γ signalling which can partially explain the potentiating effect seen in co-culture conditions. Moreover, the upregulation of

metallothionein-related genes could indicate effects on IFN- γ production.¹²¹ Importantly, previous studies on pevonedistat have found synergistic activity between the drug and with TNF- α , which has been shown to lead to rapid cell death both *in vivo* and *in vitro* using rat models.¹²² This finding could explain the increased cytotoxic effect of NK cells when combined with pevonedistat, although further validation in humans and *in vitro* would be needed. It is also worth noting that pevonedistat also downregulates *FLT3*, a driver mutation of MOLM-14, although there are no reports of it specifically affecting this target on its own. The indirect downregulation of *FLT3* is an interesting finding and deserves further investigation.

Findings made from the study of combining ruxolitinib with NK cells shed light on the role of JAK inhibitors in activating NK cell cytotoxicity through downregulation of MHC class I molecules on target cell surface. The effect of IFN- γ signalling on MHC class I molecule expression has been well established and with JAK signalling pathways being downstream of IFN- γ signalling, their inhibition can decrease the expression of MHC class I molecules that are recognised by NK cells.¹¹³ Due to their decreased expression, NK cells are more likely to attack the target cells and hence induce an increased cytotoxic effect, which gives an explanation to the increased killing observed in the DSRT.

In addition to the forementioned findings, the NK cell-inhibiting effect of midostaurin may have clinically important implications due to its use as a targeted therapy option for AML patients with *FLT3-ITD* mutations.^{17,123} In the case that NK cells would be approved and used widely for treating AML, this finding could support our understanding of the importance of not using midostaurin or other *FLT3-ITD* targeting drugs in combination with NK cell immunotherapy.

In addition to TKIs, PI3K inhibitors such as pictilisib may also induce decreased cytotoxic effects of NK cells towards malignant cells. This could be explained by the downregulation

of genes such as *WARS* and *IFI27*, which could play a role in decreasing responses to IFN- γ released by NK cells. In addition, ribosomal protein (RP) -related genes have also been linked to MHC class I molecule presentation systems, offering another possible mechanism of action.¹¹⁶

5.2 Shielding effect of NK cells

As shown by findings made in different cell lines, NK cells show some shielding activity in some compounds, which protects target cells from their function. In the case of MOLM-14, these drugs included TKIs and more specifically *FLT3*-inhibiting drugs such as midostaurin and quizartinib. One hypothesis we were exploring was that NK cells have affinity for some of these drugs, which could decrease the number of drug molecules finding their way over to the intended target on the cancer cells. However, scRNA sequencing analysis revealed that the effects may be more in line with some previous findings, which have suggested that TKIs such as midostaurin and sorafenib could inhibit the production of cytokines by NK cells and reduce lysis of leukaemia cells.¹¹⁷ Our findings highlighted the reduced ability for NK cells to target leukaemia cells through the downregulation of MHC class I molecules although direct effects of the drug on the NK cell transcriptome were not observed. These notable differences between findings highlight the need for developing new strategies to investigate such effects. The further study of these drugs and their interaction with NK cells could reveal information about NK cell biology in addition to creating new therapeutic targets for NK cell-based treatments.

5.3 Assessment of DSRT and scRNA methods

DSRT experiments combining NK cell co-cultures and drugs proved to be a functioning way of assessing NK cell-based combination therapies with oncology drugs. Drugs activating and inhibiting the cytotoxic activity of NK cells could be identified from the large pool of compounds studied, with most drugs, however, having relatively insignificant

effects on target cells or NK cell cytotoxicity. Nevertheless, significant findings were made in all cell lines, with individual drugs and families of drugs showing specific effects when in co-culture with NK cells. This not only allowed for the detailed concentration-dependent study of individual drug compounds and their inhibitory activity over target cells, but also allowed for the creation of hypotheses worth further investigation. Most notably, DSRT experiments on different cell lines allowed for the identification of similarities and differences, which could be related to genetic differences between the cell lines or the underlying pathophysiology more widely. In this study, the most notable similarities were seen between MOLM-14 and THP-1, with especially daporinad and pevonedistat showing effects that could be translated to AML treatments more widely. The AML subtype HEL, which is defined by erythroblastic proliferation, showed notable differences compared to monocytic cell lines, which highlights the importance of personalised treatments and detailed diagnostics. In essence, drug screening results can translate into more generalised findings and provide a tool for finding important drug compounds.

Single cell RNA sequencing in combination with oligo hashtags provided a tool for further analysis of drugs' effects on NK cells and target cells through the investigation of transcriptomic changes. It provided a method to study the underlying mechanisms in the target cell line affected by drugs and NK cells, which is not possible with the high-throughput drug screening alone. To better assess the effects of drugs and to investigate the reasons behind differences and similarities observed in DSRT results between cell lines, transcriptomic data would be required from THP-1 and HEL to accurately point out molecular changes resulted in by NK cell synergy with oncology drugs.

5.4 Improvements

To facilitate the discovery of new significant drug compounds, developing new custom drug screenings would be crucial. Currently, the FO5A plate used in the experiments includes large numbers of drugs with little to no effect on target cells, be it with NK cells or

with the drug only. In addition, some compounds consistently give abnormally high bioluminescence levels, indicating potential unwanted interactions with luciferase and substances used to measure it. As the molecular profile and genetic abnormalities of cancers are widely known, drug screenings could be purposefully designed to target genetic abnormalities introduced by mutations in the malignant cell line for more meaningful findings. In addition, custom screening collections of drugs could help at identifying effects of drugs used for common illnesses such as hypertension, coronary heart disease, diabetes, and different neurological malignancies. This would allow for better understanding of ways in which the effectiveness of NK cell-based immunotherapy methods can be limited due to synergy with other medications and potentially even finding compounds unrelated to cancer therapy that could enhance NK cell cytotoxicity.

In addition to creating custom drug screenings, DSRT methods could also be improved by advancements in computational analysis of large datasets obtained from DSRT measurements. Currently, the method is incapable of processing errors and outliers in luminescence measurements, creating false results in the form of extreme sDSS scores. In addition, the currently used model does not consider the possibility that the drug alone could create a proliferating effect in the target cell line. These modifications in the computational tools used for data analysis would allow for improved reliability of findings, in addition to saving time by removing the need for manual assessment of each inhibition curve. Furthermore, advancements in the data analysis could allow for automatic classification of drugs into groups depending on the effects seen in NK cell co-culture conditions in comparison to drug only.

In addition to improvements in DSRT data analysis, single cell RNA sequencing data analysis could be improved, with the introduction of the MAST statistical framework for example. This could allow for improved assessment of transcriptional changes and better characterisation of heterogeneity from the data.¹²⁴

The use of NK cells from different donors validates the findings and translates to more universal findings. However, when comparing large numbers of target cell lines, the aim should be in using the same expanded NK cells from a specific donor in both drug screenings and scRNA sequencing for improved reliability and comparability of data. Related to cells and their biology, it is also important to note that we are only able to study cells that remain viable at the point of scRNA sequencing and do not fully understand the effects of the drugs and NK cells that have been induced on those cells that have been eradicated.

5.5 Future perspectives and conclusions

The characterisation of specific drug compounds with synergetic interactions with NK cells increases the hopes for finding important targetable pathways which could be taken advantage of in improving NK cell-based immunotherapy. In the future, specific drugs of interest should be tested on a wider number of cancer cell lines for evaluation of cell line specificity of compounds such as daporinad and pevonedistat. Validation of the roles of specific transcriptional features should be performed using gene knockout experiments, made possible by advancements in genome editing technologies such as CRISPR-Cas9.

In addition, as more cell lines are studied and the significant mechanisms of action are studied in more depth, primary cells could also be studied to investigate the potential of *in vitro* findings in being translatable to clinical uses. This could facilitate the development of personalised immunotherapy options, including the combination of NK cells and anti-cancer drugs, while minimizing risks for patients.

Although the use of NK cells in clinical settings is still in its early steps, results from different studies give hope for its potential at combatting various types of cancers without strong

adverse effects. However, before they can be taken into wider uses, many questions related to their specific functions but also their efficient production remain unanswered.

In conclusion, DSRT screening provides a highly functional platform for testing the combination of drugs and NK cells against hematological malignancies such as AML. The promising findings, including significant improvements in NK cell cytotoxicity enabled by daporinad and pevonedistat in targeting MOLM-14, shed light on the remarkable potential of combining conventional drug-based therapies with emerging immunotherapy methods. Investigations of the transcriptomic landscape in different therapeutic conditions further reveal effects on gene expression at single-cell level, increasing our understanding on both NK cell function and its capabilities of being used in combination with other therapy methods. The future for NK cell therapy methods is looking increasingly promising and hopefully its combinatorial uses with different drugs could translate into improved therapy options and long-lasting outcomes in patients suffering from acute myeloid leukaemia.

Acknowledgements

First and foremost, I would like to thank my supervisors Olli Dufva and Prof. Satu Mustjoki for their continuous support and for introducing me to the exciting world of immunology and hematology. This project has made me learn tremendously about immunology, oncology, and hematology, and has allowed me to combine information from all these disciplines in a fascinating manner. I would especially like to thank Olli for his gratuitous support in all aspects of research and science during my time in the group and for all the scientific and non-scientific discussions we have had, which have allowed me to develop as a researcher and scientist. Furthermore, I would like to thank Petra Nygren for her support in my thesis project and for allowing me to take part in her PhD project. It has been a pleasure working with you and I hope we can keep on developing this work in the future. Importantly, I would also like to thank Sara Gandolfi for introducing me to tissue culture techniques and for continuously challenging me in order to develop and learn. In addition, a big thanks to Shady Awad for teaching me the use of DSRT methods and the related tools, which have formed a large part of my thesis work. Very importantly, I would like to thank Jay Klievink and Hanna Lähteenmäki for their efforts in supporting me with work in the laboratory and giving a helping hand whenever needed.

Although a lot of work was done in the laboratory and in the office, much of it was being motivated by the great atmosphere in the group. For keeping up the spirits and organising different activities, I would like to thank Hanna, Sofie, Olli, Petra, Jani, Jason, Dipabarna, Neja, Anita, Otso, Aino, Milla and Moon. Also a big thanks goes to Jenni and everyone else at the Hematology Research Unit that have made me feel welcome.

Finally, I would also like to thank my family and friends for all the support throughout my academic journey so far.

References

1. Sill H, Olipitz W, Zebisch A, Schulz E, Wölfler A. Therapy-related myeloid neoplasms: Pathobiology and clinical characteristics. *Br J Pharmacol.* 2011;162(4):792-805. doi:10.1111/j.1476-5381.2010.01100.x
2. Dong Y, Shi O, Zeng Q, et al. Leukemia incidence trends at the global, regional, and national level between 1990 and 2017. *Exp Hematol Oncol.* 2020;9(1):1-11. doi:10.1186/s40164-020-00170-6
3. Finn L, Dalovisio A, Foran J. Older patients with acute myeloid leukemia: Treatment challenges and future directions. *Ochsner J.* 2017;17(4):398-404. doi:10.1043/TOJ-17-0035
4. Licht JD, Sternberg DW. The molecular pathology of acute myeloid leukemia. *Hematology.* 2005;(212):137-142. doi:10.1182/asheducation-2005.1.137
5. Patel JP, Gönen M, Figueroa ME, et al. Prognostic Relevance of Integrated Genetic Profiling in Acute Myeloid Leukemia. *N Engl J Med.* 2012;366(12):1079-1089. doi:10.1056/NEJMoa1112304
6. Ley T, Miller C, Raphael BJ. Genomic and Epigenomic Landscapes of Adult De Novo Acute Myeloid Leukemia. *N Engl J Med.* 2013;368(22):2059-2074. doi:10.1056/nejmoa1301689
7. De Kouchkovsky I, Abdul-Hay M. 'Acute myeloid leukemia: A comprehensive review and 2016 update.' *Blood Cancer J.* 2016;6(7). doi:10.1038/bcj.2016.50
8. Gary Gilliland D, Griffin JD. The roles of FLT3 in hematopoiesis and leukemia. *Blood.* 2002;100(5):1532-1542. doi:10.1182/blood-2002-02-0492
9. Döhner H, Weisdorf DJ, Bloomfield CD. Acute Myeloid Leukemia. *N Engl J Med.* 2015;373(12):1136-1152. doi:10.1056/NEJMra1406184
10. Bennett JM, Catovsky D, Daniel M -T, et al. Proposals for the Classification of the Acute Leukaemias French-American-British (FAB) Co-operative Group. *Br J Haematol.* 1976;33(4):451-458. doi:10.1111/j.1365-2141.1976.tb03563.x
11. Arber DA, Orazi A, Hasserjian R, et al. The 2016 revision to the World Health Organization classification of myeloid neoplasms and acute leukemia. *Blood.* 2016;127(20):2391-2405. doi:10.1182/blood-2016-03-643544
12. DiNardo CD, Wei AH. How I treat acute myeloid leukemia in the era of new drugs. *Blood.* 2020;135(2):85-96. doi:10.1182/blood.2019001239
13. Liersch R, Müller-Tidow C, Berdel WE, Krug U. Prognostic factors for acute myeloid leukaemia in adults - biological significance and clinical use. *Br J Haematol.* 2014;165(1):17-38. doi:10.1111/bjh.12750
14. DeVita V, Rosenberg SA, Lawrence T. *Principles and Practice of Oncology.*; 2015. <https://www.wagecommunication.com/devita/p1.pdf>.
15. Estey EH. Treatment of acute myeloid leukemia. *Haematologica.* 2009;94(1):10-16. doi:10.3324/haematol.2008.001263
16. Nurgali K, Jagoe RT, Abalo R. Editorial: Adverse effects of cancer chemotherapy: Anything new to improve tolerance and reduce sequelae? *Front Pharmacol.*

- 2018;9(3):1-3. doi:10.3389/fphar.2018.00245
17. Stone RM, Mandrekar SJ, Sanford BL, et al. Midostaurin plus Chemotherapy for Acute Myeloid Leukemia with a FLT3 Mutation . *N Engl J Med*. 2017;377(5):454-464. doi:10.1056/nejmoa1614359
 18. Maziarz RTT, Patnaik MM, Scott BL, et al. Radius: A Phase 2 Randomized Trial Investigating Standard of Care +/- Midostaurin after Allogeneic Stem Cell Transplant in FLT3-ITD-Mutated AML. *Blood*. 2018;132(1). doi:10.1182/blood-2018-99-113582
 19. Smith CC, Zhang C, Lin KC, et al. Characterizing and overriding the structural mechanism of the quizartinib-resistant FLT3 "Gatekeeper" F691L mutation with PLX3397. *Cancer Discov*. 2016;5(6):668-679. doi:10.1158/2159-8290.CD-15-0060
 20. Roboz GJ, DiNardo CD, Stein EM, et al. Ivosidenib induces deep durable remissions in patients with newly diagnosed IDH1-mutant acute myeloid leukemia. *Blood*. 2020;135(7):463-471. doi:10.1182/blood.2019002140
 21. Singh R, Letai A, Sarosiek K. Regulation of apoptosis in health and disease: the balancing act of BCL-2 family proteins. *Nat Rev Mol Cell Biol*. 2019;20(3):175-193. doi:10.1038/s41580-018-0089-8
 22. DiNardo CD, Jonas BA, Pullarkat V, et al. Azacitidine and Venetoclax in Previously Untreated Acute Myeloid Leukemia. *N Engl J Med*. 2020;383(7):617-629. doi:10.1056/nejmoa2012971
 23. Yilmaz M, Kantarjian H, Ravandi F. Acute promyelocytic leukemia current treatment algorithms. *Blood Cancer J*. 2021;11(6). doi:10.1038/s41408-021-00514-3
 24. Dickinson AM, Norden J, Li S, et al. Graft-versus-leukemia effect following hematopoietic stem cell transplantation for leukemia. *Front Immunol*. 2017;8(6). doi:10.3389/fimmu.2017.00496
 25. Loke J, Buka R, Craddock C. Allogeneic Stem Cell Transplantation for Acute Myeloid Leukemia: Who, When, and How? *Front Immunol*. 2021;12(May):1-18. doi:10.3389/fimmu.2021.659595
 26. Gyurkocza B, Storb R, Storer BE, et al. Nonmyeloablative allogeneic hematopoietic cell transplantation in patients with acute myeloid leukemia. *J Clin Oncol*. 2010;28(17):2859-2867. doi:10.1200/JCO.2009.27.1460
 27. Saraceni F, Bruno B, Lemoli RM, et al. Autologous stem cell transplantation is still a valid option in good- and intermediate-risk AML: A GITMO survey on 809 patients autografted in first complete remission. *Bone Marrow Transplant*. 2017;52(1):163-166. doi:10.1038/bmt.2016.233
 28. Linker CA. Autologous stem cell transplantation for acute myeloid leukemia. *Bone Marrow Transplant*. 2003;31(9):731-738. doi:10.1038/sj.bmt.1704020
 29. Rein LA, Sung AD, Rizzieri DA. New approaches to manipulate minimal residual disease after allogeneic stem cell transplantation. *Int J Hematol Oncol*. 2013;2(1):39-48. doi:10.2217/ijh.13.4
 30. Jairam V, Roberts KB, Yu JB. Historical trends in the use of radiation therapy for pediatric cancers: 1973-2008. *Int J Radiat Oncol Biol Phys*. 2013;85(3):e151-e155.

doi:10.1016/j.ijrobp.2012.10.007

31. Nardi V, Winkfield KM, Ok CY, et al. Acute myeloid leukemia and myelodysplastic syndromes after radiation therapy are similar to de novo disease and differ from other therapy-related myeloid neoplasms. *J Clin Oncol.* 2012;30(19):2340-2347. doi:10.1200/JCO.2011.38.7340
32. Liu Y, Bewersdorf JP, Stahl M, Zeidan AM. Immunotherapy in acute myeloid leukemia and myelodysplastic syndromes: The dawn of a new era? *Blood Rev.* 2019;34:67-83. doi:10.1016/j.blre.2018.12.001
33. de Propriis MS, Raponi S, Diverio D, et al. High CD33 expression levels in acute myeloid leukemia cells carrying the nucleophosmin (NPM1) mutation. *Haematologica.* 2011;96(10):1548-1551. doi:10.3324/haematol.2011.043786
34. Lambert J, Pautas C, Terré C, et al. Gemtuzumab ozogamicin for de novo acute myeloid leukemia: Final efficacy and safety updates from the open-label, phase III ALFA-0701 trial. *Haematologica.* 2019;104(1):113-119. doi:10.3324/haematol.2018.188888
35. Foley B, Cooley S, Verneris MR, et al. NK cell education after allogeneic transplantation: Dissociation between recovery of cytokine-producing and cytotoxic functions. *Blood.* 2011;118(10):2784-2792. doi:10.1182/blood-2011-04-347070
36. Wiernik A, Foley B, Zhang B, et al. Targeting Natural Killer cells to Acute Myeloid Leukemia in vitro with a CD16x33 bispecific killer cell engager (BiKE) and ADAM17 inhibition. *Clin Cancer Res.* 2014;19(14):3844-3855. doi:10.1158/1078-0432.CCR-13-0505.Targeting
37. Vallera DA, Felices M, McElmurry R, McCullar V, Zhou X. IL-15 Trispecific Killer Engagers (TriKEs) Make Natural Killer Cells Specific to CD33+ Targets While Also Inducing Persistence, In Vivo Expansion, and Enhanced Function. *Clin Cancer Res.* 2016;176(3):3440-3450. doi:10.1158/1078-0432.CCR-15-2710.IL-15
38. Sarhan D, Brandt L, Felices M, et al. 161533 TriKE stimulates NK-cell function to overcome myeloid-derived suppressor cells in MDS. *Blood Adv.* 2018;2(12):1459-1469. doi:10.1182/bloodadvances.2017012369
39. Kadia TM, Cortes JE, Ghorab A, et al. Nivolumab (Nivo) maintenance (maint) in high-risk (HR) acute myeloid leukemia (AML) patients. *J Clin Oncol.* 2018;36(15_suppl):7014. doi:10.1200/JCO.2018.36.15_suppl.7014
40. Park JH, Rivière I, Gonen M, et al. Long-Term Follow-up of CD19 CAR Therapy in Acute Lymphoblastic Leukemia. *N Engl J Med.* 2018;378(5):449-459. doi:10.1056/nejmoa1709919
41. Dufva O, Koski J, Maliniemi P, et al. Integrated drug profiling and CRISPR screening identify essential pathways for CAR T-cell cytotoxicity. *Blood.* 2020;135(9):597-609.
42. Syn NL, Teng MWL, Mok TSK, Soo RA. De-novo and acquired resistance to immune checkpoint targeting. *Lancet Oncol.* 2017;18(12):e731-e741. doi:10.1016/S1470-2045(17)30607-1
43. Alfred LJ, Wojdani A, Nieto M, Perez R, Yoshida G. A chemical carcinogen, 3-methylcholanthrene, alters T-cell function and induces T-suppressor cells in a

- mouse model system. *Immunology*. 1983;50(2):207-213.
44. Dekkers F, Bijwaard H, Bouffler S, et al. A two-mutation model of radiation-induced acute myeloid leukemia using historical mouse data. *Radiat Environ Biophys*. 2011;50(1):37-45. doi:10.1007/s00411-010-0328-7
 45. Stavropoulou V, Almosaillekh M, Royo H, et al. A novel inducible mouse model of MLL-ENL -driven mixed-lineage acute leukemia. *HemaSphere*. 2018;2(4):1-11. doi:10.1097/HS9.0000000000000051
 46. Wunderlich M, Mizukawa B, Chou FS, et al. AML cells are differentially sensitive to chemotherapy treatment in a human xenograft model. *Blood*. 2013;121(12):e90-e97. doi:10.1182/blood-2012-10-464677
 47. Almosaillekh M, Schwaller J. Murine models of acute Myeloid Leukaemia. *Int J Mol Sci*. 2019;20(2). doi:10.3390/ijms20020453
 48. Matsuo Y, MacLeod RAF, Uphoff CC, et al. Two acute monocytic leukemia (AML-M5a) cell lines (MOLM-13 and MOLM-14) with interclonal phenotypic heterogeneity showing MLL-AF9 fusion resulting from an occult chromosome insertion, ins(11;9)(q23;p22p23). *Leukemia*. 1997;11(9):1469-1477. doi:10.1038/sj.leu.2400768
 49. Chanput W, Mes JJ, Wichers HJ. THP-1 cell line: an in vitro cell model for immune modulation approach. *Int Immunopharmacol*. 2014;23(1):37-45. doi:10.1016/j.intimp.2014.08.002
 50. Martin P, Papayannopoulou T. HEL cells: A new human erythroleukemia cell line with spontaneous and induced globin expression. *Science (80-)*. 1982;216(4551):1233-1235. doi:10.1126/science.6177045
 51. Marshall JS, Warrington R, Watson W, Kim HL. An introduction to immunology and immunopathology. *Allergy, Asthma Clin Immunol*. 2018;14(s2):1-10. doi:10.1186/s13223-018-0278-1
 52. Chaplin D. Overview of the immune response. *J Allergy Clin Immunol*. 2010;125(2):3-23. doi:10.1016/j.jaci.2010.01.002
 53. Colotta F, Allavena P, Sica A, Garlanda C, Mantovani A. Cancer-related inflammation, the seventh hallmark of cancer: Links to genetic instability. *Carcinogenesis*. 2009;30(7):1073-1081. doi:10.1093/carcin/bgp127
 54. Hanahan D, Weinberg RA. Hallmarks of cancer: The next generation. *Cell*. 2011;144(5):646-674. doi:10.1016/j.cell.2011.02.013
 55. Teng MWL, Galon J, Fridman WH, Smyth MJ. From mice to humans: Developments in cancer immunoediting. *J Clin Invest*. 2015;125(9):3338-3346. doi:10.1172/JCI80004
 56. Gonzalez H, Hagerling C, Werb Z. Roles of the immune system in cancer: From tumor initiation to metastatic progression. *Genes Dev*. 2018;32(19-20):1267-1284. doi:10.1101/GAD.314617.118
 57. Langers I, Renoux VM, Thiry M, Delvenne P, Jacobs N. Natural killer cells: Role in local tumor growth and metastasis. *Biol Targets Ther*. 2012;6:73-82.
 58. Lanier LL, Phillips JH, Hackett J, Tutt M, Kumar V. Natural killer cells: definition of a

- cell type rather than a function. *J Immunol.* 1987;138(2745).
59. O'Sullivan TE, Sun JC, Lanier LL. Natural Killer Cell Memory. *Immunity.* 2015;43(4):634-645. doi:10.1016/j.immuni.2015.09.013
 60. Scoville SD, Freud AG, Caligiuri MA. Modeling human natural killer cell development in the era of innate lymphoid cells. *Front Immunol.* 2017;8(MAR):4-11. doi:10.3389/fimmu.2017.00360
 61. Abel AM, Yang C, Thakar MS, Malarkannan S. Natural killer cells: Development, maturation, and clinical utilization. *Front Immunol.* 2018;9(AUG):1-23. doi:10.3389/fimmu.2018.01869
 62. Screpanti V, Wallin RPA, Ljunggren H-G, Grandien A. A Central Role for Death Receptor-Mediated Apoptosis in the Rejection of Tumors by NK Cells. *J Immunol.* 2001;167(4):2068-2073. doi:10.4049/jimmunol.167.4.2068
 63. Sonar S, Lal G. Role of tumor necrosis factor superfamily in neuroinflammation and autoimmunity. *Front Immunol.* 2015;6(7):1-13. doi:10.3389/fimmu.2015.00364
 64. Paul S, Lal G. The molecular mechanism of natural killer cells function and its importance in cancer immunotherapy. *Front Immunol.* 2017;8(9). doi:10.3389/fimmu.2017.01124
 65. Thomas R, Yang X. NK-DC Crosstalk in Immunity to Microbial Infection. *J Immunol Res.* 2016;2016. doi:10.1155/2016/6374379
 66. Zhou Z, Zhang C, Zhang J, Tian Z. Macrophages help NK cells to attack tumor cells by stimulatory NKG2D ligand but protect themselves from NK killing by inhibitory ligand Qa-1. *PLoS One.* 2012;7(5). doi:10.1371/journal.pone.0036928
 67. Karre K, Ljunggren HG, Piontek G KR. Selective rejection of H-2-deficient lymphoma variants suggests alternative immune defence strategy. *Nature.* 1986;319:675-678.
 68. Elliott J, Yokoyama W. Unifying concepts of MHC-dependent natural killer cell education. *Trends Immunol.* 2011;32(8):364-372. doi:10.1016/j.it.2011.06.001.Unifying
 69. Wu Y, Li Y, Fu B, et al. Programmed differentiated natural killer cells kill leukemia cells by engaging SLAM family receptors. *Oncotarget.* 2017;8(34):57024-57038. doi:10.18632/oncotarget.18659
 70. Fehniger TA, Cooper MA, Nuovo GJ, et al. CD56bright natural killer cells are present in human lymph nodes and are activated by T cell-derived IL-2: A potential new link between adaptive and innate immunity. *Blood.* 2003;101(8):3052-3057. doi:10.1182/blood-2002-09-2876
 71. Trinchieri G. Biology of Natural Killer Cells. *Adv Immunol.* 1989;47(C):187-376. doi:10.1016/S0065-2776(08)60664-1
 72. Fehniger TA, Cai SF, Cao X, et al. Acquisition of Murine NK Cell Cytotoxicity Requires the Translation of a Pre-existing Pool of Granzyme B and Perforin mRNAs. *Immunity.* 2007;26(6):798-811. doi:10.1016/j.immuni.2007.04.010
 73. Kobayashi BYM, Fitz L, Ryan M, et al. Identification And Purification Of Natural Killer Cell Stimulatory Factor (Nksf), A Cytokine With Multiple Biologic Effects On

Human Lymphocytes Human B lymphoblastoid cell lines facilitate the growth in vitro of human NK cells and of T cell clones (1-. *J Exp Med*. 1989;170(September):827-845.

74. Wagner JA, Berrien-Elliott MM, Rosario M, et al. Cytokine-Induced Memory-Like Differentiation Enhances Unlicensed Natural Killer Cell Antileukemia and FcγRIIIa-Triggered Responses. *Biol Blood Marrow Transplant*. 2017;23(3):398-404. doi:10.1016/j.bbmt.2016.11.018
75. Parrish-Novak J, Dillon SR, Nelson A, et al. Interleukin 21 and its receptor are involved in NK cell expansion and regulation of lymphocyte function. *Nature*. 2000;408(6808):57-63. doi:10.1038/35040504
76. Carlsten M, Järås M. Natural Killer Cells in Myeloid Malignancies: Immune Surveillance, NK Cell Dysfunction, and Pharmacological Opportunities to Bolster the Endogenous NK Cells. *Front Immunol*. 2019;10(October):1-18. doi:10.3389/fimmu.2019.02357
77. Gómez Román VR, Murray JC, Weiner LM. Chapter 1 - Antibody-Dependent Cellular Cytotoxicity (ADCC). In: Ackerman ME, Nimmerjahn F, eds. *Antibody Fc*. Boston: Academic Press; 2014:1-27. doi:https://doi.org/10.1016/B978-0-12-394802-1.00001-7
78. Costello RT, Sivori S, Marcenaro E, et al. Defective expression and function of natural killer cell-triggering receptors in patients with acute myeloid leukemia. *Blood*. 2002;99(10):3661-3667. doi:10.1182/blood.V99.10.3661
79. Nowbakht P, Ionescu MCS, Rohner A, et al. Ligands for natural killer cell-activating receptors are expressed upon the maturation of normal myelomonocytic cells but at low levels in acute myeloid leukemias. *Blood*. 2005;105(9):3615-3622. doi:10.1182/blood-2004-07-2585
80. Vitale M, Cantoni C, Pietra G, Mingari MC, Moretta L. Effect of tumor cells and tumor microenvironment on NK-cell function. *Eur J Immunol*. 2014;44(6):1582-1592. doi:10.1002/eji.201344272
81. Cheng M, Chen Y, Xiao W, Sun R, Tian Z. NK cell-based immunotherapy for malignant diseases. *Cell Mol Immunol*. 2013;10(3):230-252. doi:10.1038/cmi.2013.10
82. Ruggeri L, Capanni M, Casucci M, et al. Role of natural killer cell alloreactivity in HLA-mismatched hematopoietic stem cell transplantation. *Blood*. 1999;94(1):333-339. doi:10.1182/blood.v94.1.333.413a31_333_339
83. Choi I, Yoon SR, Park SY, et al. Donor-Derived Natural Killer Cells Infused after Human Leukocyte Antigen-Haploidentical Hematopoietic Cell Transplantation: A Dose-Escalation Study. *Biol Blood Marrow Transplant*. 2014;20(5):696-704. doi:10.1016/j.bbmt.2014.01.031
84. Choi I, Yoon SR, Park SY, et al. Donor-Derived Natural Killer Cell Infusion after Human Leukocyte Antigen–Haploidentical Hematopoietic Cell Transplantation in Patients with Refractory Acute Leukemia. *Biol Blood Marrow Transplant*. 2016;22(11):2065-2076. doi:10.1016/j.bbmt.2016.08.008

85. Miller JS, Soignier Y, Panoskaltsis-Mortari A, et al. Successful adoptive transfer and in vivo expansion of human haploidentical NK cells in patients with cancer. *Blood*. 2005;105(8):3051-3057. doi:10.1182/blood-2004-07-2974
86. Wang CJ, Huang XJ, Gong LZ, et al. Observation on the efficacy of consolidation chemotherapy combined with allogeneic natural killer cell infusion in the treatment of low and moderate risk acute myeloid leukemia. *Zhonghua xue ye xue za zhi*. 2019;40(10):812-817. doi:10.3760/cma.j.issn.0253-2727.2019.10.003
87. Curti A, Ruggeri L, Parisi S, et al. Larger size of donor alloreactive NK cell repertoire correlates with better response to NK cell immunotherapy in elderly acute myeloid leukemia patients. *Clin Cancer Res*. 2016;22(8):1914-1921. doi:10.1158/1078-0432.CCR-15-1604
88. Zhao XY, Jiang Q, Jiang H, et al. Expanded clinical-grade membrane-bound IL-21/4-1BBL NK cell products exhibit activity against acute myeloid leukemia in vivo. *Eur J Immunol*. 2020;50(9):1374-1385. doi:10.1002/eji.201948375
89. Wu Y, Tian Z, Wei H. Developmental and functional control of natural killer cells by cytokines. *Front Immunol*. 2017;8(AUG). doi:10.3389/fimmu.2017.00930
90. Cany J, van der Waart AB, Tordoir M, et al. Natural Killer Cells Generated from Cord Blood Hematopoietic Progenitor Cells Efficiently Target Bone Marrow-Residing Human Leukemia Cells in NOD/SCID/IL2Rgnull Mice. *PLoS One*. 2013;8(6):1-11. doi:10.1371/journal.pone.0064384
91. Dolstra H, Roeven MWH, Spanholtz J, et al. Successful transfer of umbilical cord blood CD34+ hematopoietic stem and progenitor-derived NK cells in older acute myeloid leukemia patients. *Clin Cancer Res*. 2017;23(15):4107-4118. doi:10.1158/1078-0432.CCR-16-2981
92. Klingemann H. Are natural killer cells superior CAR drivers? *Oncoimmunology*. 2014;3(4):1-4. doi:10.4161/onci.28147
93. Hauswirth AW, Florian S, Printz D, et al. Expression of the target receptor CD33 in CD34 +/CD38 -/CD123 + AML stem cells. *Eur J Clin Invest*. 2007;37(1):73-82. doi:10.1111/j.1365-2362.2007.01746.x
94. Pemovska T, Kontro M, Yadav B, et al. Individualized systems medicine strategy to tailor treatments for patients with chemorefractory acute myeloid leukemia. *Cancer Discov*. 2013;3(12):1416-1429. doi:10.1158/2159-8290.CD-13-0350
95. Kuleskiy E, Saarela J, Turunen L, Wennerberg K. Precision Cancer Medicine in the Acoustic Dispensing Era: Ex Vivo Primary Cell Drug Sensitivity Testing. *J Lab Autom*. 2016;21(1):27-36. doi:10.1177/2211068215618869
96. Branchini BR, Magyar RA, Murtiashaw MH, Anderson SM, Helgerson LC, Zimmer M. Site-Directed Mutagenesis of Firefly Luciferase Active Site Amino Acids: A Proposed Model for Bioluminescence Color. *Biochemistry*. 1999;38(40):13223-13230. doi:10.1021/bi991181o
97. Allard S, Kopish K. Luciferase Reporter Assays: Powerful, Adaptable Tools For Cell Biology Research. *Cell Notes*. 2008;(21):23-26. doi:10.1053/j.gastro.2006.05.006
98. Tawa P, Tam J, Cassady R, Nicholson DW, Xanthoudakis S. Quantitative analysis of

- fluorescent caspase substrate cleavage in intact cells and identification of novel inhibitors of apoptosis. *Cell Death Differ.* 2001;8(1):30-37.
99. Kummrow A, Frankowski M, Bock N, Werner C, Dziekan T, Neukammer J. Quantitative assessment of cell viability based on flow cytometry and microscopy. *Cytom Part A.* 2013;83 A(2):197-204. doi:10.1002/cyto.a.22213
 100. Ghiringhelli F, Menard C, Puig PE, et al. Metronomic cyclophosphamide regimen selectively depletes CD4 +CD25+ regulatory T cells and restores T and NK effector functions in end stage cancer patients. *Cancer Immunol Immunother.* 2007;56(5):641-648. doi:10.1007/s00262-006-0225-8
 101. Khallouf H, Märten A, Serba S, et al. 5-fluorouracil and interferon- α immunochemotherapy enhances immunogenicity of murine pancreatic cancer through upregulation of NKG2D ligands and MHC class I. *J Immunother.* 2012;35(3):245-253. doi:10.1097/CJI.0b013e31824b3a76
 102. Liu WM, Fowler DW, Smith P, Dalgleish AG. Pre-treatment with chemotherapy can enhance the antigenicity and immunogenicity of tumours by promoting adaptive immune responses. *Br J Cancer.* 2010;102(1):115-123. doi:10.1038/sj.bjc.6605465
 103. Mizoguchi I, Yoshimoto T, Katagiri S, et al. Sustained upregulation of effector natural killer cells in chronic myeloid leukemia after discontinuation of imatinib. *Cancer Sci.* 2013;104(9):1146-1153. doi:10.1111/cas.12216
 104. Iriyama N, Fujisawa S, Yoshida C, et al. Early cytotoxic lymphocyte expansion contributes to a deep molecular response to dasatinib in patients with newly diagnosed chronic myeloid leukemia in the chronic phase: Results of the D-first study. *Am J Hematol.* 2015;90(9):819-824. doi:10.1002/ajh.24096
 105. Brachène A, Dos Santos R, Marroqui L, Colli ML. IFN α induces a preferential long-lasting expression of MHC class I in human pancreatic beta cells. *Diabetologia.* 2018;61(3):636-640. doi:10.1007/s00125-017-4536-4.IFN
 106. Liu L, Mayes PA, Eastman S, et al. The BRAF and MEK inhibitors dabrafenib and trametinib: Effects on immune function and in combination with immunomodulatory antibodies targeting PD-1, PD-L1, and CTLA-4. *Clin Cancer Res.* 2015;21(7):1639-1651. doi:10.1158/1078-0432.CCR-14-2339
 107. Yadav B, Pemovska T, Szwajda A, et al. Quantitative scoring of differential drug sensitivity for individually optimized anticancer therapies. *Sci Rep.* 2014;4:1-10. doi:10.1038/srep05193
 108. Stoeckius M, Zheng S, Houck-Loomis B, et al. Cell Hashing with barcoded antibodies enables multiplexing and doublet detection for single cell genomics. *Genome Biol.* 2018;19(1):1-12. doi:10.1186/s13059-018-1603-1
 109. Luecken MD, Theis FJ. Current best practices in single-cell RNA-seq analysis: a tutorial. *Mol Syst Biol.* 2019;15(6). doi:10.15252/msb.20188746
 110. Ferris J, Espona-Fiedler M, Hamilton C, et al. Pevonedistat (MLN4924): mechanism of cell death induction and therapeutic potential in colorectal cancer. *Cell Death Discov.* 2020;6(1). doi:10.1038/s41420-020-00296-w
 111. Galli U, Colombo G, Travelli C, Tron GC, Genazzani AA, Grolla AA. Recent

- Advances in NAMPT Inhibitors: A Novel Immunotherapeutic Strategy. *Front Pharmacol.* 2020;11(May):1-20. doi:10.3389/fphar.2020.00656
112. Senkevitch E, Durum S. The promise of Janus kinase inhibitors in the treatment of hematological malignancies. *Cytokine.* 2017;98:33-41. doi:10.1016/j.cyto.2016.10.012.The
 113. Castro F, Cardoso AP, Gonçalves RM, Serre K, Oliveira MJ. Interferon-gamma at the crossroads of tumor immune surveillance or evasion. *Front Immunol.* 2018;9(5):1-19. doi:10.3389/fimmu.2018.00847
 114. Nachev M, Ali AK, Almutairi SM, Lee SH. Targeting SLC1A5 and SLC3A2/SLC7A5 as a Potential Strategy to Strengthen Anti-Tumor Immunity in the Tumor Microenvironment. *Front Immunol.* 2021;12(April):1-11. doi:10.3389/fimmu.2021.624324
 115. Sottile R, Federico G, Garofalo C, et al. Iron and ferritin modulate MHC Class I expression and NK cell recognition. *Front Immunol.* 2019;10(February):1-12. doi:10.3389/fimmu.2019.00224
 116. Wei J, Kishton RJ, Angel M, et al. Ribosomal Proteins Regulate MHC Class I Peptide Generation for Immunosurveillance. *Mol Cell.* 2019;73(6):1162-1173.e5. doi:10.1016/j.molcel.2018.12.020
 117. Salih J, Kanz L, Salih HR, Krusch M. The FLT3-Inhibitors Midostaurin, Sunitinib, Sorafenib, and TKI258 Differentially Affect NK Cell-Mediated Immunesurveillance of Acute Myeloid Leukemia. *Blood.* 2009;114(22):3785. doi:10.1182/blood.V114.22.3785.3785
 118. Chen Y, Ning J, Cao W, et al. Research Progress of TXNIP as a Tumor Suppressor Gene Participating in the Metabolic Reprogramming and Oxidative Stress of Cancer Cells in Various Cancers. *Front Oncol.* 2020;10(October):1-12.
 119. Kim DO, Byun JE, Kim WS, et al. Txnip regulates natural killer cell-mediated innate immunity by inhibiting ifn- γ production during bacterial infection. *Int J Mol Sci.* 2020;21(24):1-19. doi:10.3390/ijms21249499
 120. Fang M, Orr MT, Spee P, Egebjerg T, Lanier LL, Sigal LJ. CD94 Is Essential for NK Cell-Mediated Resistance to a Lethal Viral Disease. *Immunity.* 2011;34(4):579-589. doi:10.1016/j.immuni.2011.02.015
 121. Vignesh KS, Deepe GS. Metallothioneins: Emerging modulators in immunity and infection. *Int J Mol Sci.* 2017;18(10). doi:10.3390/ijms18102197
 122. Wolenski FS, Fisher CD, Sano T, et al. The NAE inhibitor pevonedistat (MLN4924) synergizes with TNF- α to activate apoptosis. *Cell Death Discov.* 2015;1(1):1-9. doi:10.1038/cddiscovery.2015.34
 123. Levis M. Midostaurin approved for FLT3-mutated AML. *Blood.* 2017;129(26):3403-3406. doi:10.1182/blood-2017-05-782292
 124. Finak G, McDavid A, Yajima M, et al. MAST: A flexible statistical framework for assessing transcriptional changes and characterizing heterogeneity in single-cell RNA sequencing data. *Genome Biol.* 2015;16(1):1-13. doi:10.1186/s13059-015-0844-5

Supplementary material

Equation 1. Dose calculations of radiation given to K562 feeder cells.

Radiation dose needed: 100 Gy

Original dose rate: 2.01 Gy/min

Dose factor in March 2021: 1.696028

$$\text{Time required to give 100 Gy dose} = \frac{100}{\frac{2.01 \text{ Gy/min}}{1.696028}} = 84.64 \text{ min} = 5078 \text{ s}$$

	1	2	3	4	5	6	7	8	9	10	11	12	13	14	15	16	17	18	19	20	21	22	23	24	
A	cells	BzCl	d	d	d	d	d	d	d	d	d	d	d	d	d	d	d	d	d	d	d	d	d	BzCl	
B	cells	d	d	d	d	d	d	d	DMSO	d	d	d	d	d	d	BzCl	d	d	d	d	d	d	d	d	cells
C	cells	d	d	d	d	d	d	d	d	d	d	DMSO	d	d	d	d	d	d	d	DMSO	d	d	d	d	cells
D	cells	d	d	d	DMSO	d	d	d	d	d	d	d	d	d	d	d	d	d	d	d	d	d	d	d	cells
E	cells	d	d	d	d	d	d	d	d	d	d	d	d	d	DMSO	d	d	d	d	d	d	d	d	d	cells
F	cells	d	d	d	d	d	d	d	d	d	BzCl	d	d	d	d	d	d	d	d	d	d	d	d	d	cells
G	cells	d	d	d	d	BzCl	d	d	d	d	d	d	d	d	d	d	d	d	d	d	d	d	d	d	cells
H	cells	d	d	d	d	d	d	d	d	d	d	d	d	d	d	d	d	d	d	DMSO	d	d	d	d	cells
I	cells	d	d	d	d	d	d	DMSO	d	d	d	d	d	d	d	d	d	d	d	d	d	d	d	d	cells
J	cells	d	d	d	d	d	d	d	d	d	d	d	d	BzCl	d	d	d	d	d	d	d	d	d	d	cells
K	cells	d	d	d	d	d	d	d	d	d	d	d	d	d	d	d	d	d	d	d	d	BzCl	d	d	cells
L	cells	d	d	d	d	d	d	d	d	d	d	d	d	d	d	d	DMSO	d	d	d	d	d	d	d	cells
M	cells	d	d	BzCl	d	d	d	d	d	d	d	d	d	d	d	d	d	d	d	d	d	d	d	d	cells
N	cells	d	d	d	d	d	DMSO	d	d	d	BzCl	d	d	d	d	d	d	d	d	d	d	d	d	d	cells
O	cells	d	d	d	d	d	d	d	d	d	d	DMSO	d	d	d	d	d	BzCl	d	d	d	d	d	d	cells
P	cells	d	DMSO	d	d	d	d	d	d	d	d	d	d	d	d	d	d	d	d	d	d	DMSO	d	BzCl	cells

DMSO	= NK + DMSO
DMSO	= DMSO
BzCl	= benzyl chloride
cells	= target cells only
d	= drugs

Figure 1. Plating map used for automated pipetting in DSRT. Map used to plate cells and media on 384-well micro plates including drugs from the FO5A drug library. NK + DMSO includes only NK cells in diluted DMSO as control. DMSO includes only diluted DMSO as a control, whereas BzCl is used as an indicator of absolute cell death due to its toxicity. Wells including cells only were on the far right and left sides of the plate. Wells marked as d included drugs according to the FO5A protocol by FIMM.

FOR PRE-HASHING OPTIMISATION

Drugs: Ruxolitinib, Pictilisib

1	Initial	Diluted	DMSO conc (%)	
Conc (nm)	10000000	2000000	20	Add 40 uL H2O
Amount (uL)	10	50		SAVE ALIQUOT
2				Add 500 uL 20% DMSO
Conc (nm)	2000000	1000000	20	
Amount (uL)	10	20		
3				Add 995 uL R10
Conc (nm)	1000000	5000	0,1	
Amount (uL)	5	1000		
4				Add 5 uL of diluted drug into well
Conc (nm)	5000	1000	0,02	
Amount (uL)	5	25		

Drug: Pevonedistat

1	Initial	Diluted	DMSO conc (%)	
Conc (nm)	10000000	2000000	20	Add 40 uL H2O
Amount (uL)	10	50		SAVE ALIQUOT
2				Add 950 uL 20% DMSO
Conc (nm)	2000000	100000	20	SAVE ALIQUOT
Amount (uL)	50	1000		
3				Add 995 uL R10
Conc (nm)	100000	500	0,1	
Amount (uL)	5	1000		
4				Add 5 uL of diluted drug into well
Conc (nm)	500	100	0,02	
Amount (uL)	5	25		

Drugs: Daporinad, Midostaurin

1	Initial	Diluted	DMSO conc (%)	
Conc (nm)	10000000	2000000	20	Add 40 uL H2O
Amount (uL)	10	50		SAVE ALIQUOT
2				Add 950 uL 20% DMSO
Conc (nm)	2000000	100000	20	SAVE ALIQUOT
Amount (uL)	50	1000		
3				Add 950 uL 20% DMSO
Conc (nm)	100000	5000	20	
Amount (uL)	50	1000		
4				Add 990 uL R10
Conc (nm)	5000	50	0,2	
Amount (uL)	10	1000		
5				Add 5 uL of diluted drug into well
Conc (nm)	50	10	0,04	
Amount (uL)	5	25		

Drug: Quizartinib

1	Initial	Diluted	DMSO conc (%)	
Conc (nm)	10000000	2000000	20	Add 40 uL H2O
Amount (uL)	10	50		SAVE ALIQUOT
2				Add 950 uL 20% DMSO
Conc (nm)	2000000	100000	20	SAVE ALIQUOT
Amount (uL)	50	1000		
3				Add 995 uL 20% DMSO
Conc (nm)	100000	500	20	
Amount (uL)	5	1000		
4				Add 990 uL R10
Conc (nm)	500	5	0,2	
Amount (uL)	10	1000		
5				Add 5 uL of diluted drug into well
Conc (nm)	5	1	0,04	
Amount (uL)	5	25		

	nM	mL	nM	mL
	conc. 1	vol. 1	conc. 2	vol. 2
Daporinad	50	0,005	10	0,025
Ruxolitinib	5000	0,005	1000	0,025
Pevonedistat	500	0,005	100	0,025
Pictilisib	5000	0,005	1000	0,025
Quazirtinib	5	0,005	1	0,025
Midostaurin	50	0,005	10	0,025

Stock Vol. added Final conc. Vol./well

FOR HASHING

Drugs: Ruxolitinib, Pictilisib

1	Initial	Diluted	DMSO conc (%)	
Conc (nm)	2000000	400000	20	Add 40 uL 20% DMSO
Amount (uL)	10	50		
2				Add 500 uL 20% DMSO
Conc (nm)	400000	200000	20	
Amount (uL)	10	20		
3				Add 495 uL R10
Conc (nm)	200000	2000	0,2	
Amount (uL)	5	500		
4				Add 5 uL of diluted drug into well
Conc (nm)	2000	1000	0,1	
Amount (uL)	500	1000		

Drug: Pevonedistat

1	Initial	Diluted	DMSO conc (%)	
Conc (nm)	100000	20000	20	Add 40 uL 20% DMSO
Amount (uL)	10	50		
2				Add 495 uL R10
Conc (nm)	20000	200	0,2	
Amount (uL)	5	500		
3				Add 5 uL of diluted drug into well
Conc (nm)	200	100	0,1	
Amount (uL)	500	1000		

Drugs: Daporinad, Midostaurin

1	Initial	Diluted	DMSO conc (%)	
Conc (nm)	100000	20000	20	Add 40 uL H2O
Amount (uL)	10	50		
2				Add 90 uL 20% DMSO
Conc (nm)	20000	2000	20	
Amount (uL)	10	100		
3				Add 495 uL R10
Conc (nm)	2000	20	0,2	
Amount (uL)	5	500		
4				Add 5 uL of diluted drug into well
Conc (nm)	20	10	0,1	
Amount (uL)	500	1000		

Drug: Quizartinib

1	Initial	Diluted	DMSO conc (%)	
Conc (nm)	100000	20000	20	Add 40 uL H2O
Amount (uL)	10	50		
2				Add 990 uL 20% DMSO
Conc (nm)	20000	200	20	
Amount (uL)	10	1000		
3				Add 495 uL R10
Conc (nm)	200	2	0,2	
Amount (uL)	5	500		
4				Add 5 uL of diluted drug into well
Conc (nm)	2	1	0,1	
Amount (uL)	500	1000		

Figure 2. Serial drug dilutions and related calculations. Drug dilutions used for pre-hashing optimisation and hashing experiments. Calculated with equation $c_1V_1=c_2V_2$.

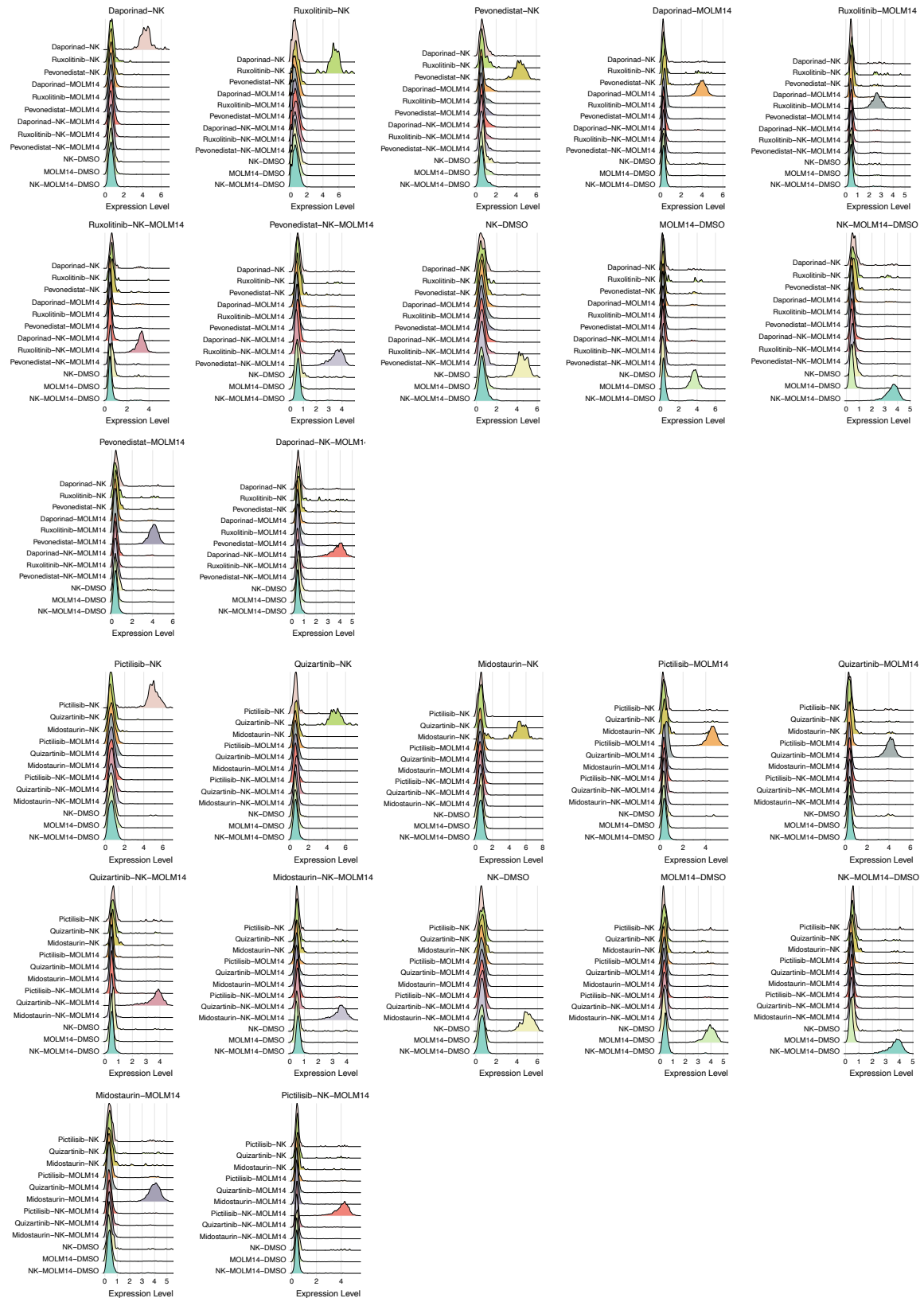


Figure 3. Quality control of hashtags indicating a specific condition. Peaks indicating specific hashtag antibody being bound to each condition and being representative of individual conditions.

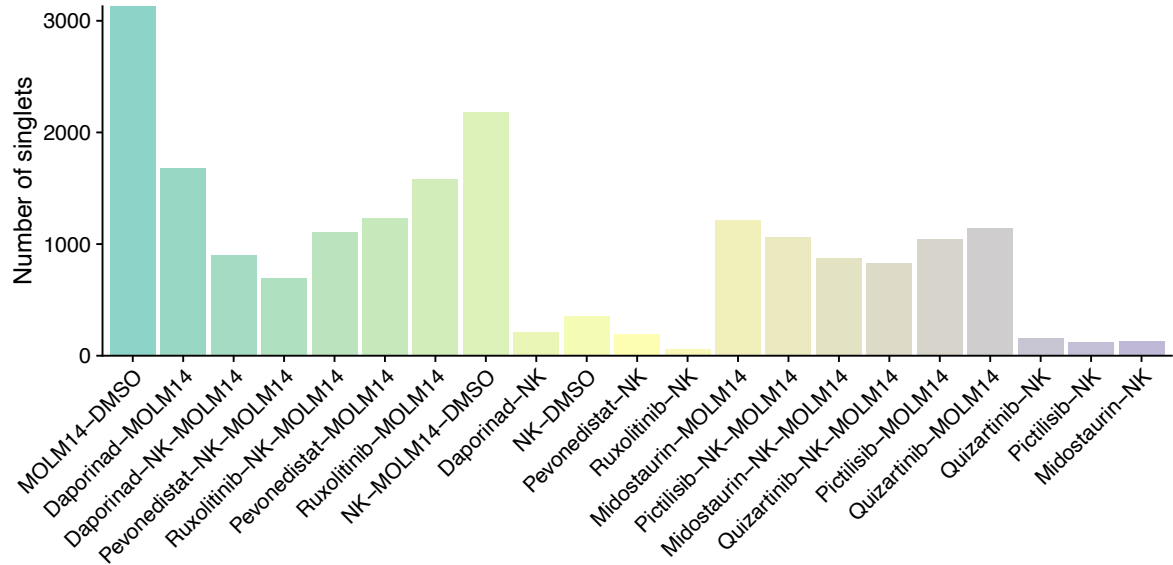


Figure 4. Cell counts in each condition in the scRNA sequencing. Cell counts in each condition of the two samples sequenced together. MOLM-14 DMSO and NK-MOLM-14-DMSO conditions have cells pooled from both samples for which higher cell counts can be observed.



Figure 5. Distribution of tagged cells on a UMAP. Hashtag-bound cells represented on a UMAP giving indication of how different conditions are portrayed on the transcriptomic landscape.

Table 1. Drugs screened in the FO5A plates and specific differential drug sensitivity (sDSS) scores obtained for each cell line. Drug compounds, their targets and phase of use together with sDSS scores across all three cell lines.

Drug compound	Mechanism/Targets	High phase/Approval status	MOLM-14 sDSS	THP-1 sDSS	HEL sDSS
1-methyl-D-tryptophan	IDO inhibitor	Investigational (Ph 2)	-1,9	9,5	0
4-hydroxytamoxifen	Estrogen receptor modulator	Investigational as a gel preparation	-5,7	0	0
8-amino-adenosine	RNA synthesis inhibitor	Probe	-0,9	-1,3	2,4
8-chloro-adenosine	RNA synthesis inhibitor	Investigational (Ph 2)	-5,7	-3,4	-0,4
A-1155463	Bcl inhibitor	Probe	4,6	-1,2	-1
A-1210477	MCL-1 inhibitor	Probe	-1,9	2,2	1,1
A-1331852	Bcl inhibitor	Probe	0	-4,2	-4,2
A-366	G9a/GLP inhibitor	Probe	-2,5	1	-7
A-419259	Src inhibitor	Probe	-7,3	-15,1	-17,4
ABC294640	Sphingosine kinase 2 inhibitor	Investigational (Ph 2)	-3,1	-1	-0,4
Abemaciclib	CDK inhibitor	Investigational (Ph 3)	4,2	0	-16,3
Abexinostat	HDAC inhibitor	Investigational (Ph 2)	11,3	-13,4	-2,5
Abiraterone	CYP inhibitor	Approved	0,3	0,3	-1,3
ABT-751	Mitotic inhibitor	Investigational (Ph 2)	-2,3	1	0
Acalabrutinib	BTK inhibitor	Investigational (Ph 3)	0	0	-2,3
Acitretin	Retinoid receptor agonist	Approved (non-oncology)	-0,8	0	0
Afatinib	RTK inhibitor	Approved	-1,6	0	0,8
Afuresertib	AKT inhibitor	Investigational (Ph 2)	0	-0,2	0
Aldoxorubicin	Topoisomerase inhibitor	Investigational (Ph 3)	-2,6	1	0
Alectinib	ALK inhibitor	Approved (Japan, US)	-3	0	0
Alisertib	Aurora inhibitor	Investigational (Ph 3)	-4,7	1,9	8,3
Allopurinol	Xanthine oxidase inhibitor	Approved	-4,6	-4,3	-11,4
Alpelisib	PI3K inhibitor	Investigational (Ph 2)	-2,7	-1,7	-2,5
Altiratinib	MET inhibitor	Investigational (Ph 1)	-15,8	-3,4	0,1
Alvocidib	CDK inhibitor	Investigational (Ph 2)	0,5	-2,8	11,1
Amcasertib	Cancer stem cell kinase inhibitor	Investigational (Ph 2)	-5,5	-0,4	-4,3
AMG-232	MDM2 inhibitor	Investigational (Ph 2)	-2,8	-2,5	-2,6
AMG-337	MET inhibitor	Investigational (Ph 2)	-0,7	0	0
AMG-925	FLT3 inhibitor	Probe	-6,5	-1,6	-10,2
AMG319	PI3K inhibitor	Investigational (Ph 2)	0	-4,1	0
Aminoglutethimide	Aromatase inhibitor	Approved	1	0,5	-1,9
Amsacrine	Topoisomerase inhibitor	Approved	-3,9	-0,3	0,4
Amuvatinib	Broad range TKI	Investigational (Ph 2)	3,4	-1,8	2,1
Anagrelide	Antithrombotic	Approved	1,7	0	-6,5
Anastrozole	Aromatase inhibitor	Approved	1,1	0,3	0
Apalutamide	AR antagonist	Investigational (Ph 2)	-3,4	-5,3	0
Apatinib	VEGFR inhibitor	Investigational (Ph 3)	-10,5	-14,4	-14,7
APR-246	p53 activator, thioredoxin reductase 1 inhibitor	Investigational (Ph 1)	0,7	0	-2,2
AR-42	HDAC inhibitor	Investigational (Ph 1)	-2	0	-6,2
Arsenic(III) oxide	Reductase inhibitor	Approved	0	1,3	0

ARV-825	BET-targeting PROTAC	Probe	-6,7	0	-11
Asciminib	Abl inhibitor	Investigational (Ph 1)	0	0	0
ASP3026	ALK inhibitor	Investigational (Ph 1)	-5,3	-4,7	-7,9
AT 101	Bcl inhibitor	Investigational (Ph 2)	-7,8	2,9	-3,1
AT-406	XIAP/clAP1/clAP2 inhibitor	Investigational (Ph 1)	1,7	2,6	-1,3
AT13148	ROCK/PKA/p7056K inhibitor	Investigational (Ph 1)	-7,8	-1,1	-8,3
AT7519	CDK inhibitor	Investigational (Ph 1)	0	1,5	-2,3
AT9283	JAK inhibitor	Investigational (Ph 2)	1,8	-8,9	-2,7
Atorvastatin	Reductase inhibitor	Approved	0,5	3,8	-3
Auranofin	Antirheumatic agent	Approved	1,6	-3,3	-3,1
AVN944	IMPDH inhibitor	Investigational (Ph 2)	5,8	3,8	-2,5
Axitinib	Broad range TKI	Approved	-32,3	0	0
AZ 3146	TTK inhibitor	Probe	-5,3	4,8	-11,7
AZ191	DYRK1A inhibitor	Probe	-8,1	-5,6	-13,5
Azacitidine	Methyl transferase inhibitor	Approved	-0,2	0,1	-5,7
AZD-1080	GSK3 inhibitor	Investigational (Ph 1)	0	0,1	-4,2
AZD-5363	AKT inhibitor	Investigational (Ph 2)	-2,1	-1,8	3
AZD-5438	CDK inhibitor	Investigational (Ph 1)	0,2	1,6	5,2
AZD-6482	PI3K inhibitor	Investigational (Ph 1)	-13,1	-1	-2,8
AZD-8186	PI3K inhibitor	Investigational (Ph 1)	-8,1	-3,2	0
AZD0156	ATM inhibitor	Investigational (Ph 1)	-1,6	-1,3	-2,9
AZD1152-HQPA	Aurora inhibitor	Investigational (Ph 3)	-12,2	0	0
AZD1208	PIM inhibitor	Investigational (Ph 1)	-4,2	-5,6	-7
AZD1480	JAK inhibitor	Investigational (Ph 1)	-0,2	0	2
AZD1775	Wee1 inhibitor	Investigational (Ph 2)	-4,8	2,1	8,2
AZD3759	EGFR Inhibitor	Investigational (Ph 2)	-1,6	0	0
AZD3965	MCT1 inhibitor	Investigational (Ph 1)	0	0	0
AZD4547	FGFR inhibitor	Investigational (Ph 2)	1,1	1,1	0
AZD6738	ATR inhibitor	Investigational (Ph 1)	-3,1	-7,1	0
AZD7545	PDHK inhibitor	Probe	2,6	4,2	-3,1
AZD7762	Chk1 inhibitor	Investigational (Ph 1)	-4,8	-4,3	-16,4
AZD8055	mTOR inhibitor	Investigational (Ph 1)	-2,2	-0,5	-1,8
Bafetinib	Abl inhibitor	Investigational (Ph 2)	-4,6	-0,9	3,2
Baricitinib	JAK inhibitor	Approved (EU)	8,7	-10,3	3,6
BAY 87-2243	HIF1alpha inhibitor	Investigational (Ph 1)	0	0	5,1
BAY-1436032	IDH1 R132H/R132C inhibitor	Investigational (Ph 1)	-0,6	0	0,6
BCI	Dusp6 inhibitor	Probe	-1,5	-1,3	-0,4
Belinostat	HDAC inhibitor	Approved (US)	-1,9	-5,1	-5,2
Bentamapimod	JNK inhibitor	Investigational (Ph 1)	-21,4	0	0
Bexarotene	Antineoplastic agent	Approved	-2,2	1,6	-1,3
BGB-283	RAF inhibitor	Investigational (Ph 1)	-1,5	-2,4	-1,5
BGB324	Axl inhibitor	Investigational (Ph 1)	-3,8	0	0
BI 2536	PLK1 inhibitor	Investigational (Ph 2)	-5,6	2,8	-5,4
Bicalutamide	Nonsteroidal antiandrogen	Approved	-0,7	-1,3	-1,1
BIIB021	HSP90 inhibitor	Investigational (Ph 2)	-4,5	-2,6	2,9
Bimatoprost	Prostaglandin analog	Approved	0	0	0
Binimetinib	MEK inhibitor	Investigational (Ph 2)	-4	-7,7	-5
Birabresib	BET inhibitor	Investigational (Ph 2)	-4,6	-1,1	-12

Birinapant	SMAC mimetic	Investigational (Ph 2)	-4,2	0	-2,8
Bleomycin	Antibiotic	Approved	-0,1	-0,5	0
BMS-754807	IGF1R inhibitor	Investigational (Ph 2)	-4,8	-3,9	6,2
BMS-777607	MET inhibitor	Investigational (Ph 2)	-1,4	0	-1
BMS-911543	JAK inhibitor	Investigational (Ph 1)	-0,7	0	4,7
BMS863233	Cdc7 inhibitor	Investigational (Ph 2)	1,6	-3,7	-4,2
Bortezomib	Proteasome inhibitor	Approved	0,4	9	8
Bosutinib	Abl-Src inhibitor	Approved	-1,7	-1,9	13,4
BRD7116	Leukemic stem cell inhibitor	Probe	0,4	-7,1	-1,5
Brigatinib	ALK inhibitor	Approved (US)	-0,8	-1,7	-9,3
Brivanib	VEGFR inhibitor	Investigational (Ph 3)	2,9	0	0
Bryostatin 1	PKC activator	Investigational (Ph 1)	8,5	8	0
Buparlisib	PI3K inhibitor	Investigational (Ph 2)	-5,2	-1,2	0
BX-912	PDK1 inhibitor	Probe	-8	-5,6	-1,7
C646	CBP inhibitor	Probe	-0,7	-0,2	0
Cabazitaxel	Mitotic inhibitor	Approved	-2,2	1,7	8
Cabozantinib	Broad range TKI	Approved	-6,4	1,5	0
Canertinib	HER inhibitor	Investigational (Ph 3)	-2,7	-2,6	0
Capecitabine	Synthase inhibitor	Approved	0	0	0
Capmatinib	MET inhibitor	Investigational (Ph 2)	-0,6	3,2	-0,3
Carboplatin	Antineoplastic agent	Approved	0	3,9	0,3
Carfilzomib	Proteasome inhibitor	Approved	-3	2,3	7
CC-115	mTOR inhibitor	Investigational (Ph 1)	-5,6	-0,5	-7,8
CC-223	mTOR inhibitor	Investigational (Ph 2)	-2	-2,4	2,1
CC122	Immunomodulator	Investigational (Ph 2)	0	0	0
CCT196969	RAF/Src inhibitor	Probe	0,2	-6,1	-4,3
Cediranib	Broad range TKI	Investigational (Ph 3)	-2,7	0	0
Celecoxib	COX-2 inhibitor	Approved	3,5	7,3	-1,6
CEP-32496	B-Raf inhibitor	Investigational (Ph 2)	0	-3,7	0
CEP-37440	ALK inhibitor	Investigational (Ph 1)	-10,1	-4,6	-6,2
Cerdulatinib	JAK/SYK inhibitor	Investigational (Ph 1)	0,7	-26,4	-14,2
Ceritinib	ALK inhibitor	Approved	-7,1	-2	-0,3
Chloroquine	Antimalaria agent	Approved	-7,8	2,7	-13,2
Cilengitide	alphaVbeta3 integrin inhibitor	Investigational (Ph 3)	0	0	0
Cisplatin	Antineoplastic agent	Approved	0,3	-0,8	2,3
Cladribine	Antimetabolite	Approved	-2,5	0,7	1,6
Clofarabine	Antimetabolite	Approved	-5	-0,8	-15,2
Clomifene	Estrogen receptor modulator	Approved	-2,5	0	-6
Cobimetinib	MEK inhibitor	Approved (US)	1	-10	-0,7
Copanlisib	PI3K inhibitor	Investigational (Ph 2)	-7,5	-9,1	-3,7
CPI-0610	BET inhibitor	Investigational (Ph 1)	0,1	0	-8,6
CPI-360	EZH2 inhibitor	Probe	-5,4	0	0
CPI-613	pyruvate dehydrogenase/alpha-ketoglutarate dehydrogenase inhibitor	Investigational (Ph 2)	0	0	0
Crenolanib	PDGFR inhibitor	Investigational (Ph 2)	-1,7	-0,7	8,1
Crizotinib	ALK inhibitor	Approved	2,7	0	0,2
CUDC-305	HSP90 inhibitor	Investigational (Ph 1)	-3,8	-1,2	-3,1

CUDC-907	HDAC inhibitor	Investigational (Ph 2)	-7,6	-19,6	-6,5
Cytarabine	Antimetabolite	Approved	-0,1	-3,1	0,5
Dabrafenib	B-Raf inhibitor	Approved	-0,9	4,7	-1,5
Dacomitinib	HER inhibitor	Investigational (Ph 3)	-1,2	0	0
Dactinomycin	DNA/RNA synthesis inhibitor	Approved	-9,2	1,1	0,7
Dactolisib	mTOR inhibitor	Investigational (Ph 2)	1	1,1	3,9
Danusertib	Aurora inhibitor	Investigational (Ph 2)	-3,4	2,7	3
Daporinad	NAMPT inhibitor	Investigational (Ph 2)	14,9	13,7	4,2
Darapladib	phospholipase A2 inhibitor	Investigational (Ph 3)	0	0	0
Dasatinib	Broad range TKI	Approved	-9,3	-12,4	-17,6
Daunorubicin	Topoisomerase inhibitor	Approved	-4,5	0,8	-2,9
dBET1	BET-targeting PROTAC	Probe	-2	0,9	-10,7
Decernotinib	JAK inhibitor	Investigational (Ph 3)	1,2	-5,4	1,9
Decitabine	Methyl transferase inhibitor	Approved	-0,7	1,3	-3,1
Deferoxamine	Iron chelator	Approved (non-oncology)	-1	0	-6,2
DEL-22379	ERK inhibitor	Probe	-5,5	-2,4	-0,2
Dexamethasone	Glucocorticoid	Approved	0	-6	0
Digoxin	Cardiac glycoside	Approved (non-oncology)	0,1	1,9	-2,5
Dinaciclib	CDK inhibitor	Investigational (Ph 3)	-1,4	1,4	5,8
Disulfiram(+CuCl2)	alcohol dehydrogenase inhibitor	Approved (non-oncology)	2,7	0	-0,3
Docetaxel	Mitotic inhibitor	Approved	-0,7	3,3	3,5
Doramapimod	MAPK inhibitor	Investigational (Ph 1)	-1,6	-8,5	0,5
Dovitinib	RTK inhibitor	Investigational (Ph 3)	-17,3	-2,4	-6,2
Doxorubicin	Topoisomerase inhibitor	Approved	-8,5	2,4	0
Duvelisib	PI3K inhibitor	Investigational (Ph 3)	-8	-3,7	0
E7820	Integrin alpha2 expression inhibitor	Investigational (Ph 2)	-4,4	3,1	-6,5
Eltanexor	XPO1/CRM1 inhibitor	Investigational (Ph 2)	-7,2	-5,9	-4,6
Enasidenib	IDH2-R140Q inhibitor	Approved (US)	0	-5	1,3
Encorafenib	B-Raf inhibitor	Investigational (Ph 2)	0,2	8,8	-2,5
ENMD-2076	Kinase inhibitor	Investigational (Ph 2)	-4,7	-5,6	0
Ensartinib	ALK inhibitor	Investigational (Ph 3)	-0,1	-0,4	1,7
Entinostat	HDAC inhibitor	Investigational (Ph 2)	-4,2	-0,2	-8,4
Entospletinib	Syk inhibitor	Investigational (Ph 2)	-33,2	0	-34,8
Entrectinib	TRK/ROS1/ALK inhibitor	Investigational (Ph 2)	-1,8	-6	-1,4
Enzalutamide	AR antagonist	Approved	-4,2	0	0
Enzastaurin	PKC inhibitor	Investigational (Ph 3)	-1,6	0	-3,1
Epacadostat	IDO inhibitor	Investigational (Ph 3)	0	-0,1	0
Epirubicin	Topoisomerase inhibitor	Approved	-5,4	-0,4	-1,1
EPZ-5687	EZH2 inhibitor	Probe	-1,6	0	0
EPZ015666	PRMT5 inhibitor	Probe	0	-0,1	0
EPZ031686	SMYD3 inhibitor	Probe	0	0	0
Erastin	VDAC inhibitor	Probe	-4,2	0	2,9
Erdafitinib	FGFR inhibitor	Investigational (Ph 2)	-0,3	0	3,5
Eribulin	Mitotic inhibitor	Approved	-7,8	2	0
Erlotinib	EGFR Inhibitor	Approved	-5,4	0	-5,4
Etoposide	Topoisomerase inhibitor	Approved	-1,5	0,3	-3,2
Everolimus	mTORC inhibitor	Approved	-0,8	-0,7	-1,3

Exemestane	Aromatase inhibitor	Approved	1,5	0,4	0
Fedratinib	JAK inhibitor	Investigational (Ph 2)	-0,8	-1,9	-0,2
Filanesib	KSP/Eg5 inhibitor	Investigational (Ph 2)	-3,3	-0,2	6,7
Filgotinib	JAK inhibitor	Investigational (Ph 2)	0	-9	0
Finasteride	Reductase inhibitor	Approved	0	0	0
Fingolimod	Immunomodulator	Approved	-5,1	-1,9	-10,2
Floxuridine	Antimetabolite	Approved	2	-3	0
Fludarabine	Antimetabolite	Approved	0	-0,4	0
Fluorouracil	Antimetabolite	Approved	0,8	0,8	0
Flutamide	Nonsteroidal antiandrogen	Approved	-1,1	0	0
Foretinib	Antineoplastic agent	Investigational (Ph 2)	-17,3	-1,7	2,8
Fostamatinib	Syk inhibitor	Investigational (Ph 2)	0,5	-0,2	-4,6
FRAX486	PAK inhibitor	Probe	2	3,2	16,5
Fulvestrant	Estrogen receptor modulator	Approved	0	0	0
Galiellalactone	STAT3-DNA interaction inhibitor	Probe	1,6	0,1	0
Galunisertib	TGF-B/Smad inhibitor	Investigational (Ph 2)	-0,4	0	1,5
Gandotinib	JAK inhibitor	Investigational (Ph 2)	-0,2	-15,8	1,1
Ganetespib	HSP90 inhibitor	Investigational (Ph 3)	-7,1	-0,4	-3,6
GDC-0084	PI3K/mTOR inhibitor	Investigational (Ph 1)	-7,9	-9	-6,7
GDC-0623	MEK inhibitor	Investigational (Ph 2)	-0,8	-7,4	-0,9
GDC-0853	BTK inhibitor	Investigational (Ph 2)	0	0	0
GDC-0919	IDO inhibitor	Investigational (Ph 1)	-2,2	-0,1	0,4
Gedatolisib	PI3K/mTOR inhibitor	Investigational (Ph 2))	6	0,1	-1
Gefitinib	Broad range TKI	Approved	-0,3	0	-1,7
Gemcitabine	Antimetabolite	Approved	-4,7	0,1	0,4
Gilteritinib	FLT3/AXL inhibitor	Investigational (Ph 2)	-2,4	-0,1	-4,4
Givinostat	HDAC inhibitor	Investigational (Ph 2)	2,5	0	-1,3
Glasdegib	Smo inhibitor	Investigational (Ph 2)	0	-2,5	0
Glesatinib	Broad range TKI	Investigational (Ph 2)	-4,6	-0,5	0
GNE-0877	LRRK2 inhibitor	Probe	-0,1	-0,2	0
GNE-7915	LRRK2 inhibitor	Probe	-2,7	0	-7,1
Golvatinib	MET/VEGFR inhibitor	Investigational (Ph 2)	1	0	-0,2
Goserelin	Hormone superagonist	Approved	0	0,1	-1,2
GSK-1070916	Aurora inhibitor	Investigational (Ph 1)	-3,5	0,8	0
GSK-2334470	PDK1 inhibitor	Probe	-5,8	-4,6	-3,7
GSK-461364	PLK1 inhibitor	Investigational (Ph 1)	-0,9	-6,5	-9,6
GSK-690693	AKT/PKA/PKC inhibitor	Investigational (Ph 1)	-7,8	0	-6
GSK-J4	Histone demethylase inhibitor	Probe	-2,8	2,1	2,4
GSK2256098	FAK inhibitor	Investigational (Ph 2)	0,2	-6,6	0
GSK2636771	PI3K inhibitor	Investigational (Ph 1)	-2	-5,9	0
GSK2656157	PERK inhibitor	Probe	-0,4	0	-2,5
GSK269962	ROCK inhibitor	Probe	-12,5	-2,5	-24,7
GSK2801	BAZ2B/A bromodomain inhibitor	Probe	-2,5	-2,2	0
GSK2830371	Wip1 inhibitor	Probe	0,3	0	-1,1
GSK2879552	LSD1 inhibitor	Investigational (Ph 1)	3,8	0	-7
GSK343	EZH2 inhibitor	Probe	-0,1	0	0
GSK650394	SGK inhibitor	Probe	-3,1	1	-1,5

GSK923295	CENP-E inhibitor	Investigational (Ph 1)	0,4	3,8	0
Hydroxyfasudil	ROCK inhibitor	(Approved Japan)	0	0,2	-4,5
Hydroxyurea	Antineoplastic agent	Approved	0,1	-3,4	0
I-BET151	BET inhibitor	Probe	-3,2	0	-13,7
Ibrutinib	Btk inhibitor	Approved	-2,5	-7,3	0
Icotinib	EGFR Inhibitor	Investigational (Ph 2)	-1	2,8	0
Idarubicin	Topoisomerase inhibitor	Approved	-7,6	1,1	-2,9
Idasanutlin	p53-MDM2 inhibitor	Investigational (Ph 3)	-2,7	0	-4
Idelalisib	PI3K inhibitor	Approved	-6,2	-2,4	-6,9
Imatinib	Broad range TKI	Approved	0	-1,9	0
Imiquimod	Immunomodulator	Approved	0	0	0
Indibulin	Mitotic inhibitor	Investigational (Ph 2)	0,6	0	0
Infigratinib	FGFR inhibitor	Investigational (Ph 1)	-0,2	0	-0,1
IOX-1	2-Oxoglutarate Oxygenase Inhibitor	Probe	4	0,5	-0,1
IOX-2	PHD2 inhibitor	Probe	0	-6,5	0
Ipatasertib	AKT inhibitor	Investigational (Ph 2)	0,3	3,5	-2,8
Itraconazole	Hedgehog signaling inhibitor	Approved (non-oncology)	0,5	0,3	-0,5
Ivosidenib	IDH1 R132H/R132C inhibitor	Investigational (Ph 3)	0	0	1,9
Ixabepilone	Mitotic inhibitor	Approved	-2,4	-3,8	-3
Ixazomib	Proteasome inhibitor	Approved	-3,1	3,2	1,8
JPH203	LAT1 inhibitor	Probe	5,1	0	-0,1
JQ1	BET inhibitor	Probe	-7,2	5,7	-12,3
KD025	ROCK2 inhibitor	Investigational (Ph 2)	0	-10,6	-6,8
KU-60019	ATM inhibitor	Probe	-5,5	-3	0
Lapatinib	Broad range TKI	Approved	-1,9	-3,8	-4,8
Larotrectinib	TRK inhibitor	Investigational (Ph 2)	0	0	0
Lasofixifene	Estrogen receptor modulator	Approved	-2,7	0	-2,4
Lenalidomide	Immunomodulator	Approved	-3,1	0	2,1
Lenvatinib	Broad range TKI	Approved (US)	-3,6	0	1,1
Letrozole	Aromatase inhibitor	Approved	13,1	0	-1,9
Linifanib	Broad range TKI	Investigational (Ph 3)	-5,8	0	0
Linsitinib	IGF1R inhibitor	Investigational (Ph 2)	0	0	-0,7
Litronesib	Eg5 inhibitor	Investigational (Ph 2)	-1,2	5,7	4,2
Lomeguatrib	Methyl transferase inhibitor	Investigational (Ph 2)	-0,6	-4,7	2,6
Lonafarnib	Farnesyl transferase inhibitor	Investigational (Ph 3)	-2,6	-4,6	0,6
Losmapimod	MAPK inhibitor	Investigational (Ph 3)	0	-1,6	5,4
Lovastatin	Reductase inhibitor	approved (non-oncology)	-4,3	0	-2,7
Lucitanib	FGFR1/VEGFR inhibitor	Investigational (Ph 2)	-2,3	-1,9	0,7
Luminespib	HSP90 inhibitor	Investigational (Ph 2)	-6,9	0,2	-0,5
LY-2584702	p70S6K inhibitor	Investigational (Ph 1)	-1,7	4,1	0
LY-2874455	FGFR inhibitor	Investigational (Ph 1)	-5,2	-15,2	-1,2
LY3009120	RAF inhibitor	Investigational (Ph 1)	-1	-6,9	-7,1
LY3023414	PI3K/mTOR inhibitor	Investigational (Ph 2)	3	-6,1	-2,2
Marimastat	MMP inhibitor	Investigational (Ph 3)	0	-0,4	-1
Masitinib	KIT inhibitor	Investigational (Ph 3)	-12,6	-11,8	0
Megestrol acetate	Progestogen	Approved	0	0	-2,5
Mepacrine	NF-kB inhibitor, p53 activator	Approved	-1,1	1,6	-1,3

Mercaptopurine	Antimetabolite	Approved	4,1	-5,6	-0,1
Merestinib	MET inhibitor	Investigational (Ph 2)	-12,8	-0,6	0,9
Metformin	AMPK activator	Approved (non-oncology)	0	0	0
Methotrexate	Antimetabolite	Approved	-0,3	-11,6	-15,9
Methylprednisolone	Glucocorticoid	Approved	-30,1	-8,1	-10,1
Midostaurin	Broad range TKI	Approved (US)	-10	-4,1	0
Miliciclib	CDK inhibitor	Investigational (Ph 2)	-1	-5,2	-10,9
Miltefosine	PI3K/AKT inhibitor	Approved	-5,1	1	-2,3
Mitomycin C	Antineoplastic agent	Approved	0	4,9	-0,2
Mitotane	Antineoplastic agent	Approved	1,2	-8,8	-7,2
Mitoxantrone	Topoisomerase inhibitor	Approved	-4,8	-1,6	-2,1
Mivebresib	BET inhibitor	Investigational (Ph 1)	-2,2	2,9	-13,6
MK-0752	gamma-secretase/notch inhibitor	Investigational (Ph 2)	0	0	0
MK-2206	AKT inhibitor	Investigational (Ph 2)	-0,9	1,1	0,8
MK-8745	Aurora inhibitor	Probe	0,2	2,5	7,3
MK-8776	CHEK1 inhibitor	Investigational (Ph 1)	-3,2	-2,5	-0,8
ML323	USP1-UAF1 inhibitor	Probe	2,3	-0,7	-0,5
ML390	DHODH inhibitor	Probe	2,3	0	-0,4
Mocetinostat	HDAC inhibitor	Investigational (Ph 2)	-0,4	-1,8	-7,5
Molibresib	BET inhibitor	Investigational (Ph 1)	-1,9	-1	-7,3
Momelotinib	JAK inhibitor	Investigational (Ph 2)	-0,6	0	0
Motesanib	Broad range TKI	Investigational (Ph 2)	0	-7,3	-8,5
Motolimod	TLR agonist	Investigational (Ph 2)	0	1,7	0
MST-312	Telomerase inhibitor	Probe	-10,2	3,8	-1,3
Mubritinib	HER inhibitor	Investigational (Ph 1)	2,6	-3,2	0,7
Napabucasin	CSC inhibitor	Investigational (Ph 3)	-8,4	0	-3
Navitoclax	Bcl inhibitor	Investigational (Ph 2)	-3,1	0	-1,8
Necrostatin 2	Necroptosis inhibitor	Probe	0	-0,8	0
Neflamapimod	MAPK inhibitor	Investigational (Ph 2)	0	0	8
Nelarabine	Synthase inhibitor	Approved	-1,9	2	7,4
Neratinib	HER2/EGFR inhibitor	Approved (US)	-3,5	2	-0,6
Nilotinib	Abl inhibitor	Approved	-2,6	-0,6	0
Nilutamide	Nonsteroidal antiandrogen	Approved	-0,7	0	3
Nintedanib	RTK inhibitor	Approved	-6,5	0	9,7
Niraparib	PARP inhibitor	Approved (US)	-1,7	0	-7,4
NMS-873	p97/VCP inhibitor	Probe	-1,4	-2,2	0
NVP-AEW541	IGF1R inhibitor	Investigational (Ph 1)	-9,2	-3	0
NVP-BGT226	PI3K/mTOR inhibitor	Investigational (Ph 2)	-1	1	-1,7
NVP-BHG712	EphB4 inhibitor	Probe	-4,5	0,6	-0,4
NVP-CGM097	p53-MDM2 inhibitor	Investigational (Ph 1)	-8,1	-3,9	-2,6
NVP-LCL161	SMAC mimetic	Investigational (Ph 2)	-2,5	-0,7	-1,1
NVP-LGK974	PORCN inhibitor	Investigational (Ph 1)	-5	-0,6	0
NVP-RAF265	C-Raf inhibitor	Investigational (Ph 2)	-4	-2,4	-0,6
NVP-SHP099	SHP2 inhibitor	Probe	-0,8	-0,4	0
ODM-201	AR antagonist	Investigational (Ph 3)	-0,5	4,3	-6
Olaparib	PARP inhibitor	Approved	0,8	-0,9	0
Olmudinib	EGFR Inhibitor	Investigational (Ph 2)	-2,9	-11,6	-11,8

Omacetaxine	Protein synthesis inhibitor	Approved	-5,9	0,5	4,4
Omaveloxolone	Nrf2 activator	Investigational (Ph 2)	6,7	2,9	-5,1
Omipalisib	PI3K/mTOR inhibitor	Investigational (Ph 1)	-7,9	-9,1	-7,9
Onalespib	HSP90 inhibitor	Investigational (Ph 2)	-5	-6,1	-6,5
ONX-0914	LMP7	Probe	1	3,3	6,5
Oprozomib	Proteasome inhibitor	Investigational (Ph 1)	-2,8	2,3	1,8
Orteronel	Androgen synthesis inhibitor	Investigational (Ph 3)	0,6	0	-3,3
Osimertinib	RTK inhibitor	Approved	-7,7	-1,1	-7,9
OSU-03012	PDPK1 inhibitor	Investigational (Ph 1)	0	0	0
OTS-964	TOPK inhibitor	Probe	-4,1	-0,2	0
OTS167	MELK inhibitor	Investigational (Ph 2)	1,1	-1,3	-1,5
Oxaliplatin	Antineoplastic agent	Approved	-1,9	4,7	1
PAC-1	procaspase-3 activator	Investigational (Ph 1)	0,4	0	-0,9
Paclitaxel	Mitotic inhibitor	Approved	-0,4	-0,1	-10,8
Pacritinib	FLT3/JAK inhibitor	Investigational (Ph 3)	-8,9	-3,2	-5,5
Palbociclib	CDK inhibitor	Approved	-5,1	-1,8	-10
Palomid-529	AKT/mTOR/PI3K inhibitor	Investigational (Ph 1)	-6,9	0	-4,7
Panobinostat	HDAC inhibitor	Approved	0,3	0	-3,5
Pazopanib	Broad range TKI	Approved	-5,3	0	-0,5
PCI-34051	HDAC inhibitor	Probe	-2,9	0	-1,7
PD0325901	MEK inhibitor	Investigational (Ph 2)	0,5	-12,6	-4,2
Peficitinb	JAK inhibitor	Investigational (Ph 3)	1	-5,5	-0,4
Pemetrexed	Reductase inhibitor	Approved	3,3	-1,5	-4,5
Pentostatin	Antimetabolite	Approved	3,4	-5,5	-8
Perifosine	AKT inhibitor	Investigational (Ph 3)	-0,7	0,2	-2,2
Pevonedistat	NAE inhibitor	Investigational (Ph 1)	7,5	13,8	6,6
Pexidartinib	Broad range TKI	Investigational (Ph 3)	-9,9	0	0
PF-00477736	Chk1 inhibitor	Investigational (Ph 1)	-1,1	-6,8	-8,8
PF-00562271	FAK inhibitor	Investigational (Ph 1)	-7,7	-7,3	0
PF-03758309	PAK inhibitor	Investigational (Ph 1)	-5,8	-4,1	0
PF-04708671	p70S6K inhibitor	Probe	-1,6	0	-3,5
PF-06463922	ALK inhibitor	Investigational (Ph 2)	0	0	0
PF-3845	FAAH inhibitor	Probe	1,5	-5	1,8
PF-4800567	CK1 inhibitor	Probe	-2,2	0	-0,5
PF-670462	CK1 inhibitor	Probe	-1,6	-1	0,4
PF06650833	IRAK4 inhibitor	Investigational (Ph 2)	0,7	0	-0,4
PFI-1	BET inhibitor	Probe	0	0,8	0
PH-797804	MAPK inhibitor	Investigational (Ph 2)	0	-0,2	12,9
PHA 408	IKK-2 inhibitor	Probe	-3,6	-1,8	-6,3
Pictilisib	PI3K inhibitor	Investigational (Ph 2)	-10,5	-10,5	-5
Pilocarpine	Muscarinic receptor agonist	Approved	0	0	0
PIM-447	PIM inhibitor	Investigational (Ph 1)	1,3	-3,2	-10,4
Pinometostat	DOT1L inhibitor	Investigational (Ph 1)	-2	0	-0,3
Pirfenidone	Antifibrotic	Approved	-2,1	0	0
Pixantrone	Topoisomerase inhibitor	Investigational (Ph 3)	-3	2,3	0
Plerixafor	CXCR4 agonist	Approved	0,5	4,6	0
Plicamycin	DNA/RNA synthesis inhibitor	Approved	2,4	0	0
Pomalidomide	Anti-angiogenic	Approved	-8	1,3	0

Ponatinib	Broad range TKI	Approved	-7,6	-3,6	-4,7
Poziotinib	HER inhibitor	Investigational (Ph 2)	-1,5	-19,3	-1,6
Pracinostat	HDAC inhibitor	Investigational (Ph 2)	3,1	0	-5
Pravastatin	Reductase inhibitor	Approved (non-oncology)	0,9	2,2	-1
Prednisolone	Glucocorticoid	Approved	-14,6	-12,9	0
Prexasertib	Chk1 inhibitor	Investigational (Ph 2)	23,8	-18,5	11
PS-1145	IKK-2 inhibitor	Probe	0	-0,5	2,4
PTC-209	BMI-1 inhibitor	Probe	-6,5	-0,2	0,6
Quisinostat	HDAC inhibitor	Investigational (Ph 2)	-0,1	0	-10
Quizartinib	FLT3 inhibitor	Investigational (Ph 3)	-13,3	0	0
Rabusertib	Chk1 inhibitor	Investigational (Ph 2)	5,8	-0,4	-2,6
Radotinib	BCR-ABL1 inhibitor	Investigational (Ph 3)	0	0	0
Ralimetinib	MAPK inhibitor	Investigational (Ph 2)	-0,7	-0,1	3,5
Raloxifene	Estrogen receptor modulator	Approved	-1,2	-3,7	-8,7
Raltitrexed	Synthase inhibitor	Approved	10,4	0,3	-10,5
Ravoxertinib	ERK inhibitor	Investigational (Ph 1)	-0,7	-5,7	-6,3
Regorafenib	B-Raf inhibitor	Approved	-2,1	-6,3	1,6
Resatorvid	TLR agonist	Investigational (Ph 3)	0	0	0
Resiquimod	TLR agonist	Investigational (Ph 2)	8	0	0
Resminostat	HDAC inhibitor	Investigational (Ph 2)	-4,7	-5	-9,4
RGFP966	HDAC inhibitor	Probe	-6,9	0	0
Ribociclib	CDK inhibitor	Approved (US)	-0,9	-0,6	-6,4
Ridaforolimus	mTOR inhibitor	Investigational (Ph 3)	4,1	-2,1	-3,1
Rigosertib	Ras-Raf interaction inhibitor	Investigational (Ph 3)	-6,6	-0,1	-14,7
Ripasudil	ROCK inhibitor	Approved (Japan)	-7,4	-0,1	-2,1
RO5126766	RAF/MEK inhibitor	Investigational (Ph 1)	-0,2	-2,7	-0,9
Rociletinib	EGFR Inhibitor	Investigational (Ph 3)	-3,2	-4,6	-5
Rocilinostat	HDAC inhibitor	Investigational (Ph 1)	1,7	-6,1	-4
Romidepsin	HDAC inhibitor	Approved	3,7	-15,8	-2,9
Roxadustat	HIF prolyl hydroxylase inhibitor	Investigational (Ph 2)	3,6	0	-0,4
RSL3	GPX4 inhibitor	Probe	3,6	0	-0,1
Ruboxistaurin	PKC inhibitor	Investigational (Ph 3)	-4,6	-2,2	-8,9
Rucaparib	PARP inhibitor	Approved (US)	-2,5	1,2	0
Ruxolitinib	JAK inhibitor	Approved	7,9	-18	0,3
S-63845	MCL-1 inhibitor	Probe	-5,9	-0,1	0
Sabutoclax	Bcl inhibitor	Probe	-5,2	0,1	-4,5
Salinomycin	Ionophore	Veterinary approval	-0,6	7,8	5,7
Sapanisertib	mTOR inhibitor	Investigational (Ph 1)	3,5	-5,3	-4,8
Sapitinib	HER inhibitor	Investigational (Ph 2)	-0,3	0	2
SAR405838	MDM2 inhibitor	Investigational (Ph 1)	-5,8	0,7	-4
Saracatinib	Abl-Src inhibitor	Investigational (Ph 3)	-7,3	0	0
Saridegib	Hedgehog signaling inhibitor	Investigational (Ph 2)	-5,6	0	0
SB 743921	Mitotic inhibitor	Investigational (Ph 2)	7,9	-1,2	9,7
SCH772984	ERK inhibitor	Probe	-8,6	-15,7	-12,2
Seliciclib	CDK inhibitor	Investigational (Ph 2)	1,8	-1,2	-1,5
Selinexor	XPO1/CRM1 inhibitor	Investigational (Ph 2)	-1,6	-7,6	-8,4
Selonsertib	ASK1 inhibitor	Investigational (Ph 2)	-1,4	0	0

Selumetinib	MEK inhibitor	Investigational (Ph 3)	-3,8	-10,2	-2,9
Senexin B	CDK inhibitor	Probe	-4,2	-0,2	-2
Sepantronium bromide	Survivin inhibitor	Investigational (Ph 2)	-1	2	-3,8
Serabelisib	PI3K inhibitor	Investigational (Ph 2)	-11,5	-1,7	0
SGC-CBP30	CREBBP/EP300 bromodomain inhibitor	Probe	-2,3	-2,7	-16,3
SGC0946	DOT1L inhibitor	Probe	-4,6	0	1,8
SGL-1776	PIM inhibitor	Investigational (Ph 1)	-12,6	-4,9	-2,7
SH-4-54	STAT3 inhibitor	Probe	-1,6	-5,7	-3
Silmitasertib	CSNK2A1 inhibitor	Investigational (Ph 2)	-0,3	0,7	-7,9
Simvastatin	Reductase inhibitor	Approved (non-oncology)	0	2,9	-0,9
Sirolimus	mTORC inhibitor	Approved	1,3	-0,1	-3,7
Sitravatinib	Broad range TKI	Investigational (Ph 1)	-15	-2,4	2,3
SN-38	Topoisomerase inhibitor	(Approved)	-3,4	-5,6	-0,4
SNS-032	CDK inhibitor	Investigational (Ph 2)	-0,3	0,1	3,5
Sonidegib	Hedgehog signaling inhibitor	Approved	0	-0,7	-0,4
Sonolisib	PI3K inhibitor	Investigational (Ph 2)	-2,6	0	0
Sorafenib	Broad range TKI	Approved	-12,9	0	-1,2
Sotrastaurin	PKC inhibitor	Investigational (Ph 2)	-1,9	-4,6	-15,2
Spebrutinib	BTK inhibitor	Investigational (Ph 2)	-5,7	-10,4	-7,1
StemRegenin 1	AHR antagonist	Probe	-1,9	0	-0,2
Sunitinib	Broad range TKI	Approved	-5,8	-0,4	0
Tacedinaline	HDAC inhibitor	Investigational (Ph 3)	0	0	0
Tacrolimus	Calcineurin inhibitor	Approved	-0,2	0	31,2
TAK-285	HER inhibitor	Investigational (Ph 1)	-1,7	0	-0,4
TAK-530	RAF inhibitor	Investigational (Ph 1)	-2,1	-2,6	4,8
TAK-901	Broad range TKI	Investigational (Ph 1)	-3,3	-3,5	0
Taladegib	Hedgehog signaling inhibitor	Investigational (Ph 2)	3,8	0	0
Talazoparib	PARP inhibitor	Investigational (Ph 3)	-1,1	0	0
Talmapimod	MAPK inhibitor	Investigational (Ph 2)	-0,5	-0,4	6,5
Tamatinib	Syk inhibitor	Investigational (Ph 1)	-2,3	-12,3	-2,8
Tamoxifen	Estrogen receptor modulator	Approved	1,6	-1,3	-4,2
Tandutinib	Broad range TKI	Investigational (Ph 2)	-3,2	0	0
Tanzisertib	JNK inhibitor	Investigational (Ph 2)	-0,1	-2,9	4,3
Tarenflurbil	Gamma-secretase inhibitor	Investigational (Ph 3)	0	0	0
Taselisib	PI3K inhibitor	Investigational (Ph 3)	-8,9	-6,2	-5,1
Tasquinimod	Immunomodulator	Investigational (Ph 3)	-0,4	0	-4
Tazemetostat	EZH2 inhibitor	Investigational (Ph 2)	-0,6	-1,1	2
Telatinib	VEGFR inhibitor	Investigational (Ph 2)	0,3	0,1	0
Temozolomide	Alkylating agent	Approved	0	0,2	-0,4
Temsirolimus	mTORC inhibitor	Approved	7,9	-0,1	0
Teniposide	Topoisomerase inhibitor	Approved	0	-0,8	1
Tepotinib	MET inhibitor	Investigational (Ph 1)	0	-2,9	0
Tesevatinib	RTK inhibitor	Investigational (Ph 2)	-4	0	-4,2
TEW-7197	ALK inhibitor	Investigational (Ph 1)	0	0	5,6
TG100-115	PI3K inhibitor	Investigational (Ph 2)	0,9	0	-0,9
TGR-1202	PI3K inhibitor	Investigational (Ph 3)	0,1	0	-5,6
TGX-221	PI3K inhibitor	Probe	-2,6	-5,3	-8,2

TH588	MTH1 inhibitor	Probe	-2,2	-0,5	-2,3
Thalidomide	Immunosuppressant	Approved	-1,3	-6,6	-7,2
Thioguanine	Antimetabolite	Approved	-0,9	-2,4	-2,3
THZ2	CDK inhibitor	Probe	-13,7	0,4	1,3
TIC10	ERK/AKT inhibitor	Investigational (Ph 2)	-0,4	0,1	9,7
Tideglusib	GSK3 inhibitor	Investigational (Ph 2)	0	-1,4	0
Tipifarnib	Farnesyltransferase inhibitor	Investigational (Ph 3)	-3,3	-22	3,2
Tirabrutinib	BTK inhibitor	Investigational (Ph 1)	0	-7,1	-3,7
Tivantinib	MET inhibitor	Investigational (Ph 2)	4	0,4	5,5
Tivozanib	VEGFR inhibitor	Investigational (Ph 3)	-10,9	5,8	6,3
Tofacitinib	JAK inhibitor	Approved	5,7	-7,6	1,2
Topotecan	Topoisomerase inhibitor	Approved	-1	-1,8	1,8
Toremifene	Estrogen receptor modulator	Approved	-2,1	0	-4,8
Tosedostat	Aminopeptidase inhibitor	Investigational (Ph 3)	5,2	-1,4	-6,1
Tozasertib	Aurora inhibitor	Investigational (Ph 2)	-4,9	6,9	6,5
TRAM-34	Ca ²⁺ -activated K ⁺ channel inh.	Probe	0,7	2,5	0
Trametinib	MEK inhibitor	Approved	-4,3	-9,5	-4,4
Tretinoin	Retinoic acid receptor agonist	Approved	-1,7	4	-4,4
Triapine	Reductase inhibitor	Investigational (Ph 2)	-1,1	-6,4	-5,3
Triciribine	AKT inhibitor	Investigational (Ph 2)	1,2	-1,1	11,3
Trifluridine	Antimetabolite	Approved	-0,8	-7,3	0
Tubacin	HDAC inhibitor	Probe	-4,4	0	2,8
Tubastatin A	HDAC inhibitor	Probe	-3,6	-1,9	2,1
Tucatinib	HER inhibitor	Investigational (Ph 1)	-4,1	1,4	0
Tucidinostat	HDAC inhibitor	Investigational (Ph 2)	-2,1	-0,7	-4,6
UCN-01	Protein kinase inhibitor	Investigational (Ph 2)	-4,1	-3,5	-5,6
Ulixertinib	ERK inhibitor	Investigational (Ph 2)	-1,9	-8,2	-5
UM729	AHR antagonist enhancer	Probe	-5,8	0	-4,9
UNC0638	G9a/GLP inhibitor	Probe	-5	-0,6	-4,7
UNC0642	G9a/GLP inhibitor	Probe	0	-0,8	-1,2
UNC1215	L3MBTL3 inhibitor	Probe	0	0,1	0
UNC2881	MER inhibitor	Probe	-5,8	-1,5	-0,4
Upadacitinib	JAK inhibitor	Investigational (Ph 3)	5,5	-11,1	4
Uprosertib	AKT inhibitor	Investigational (Ph 2)	-2,1	0	-1
URB597	FAAH inhibitor	Investigational (Ph 1)	0	-4,6	0
Valproic acid	HDAC inhibitor	Approved	0	0,5	2,2
Valrubicin	Topoisomerase inhibitor	Approved	-3,7	-1,4	-6
Vandetanib	Broad range TKI	Approved	-2,9	2,7	6,4
Varespladib	Secretory phospholipase A2 inhibitor	Investigational (Ph 2)	0	-1,5	0
Varlitinib	HER2/EGFR inhibitor	Investigational (Ph 2)	0	2,2	0
Vatalanib	VEGFR inhibitor	Investigational (Ph 3)	0	0	-2,9
VE-821	ATR inhibitor	Probe	-3,1	0	0
Veliparib	PARP inhibitor	Investigational (Ph 3)	0	-0,5	-1,4
Vemurafenib	B-Raf inhibitor	Approved	-1	0	0,3
Venetoclax	Bcl inhibitor	Approved (US)	-2,8	3,4	-1,7
VER 155008	HSP70 inhibitor	Probe	0	0,2	6,1
Verdinexor	XPO1/CRM1 inhibitor	Investigational (Ph 1)	-5,1	2,6	-1,7

Vesatolimod	TLR agonist	Investigational (Ph 2)	0	0	0
VGX-1027	Immunomodulator	Investigational (Ph 1)	0,4	0	0
Vidofludimus	DHODH inhibitor	Investigational (Ph 2)	-10,2	0	-9
Vinblastine	Mitotic inhibitor	Approved	-0,1	5,1	-2,3
Vincristine	Mitotic inhibitor	Approved	-0,7	1,4	-0,4
Vinflunine	Mitotic inhibitor	Approved	-1,6	1,3	0
Vinorelbine	Mitotic inhibitor	Approved	-13,6	-6,3	-13,2
Vismodegib	Hedgehog signaling inhibitor	Approved	-0,1	0	-0,1
Vistusertib	mTOR inhibitor	Investigational (Ph 2)	2,4	1,2	-3
VLX1570	proteasome deubiquitinase inhibitor	Investigational (Ph 2)	-2	2,9	6,2
Volasertib	PLK1 inhibitor	Investigational (Ph 3)	-2,5	0,8	-4,5
Vorinostat	HDAC inhibitor	Approved	1,1	-3,8	-2,9
VS-4718	FAK inhibitor	Investigational (Ph 1)	-5,6	-3,9	5,3
WEHI-539	Bcl inhibitor	Probe	0	-6,1	0
XAV-939	Tankyrase-1 and -2	Probe	0	-0,6	-1
ZSTK474	PI3K inhibitor	Investigational (Ph 1)	-8,9	-8,4	0